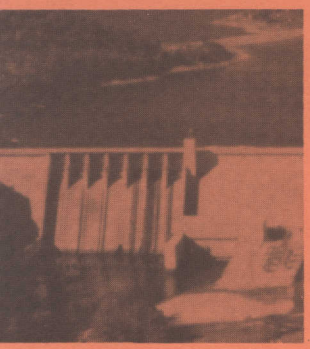

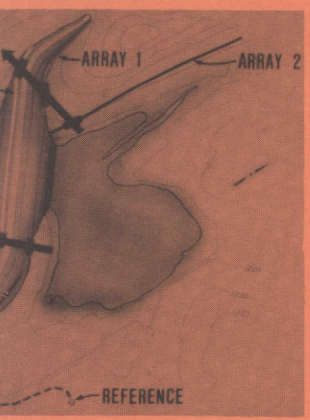

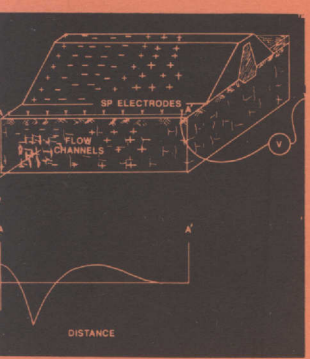

REMR RESEARCH PROGRAM

REPAIR, EVALUATION, MAINTENANCE, AND REHABILITATION RESEARCH PROGRAM

TECHNICAL REPORT REMR-GT-6

GEOTECHNICAL APPLICATIONS OF THE SELF-POTENTIAL METHOD

Report 3

DEVELOPMENT OF SELF-POTENTIAL INTERPRETATION TECHNIQUES FOR SEEPAGE DETECTION

by

Robert W. Corwin

Consulting Geophysicist
Harding-Lawson Associates
PO Box 578, Navato, California 94948

Foreword by

Dwain K. Butler

Geotechnical Laboratory

DEPARTMENT OF THE ARMY
Waterways Experiment Station, Corps of Engineers
PO Box 631, Vicksburg, Mississippi 39181-0631

February 1989
Report 3 of a Series

Prepared for DEPARTMENT OF THE ARMY
US Army Corps of Engineers
Washington, DC 20314-1000

Unclassified

SECURITY CLASSIFICATION OF THIS PAGE

REPORT DOCUMENTATION PAGE

Form Approved OMB No. 0704-0188

1a. REPORT SECURITY CLASSIFICATION: Unclassified	1b. RESTRICTIVE MARKINGS
2a. SECURITY CLASSIFICATION AUTHORITY	3. DISTRIBUTION/AVAILABILITY OF REPORT: Approved for public release; distribution unlimited.
2b. DECLASSIFICATION/DOWNGRADING SCHEDULE	
4. PERFORMING ORGANIZATION REPORT NUMBER(S): Technical Report REMR-GT-6	5. MONITORING ORGANIZATION REPORT NUMBER(S)
6a. NAME OF PERFORMING ORGANIZATION: Harding-Lawson Associates; 6b. OFFICE SYMBOL (If applicable)	7a. NAME OF MONITORING ORGANIZATION
6c. ADDRESS (City, State, and ZIP Code): PO Box 578, Navato, CA 94948	7b. ADDRESS (City, State, and ZIP Code)
8a. NAME OF FUNDING/SPONSORING ORGANIZATION: US Army Corps of Engineers; 8b. OFFICE SYMBOL (If applicable)	9. PROCUREMENT INSTRUMENT IDENTIFICATION NUMBER: Contract No. DACW39-86-C-0059
8c. ADDRESS (City, State, and ZIP Code): Washington, DC 20314-1000	10. SOURCE OF FUNDING NUMBERS: PROGRAM ELEMENT NO. / PROJECT NO. / TASK NO. / WORK UNIT ACCESSION NO. WU-I-32315

11. TITLE (Include Security Classification)
Geotechnical Applications of the Self-Potential Method; Report 3: Development of Self-Potential Interpretation Techniques for Seepage Detection

12. PERSONAL AUTHOR(S)
Corwin, Robert W., Butler, Dwain K.

13a. TYPE OF REPORT	13b. TIME COVERED	14. DATE OF REPORT (Year, Month, Day)	15. PAGE COUNT
Report 3 in a Series	FROM Aug 86 TO Feb 88	February 1989	158

16. SUPPLEMENTARY NOTATION
(See reverse)

17. COSATI CODES			18. SUBJECT TERMS (Continue on reverse if necessary and identify by block number)
FIELD	GROUP	SUB-GROUP	Geophysics; Self potential; Seepage; Subsurface fluid flow

19. ABSTRACT (Continue on reverse if necessary and identify by block number)

This report consists of four distinct but complementary parts: (a) a laboratory/field study of environmental effects on self-potential (SP) electrodes and long-term stability of the electrodes; (b) field investigations at Beaver Dam, Arkansas; (c) development of a computer program for interpretation of seepage-related SP field survey data; (d) development of an extensive bibliography and data base for acquisition and interpretation of seepage-related SP data.

The Beaver Dam, Arkansas, site was selected as the major field test site for a Repair, Evaluation, Maintenance, and Rehabilitation research work unit. The geotechnical problem at the site was anomalous underseepage in the foundation of a large embankment dike. SP data were effectively used to map the seepage paths.

(Continued)

20. DISTRIBUTION/AVAILABILITY OF ABSTRACT	21. ABSTRACT SECURITY CLASSIFICATION
☒ UNCLASSIFIED/UNLIMITED ☐ SAME AS RPT. ☐ DTIC USERS	Unclassified
22a. NAME OF RESPONSIBLE INDIVIDUAL	22b. TELEPHONE (Include Area Code) / 22c. OFFICE SYMBOL

16. SUPPLEMENTARY NOTATION (Continued).

A report of the Geotechnical problem area of the Repair, Evaluation, Maintenance, and Rehabilitation (REMR) Research Program. This report is available from the National Technical Information Service, 5285 Port Royal Road, Springfield, VA 22161.

19. ABSTRACT (Continued).

Three electrodes--nonpolarizing copper-copper sulfate (CS), copper-clad steel (CCS), and lead--were investigated. Of the three, the commercial-grade lead electrodes are least suitable for long-term monitoring of SP. CS electrodes with gelled electrolyte appear capable of surviving at least a few years without maintenance or significant deterioration of physical properties or performance. For SP measurements, CCS electrodes have a lower signal to noise (S/N) ratio than do CS electrodes. Field and laboratory measurements indicate that responses CCS electrodes to environmental disturbances are an order of magnitude or greater than CS electrodes. The higher noise level is due both to the direct exposure of the metal to the soil as well as the exposure of the unburied portion of the electrodes to solar heating and rainfall. Thus, the considerably higher initial cost and extra effort involved in installation of the CS electrodes are justified, and CS electrodes are recommended for geotechnical applications of the SP method.

The SP contours taken with CS electrodes during high and low pool levels at Beaver Dam are strongly related to seepage flow patterns. Even though the data are affected to some extent by topography and by seasonal changes in soil and pore water resistivity, negative SP anomalies are associated with subsurface seepage flow paths and positive SP anomalies are associated with areas of seepage outflow. Comparison of CS and CCS SP data indicate a lower S/N ratio for the CCS data and lack of correlation with the CS data in many locations. However, large amplitude SP responses from CCS electrodes, which are apparently correlated with pool level, may be due to different input parameters than those which affect CS electrodes.

Several geometric SP source models are included in a computer program for modeling SP effects. Procedures for using these source models to iteratively interpret SP field data are discussed. The computer program is utilized to estimate source depths for the seepage at Beaver Dam.

The bibliography and data base contain 144 references. The reference entries are annotated to indicate the key topics discussed, such as electrode studies, dam seepage investigations, and streaming potential theory.

FOREWORD

by

Dwain K. Butler

Flow of fluids through a porous soil on rock generates electrical voltages (potentials) through a process known as electrokinesis. These potentials are called streaming or self potentials (SP). The magnitude of the SP depends on the electrical resistivity, dielectric constant and viscosity of the fluid, on a coupling constant between the fluid and the soil/rock, and on the pressure drop along the flow path. The SP anomaly caused by the flow can be measured on the surface above the flow path; this is the basis of the SP method for seepage detection and mapping.

The US Army Engineer Waterways Experiment Station (WES) has successfully applied the self-potential (SP) and other geophysical methods to detect, map, and monitor anomalous seepage conditions at water retention and hazardous waste disposal sites throughout the United States. The keystone of this successful methodology has been the self-potential method, which has been applied using permanent arrays of inexpensive copper-clad steel electrodes (cut from common grounding rod stock). Use of the metallic electrodes for SP measurements is contrary to commonly accepted geophysical practice; however, cost, ease of installation and maintenance, and general success considerations seemed to outweigh other factors. Data processing techniques were developed which attempted to compensate for electrode polarization effects and sensitivity to environmental variables (see References below). In spite of the general success of the methodology, cases were encountered where the data were extremely noisy, and straightforward interpretation was not possible. In recent years, partly as a result of WES successes, geotechnical applications of the SP method have increased in the United States, and nonpolarizing electrodes which are more rugged and maintenance-free have been developed and applied. Although there has always been the promise for quantitative interpretation of the SP data to give flow rates and depths, data quality has generally not permitted it, and the primary need was for mapping flow paths in plan.

This report is pivotal in the development of geotechnical applications of the SP method for anomalous seepage detection, mapping, and monitoring. Many of the environmental factors which can affect SP measurements with metallic electrodes are compared in detail with the general lack of effect of the same factors on nonpolarizing electrodes. The application of nonpolarizing electrodes at Beaver Dam, Arkansas, "side-by-side" with a metallic electrode monitoring network illustrates that the metallic electrode data are not just shifted up or down in magnitude, while showing qualitative agreement, as has been postulated earlier. In many locations, the metallic electrodes are clearly responding to phenomena not detected at all by the nonpolarizing electrodes. Also, nonpolarizing electrodes now exist which can be installed in a monitoring network that will require no maintenance over a several year period. Thus, the advantages of nonpolarizing electrodes seem to outweigh the lower cost and ease of installation of metallic electrodes for seepage monitoring.

Appendix B presents a summary of recommended field procedures and data reduction methods for SP surveys with nonpolarizing electrodes. This procedure is for a single pass survey, and monitoring applications would require repetition of the survey at later times. Details of field procedure for long-term monitoring permanent arrays of nonpolarizing electrodes have been developed and proposed for application at the Beaver Dam site.

Also, this report presents initial attempts to model quantitatively SP survey results acquired at a Corps damsite. The computer program documented in this report utilizes geometric SP source models, and data can be interpreted by iterative adjustment of source model parameters. These geometric source models are relatively simple compared with quantitative modeling which treats SP from first principle considerations of streaming potential generation from flow through a porous medium. Computer programs which model cross-coupled phenomena in a two- or three-dimensional medium are complex to use and require considerable computer memory and execution time; efforts are underway to streamline and simplify these sophisticated computer programs. This report presents the results of a preliminary run of the quantitative modeling program on a "Beaver Dam-like" problem. More detailed results of modeling the Beaver Dam SP data were presented at an International Symposium on Detection of Subsurface Flow Phenomena at Karlsruhe, Germany.

FOREWORD References--

Butler, D. K. 1984. "Geophysical Methods for Seepage Detection, Mapping and Monitoring," Proceedings, Fifty-Fourth Annual International Meeting of the Society of Exploration Geophysicists, Atlanta, GA.

Butler, D. K., Wahl, R. E., and Sharp, M. K. 1984. "Geophysical Seepage Detection Studies, Mill Creek Dam, Walla Walla, Washington," Miscellaneous Paper GL-84-16, US Army Engineer Waterways Experiment Station, Vicksburg, MS.

Koester, J. P., Butler, D. K., Cooper, S. S., and Llopis, J. L. 1984. "Geophysical Investigations in Support of Clearwater Dam Comprehensive Seepage Analysis," Miscellaneous Paper GL-84-3, US Army Engineer Waterways Experiment Station, Vicksburg, MS.

PREFACE

The work described herein was performed during the period August 1986 to February 1988 by Dr. Robert W. Corwin, Consulting Geophysicist to Harding-Lawson Associates, Navato, California. The work was performed under Contract No. DACW39-86-C-0059, and funded by the Repair, Evaluation, Maintenance, and Rehabilitation (REMR) Research Project "Geophysical Techniques for Assessment of Existing Structures and Structural Foundations," Work Unit No. WU I-32315.

This report was prepared by Dr. Corwin. Principal Investigator for the REMR Research Project was Dr. Dwain K. Butler, Earthquake Engineering and Geophysics Division (EEGD), Geotechnical Laboratory (GL), WES. Dr. Butler also prepared the Foreword and conducted an extensive technical review of the report. The field work was performed at Beaver Dam, Arkansas, in close coordination with other work at the site performed by EEGD, Little Rock District, Corps of Engineers, and other contractors. The report was prepared under the general supervision of Dr. Arley G. Franklin, Chief, EEGD, and Dr. William F. Marcuson, Chief, GL. Senior technical reviewer of this report was Dr. Paul F. Hadala, Assistant Chief, GL. Mrs. Joyce H. Walker, Information Products Division, Information Technology Laboratory, edited the report.

COL Dwayne G. Lee, EN, is Commander and Director of WES. Dr. Robert W. Whalin is Technical Director.

CONTENTS

CONVERSION FACTORS, NON-SI TO SI (METRIC)
UNITS OF MEASUREMENT

Non-SI units of measurement used in this report can be converted to SI (metric) units as follows:

Multiply	By	To Obtain
atmospheres (standard)	101.325	kilopascals
degrees (angle)	0.01745329	radians
Fahrenheit degrees	5/9	Celsius degrees or Kelvins*
feet	0.3048	metres
inches	2.54	centimetres
pounds (mass)	0.4536	kilograms

* To obtain Celsius (C) temperature readings from Fahrenheit (F) readings, use the following formula: $C = (5/9)(F - 32)$. To obtain Kelvin (K) readings, use: $K = (5/9)(F - 32) + 273.15$.

DEVELOPMENT OF SELF-POTENTIAL INTERPRETATION TECHNIQUES FOR SEEPAGE DETECTION

PART I: INTRODUCTION

1. This report describes the results of a research program conducted to develop and document field techniques, analytical methods, and computer programs to improve data acquisition and interpretation procedures for the use of the self-potential (SP) method for dam seepage investigations. As the third in a series of reports on geotechnical applications of the SP method (Erchul 1988; Erchul and Slifer 1989), this report addresses key fundamental questions related to past, present, and future practice. The key questions relate to (a) electrode comparisons and long-term stability concerns; (b) data acquisition procedures; and (c) modeling and quantitative interpretation of SP data.

2. The research program included four major components:

   a. Studies of electrodes to determine their suitability and characteristics for long-term SP monitoring (Part II).

   b. Field investigations conducted as part of a large-scale geophysical study at Beaver Lake Dam, Arkansas (Part III).

   c. Development of computer programs for interpretation of SP data (Part IV and Appendix A).

   d. Compilation of a bibliographic data base of publications relating to SP methods for dam seepage investigations (Part VI).

The results developed for each of these components are described in the indicated parts of this report. A summary of the findings of this study and recommended procedures is presented in Part V. Appendix B is a stand-alone guide to SP field procedures and data reduction. Appendix C is a reprint of a paper which gives details of the Beaver Dam, Arkansas, site, as a reference for Part III.

PART II: ELECTRODE STUDIES

Introduction

3. The objective of this component of the research program was to determine the suitability of various electrode types for long-term monitoring of SP variations related to seepage flow, and to establish the responses of these electrodes to environmental noise sources such as rainfall, temperature, and soil property variations. Investigations within this component included studies of previous publications on this topic and laboratory and field measurements. Results of field electrode studies at Beaver Lake Dam, Arkansas, are included in Part III of this report.

4. As discussed in the early publications on telluric current monitoring referenced below, the electrodes are the most critical component of a system designed to monitor SP variations over long periods of time. Contact potentials caused by interactions between the electrodes and local soil conditions may be larger than the SP voltages generated by streaming potentials related to seepage flow, and time variations of these contact potentials may be greater than those related to seepage. Therefore, selection of the proper electrode type and installation procedures is crucial to the successful performance of a seepage monitoring array.

5. Initial plans had been to study a wide variety of polarizing and nonpolarizing electrode types (e.g., copper-copper sulfate, silver-silver chloride, cadmium-cadmium chloride, lead-lead chloride, etc.) as well as several types of metallic electrodes. Also, it was planned to study nonpolarizing electrodes in which the liquid electrolyte and porous junction are replaced with a block of plaster of pairs mixed with electrolyte solution. However, results of initial studies, time constraints, and the desirability of focusing on previous usage led to a change in emphasis in which laboratory and field investigations were confined to three electrode types: copper-copper sulfate (for brevity, these are subsequently referred to as copper sulfate), copper-clad steel (CCS) stakes, and metallic lead. Copper sulfate was selected in preference to other nonpolarizing electrode types because of commercial availability and extensive previous usage for field SP measurements.

Previous Investigations

6. Installed pairs or arrays of electrodes have been used for long-term monitoring of natural earth currents (tellurics) related to magnetospheric activity, SP variations that could be earthquake precursors, and of SP signals caused by possible seepage-related ground-water flow in the vicinity of dams, dikes, and other containment structures.

7. Van Nostrand and Cook (1966) give an excellent summary of the work of early investigators such as Matteucci, Mauchley, Gish, and Rooney in measuring telluric currents using permanently installed arrays of lead electrodes. These references are included in the bibliography of Part V.

8. Lead electrode pairs, carefully prepared and installed, were found to be superior to nonpolarizing electrodes for this type of measurement (Mauchley 1918), which is similar in concept to the type of long-term monitoring desired for seepage detection. However, as discussed later, factors other than those important for telluric monitoring must be considered in designing a practical seepage monitoring array.

9. Electrode dipole pairs and arrays intended to measure possible SP precursors to earthquakes have been installed in the United States, the Soviet Union, and China. An installation of this type is described in Corwin and Morrison (1977). Pairs of steel plates were used as current transmitters, and lead and copper sulfate electrodes were used as potential receivers in an experiment to determine whether electrical resistivity variations preceded earthquakes in the study area (near Hollister, California). Before and after the resistivity measurements, SP was continuously monitored across most of the transmitter and receiver electrode pairs. This provided a nearly continuous record of SP variations across steel, copper sulfate, and lead electrodes for a period of several years. Similar records probably are available from investigators involved in such studies in other locations, but little of the data has been published.

10. Electrode arrays designed to detect and monitor SP variations related to seepage flow have been installed at a number of locations by the US Army Engineer Waterways Experiment Station (WES). Descriptions of some of these installations are given by Llopis (1987), Llopis and Butler (1988) Koester, Butler, Cooper and Llopis (1984), Cooper, Koester, and Franklin (1982), and US Army Corps of Engineers, Little Rock District (1987). All of

these arrays utilized copper-clad steel (CCS) stakes as measuring electrodes. CCS stakes also were used in a monitoring array to detect sinkhole drainage patterns in Virginia (Erchul 1986). An array designed to monitor seepage through a dike, installed by the Tennessee Valley Authority (TVA) at Colbert, Alabama, used both metal stakes and copper sulfate electrodes (R. Hopkins*).

11. An experiment of particular interest to this study is presently being conducted by the University of California at a field site in Richmond, California (Wilt et al. 1987). The purpose of the experiment is to determine variations of resistivity and SP in response to downhole saltwater injection. Instrumentation for this experiment consists of arrays of surface and downhole transmitter and receiver electrodes along with a computerized data acquisition and control system. This installation is very similar in concept and instrumentation to one which could be used for long-term dam seepage monitoring.

12. The receiver electrode array at the Richmond field site consists of about 80 gelled copper sulfate electrodes, 6 of which are installed in boreholes and the remainder in a surface array buried at depths of 12- to 18-in.** These copper sulfate electrodes, which are of the same type as those described below, have been in place for about 1 year and have not shown any signs of deterioration.

13. Results of these previous studies indicate the following important points regarding selection of electrodes for long-term seepage monitoring arrays:

a. Lead electrodes for telluric monitoring arrays consist of large (several feet) grids of chemically pure lead wire buried at depths of 4-8 ft (Rooney 1932; 1937). These preparation and burial requirements increase the cost of lead electrode installations to the point where they would not be competitive with copper sulfate or CCS stake installations. Even with such elaborate installations, yearly drift of lead electrodes may be several to several tens of millivolts (mV) per year. As indicated by the results of the field experiment described later, electrodes fabricated of industrial (rather than laboratory) purity lead and installed at relatively shallow depth may not give stable readings for long-term measurements.

b. Copper sulfate (and other similar types of nonpolarizing electrodes consisting of a metal rod inserted in an electrolyte solution consisting of a salt of the metal and connected to

---

* Personal Communication, 1987, R. Hopkins, TVA.

** A table of factors for converting non-SI units of measurement to SI (metric) units is presented on page 6.

the soil through an inert porous membrane) gives very stable potentials even in the presence of environmental variations such as rainfall and temperature changes. Drawbacks of such electrodes include relatively high initial cost, care needed in installation, and the possibility of electrolyte leakage or freezing and subsequent failure of the electrode. Rooney (1937) states

> It is sometimes possible, using certain reversible [nonpolarizing] electrodes - metallic copper in copper-sulphate solution, for instance - to reduce the absolute values of potential recorded between two given points in the ground, and it should be possible, theoretically, to keep such electrodes more constant than the simple metallic ones. However, it is found in practice that the advantages of reversible electrodes for earth-current work are not readily realized. In order to make contact with the ground there must inevitably be a slow seepage of the electrode-solution into the ground about the electrode. This results in a constantly changing electrode-environment and the constancy of such an electrode turns out to be pretty much a myth."

c. CCS electrodes offer relatively low initial cost, ease of installation, and low maintenance (assuming that the electrodes are not damaged by on-site activity). The data published by WES indicate that CCS electrodes may in some way amplify the SP signals generated by seepage-related streaming potentials, and that geologic noise levels (point-to-point contact potential variations caused by local soil conditions) are considerably greater than those for copper sulfate and other nonpolarizing electrodes.

14. The most important questions raised by the results of these previous studies are:

a. Are the careful installation procedures necessary for lead electrodes cost-effective for seepage monitoring arrays?

b. Is the larger amplitude of the variations observed on CCS electrode arrays a true amplification of seepage-related signals or an apparent effect due to other causes?

c. If the CCS electrodes provide true signal amplifications, what is its cause?

d. How do signal-to-noise ratios compare for CCS, copper sulfate, and lead electrodes?

e. Considering the above factors, which electrode type provides the best combination of accuracy and cost-effectiveness for seepage monitoring arrays.

The studies described below were designed to help answer these questions.

Long-Term Monitoring Study

15. This section describes the results of a study in which three electrode pairs (copper sulfate, metallic lead, and CCS stakes) were installed in a location protected from disturbance in a suburban residential area and monitored for a period of about 1 year. The purposes of the study were to determine the time needed for the electrode pairs to stabilize, the response of the different electrode types to environmental variations such as rainfall and temperature changes, and the long-term stability of the different electrode types.

Description of installation

16. Plate 1 shows the arrangement of the electrodes. Electrode types were as follows:

a. Copper sulfate: Tinker and Rasor Model 6B, 1-in. diam by 6-in. length plastic body with 1-in. diam porous ceramic junction, initially filled with saturated copper sulfate solution (as discussed later, the liquid electrolyte was replaced with gelled electrolyte after about 6 months of operation). The electrodes were fitted with submersible waterproof adaptors (Model W-7) to allow full burial. The relatively small porous junction area and O-ring seals of these electrodes should have rendered them as leakproof as possible for commercially available off-the-shelf copper sulfate electrodes. The electrodes were installed vertically, with the tips at a depth of about 1 ft, and completely covered with soil.

b. Copper-clad steel (CCS) stakes: These electrodes were 1/2-in. diam by 2-ft-long copper-clad steel grounding rods. They were driven to a depth of 1 ft into the soil, and stranded cooper lead-in wires were clamped to the tops of the rods with stainless steel hose clamps. The CCS stakes were left partially exposed (and not completely buried) to duplicate previous Corps of Engineers field procedure. The clamps were coated with insulating compound (Scotchkote) to minimize galvanic corrosion between the stainless steel clamps and the copper rod cladding.

c. Metallic lead electrodes: These electrodes were cut to a size of 2 in. by 4.5 in. from 99 percent pure lead sheet of 0.042-in. thickness (2.5-lb/sq ft roof flashing). Stranded copper lead-in wire was soldered to the top of the long side of each electrode and the solder joint coated with Scotchkote.

The electrodes were buffed with steel wool, washed with soap and water, and rinsed before installation. They were buried with the 4.5-in. side vertical, with their center points at a depth of about 8 in.

The chronology of the installation was as follows:

a. 31 January 1986: Installation of copper sulfate and CCS electrodes.

b. 4 March 1987: Installation of lead electrodes.

c. 22 August 1987: As the data were indicating problems with the copper sulfate electrodes, they were removed for inspection and found to be dry (i.e., all the electrolyte solution had leaked out). The electrolyte was replaced with a gel consisting of two Knox gelatins (by weight) added to heated saturated copper sulfate solution and allowed to set. This conductive gel had a consistency similar to that of Jell-O, which it was hoped would eliminate or greatly retard electrolyte leakage.

d. 15 January 1988: The copper sulfate electrodes were removed for inspection and found to be in good condition, with no evidence of electrolyte leakage or junction deterioration.

17. The potentials across these three electrode pairs were monitored using a combination of strip chart recorders and digital multimeters. A rain gage installed as shown in Plate 1 was used to monitor precipitation beginning in the fall of 1987. Due to occasional equipment problems and absence of personnel from the site the records are not fully continuous. However, sufficient data were obtained to meet the objectives of the experiment.

Results

18. A strip chart record of the data from the copper sulfate and CCS electrodes for a period of about 6.5 min is shown in Plate 2. The record shows continuous variations with amplitudes ranging from a few tenths of a millivolt (mV) to a few mV, with periods of a few seconds to several tens of seconds. These variations are caused by stray currents from the electrically operated Bay Area Rapid Transit System (BART), located about 1 mile east of the monitoring electrode (the daily records discussed below show the elimination of these variations when BART is not operating).

19. The important conclusion reached from this record is that copper sulfate and CCS electrodes show essentially identical responses to electric fields generated by outside sources (the response of the lead electrodes to the BART-generated signals also was identical to that of the copper sulfate and CCS electrodes). Thus if SP signals generated by seepage flow are of

similar nature to those generated by stray currents, the SP voltage measured by copper sulfate, CCS, or lead electrodes should be identical.

20. A sample record of copper sulfate and lead electrode potentials for a period of about 3 days is shown in Plate 3. Note the strong reduction of the short-period noise level between about 11 p.m. and 3 a.m. each day, when the BART system is not operating. The intrinsic short-period noise level for both electrode pairs is of the order of about 1 mV during these intervals. Similar results were seen for the CCS electrodes.

21. Intermittent rain fell during the period shown in Plate 3, which illustrates the response of lead and copper sulfate electrodes. The responses of the copper sulfate and lead electrodes during this rainfall were representative of that seen during most of the experiment: little or no variation for the copper sulfate electrodes and the intermittent appearance of DC offsets on the lead electrodes. The copper sulfate electrodes responded only to very heavy rainfall, with DC levels returning to previous values once the rain ended. The response of the CCS electrodes is similar to that of the lead electrodes. Note that CCS and copper sulfalte electrode response to rainfall is also discussed in Part III of this report.

22. Plate 4 shows the effects of temperature variations on the copper sulfate and CCS electrode pairs. Potential for both the copper sulfate and CCS electrodes was relatively stable on 6 November, which was cool and overcast. On 7 November, a warm and sunny day, the CCS electrodes showed a positive excursion of about 15 mV corresponding to the heating of the electrodes by direct sunlight. The buried copper sulfate (and lead) electrodes showed no such diurnal response. Although of variable magnitude, this temperature response of the CCS electrodes was seen on most sunny days. Diurnal variations of this type would not be critical for long-term monitoring over periods of several months or more, but seasonal DC offsets caused by electrode temperature variations could be of concern. Complete burial of the CCS electrodes would probably reduce the SP "noise" due to temperature variation.

23. Summarized data for the entire term of the monitoring experiment are shown in Plate 5. The plotted values are estimates of the daily DC potential levels that a long-term seepage monitoring network would be designed to record. Gaps in the records are periods when the recording instruments malfunctioned and/or no personnel were available to record the data.

24. Several conclusions may be reached from the data shown in Plate 5:

a. The copper sulfate electrodes reached a stable potential value almost immediately (within a few minutes) after installation. The CCS and lead electrodes showed large potential excursions (several hundred mV) over a period of 1- to 2-months after installation before reaching more stable values.

b. During the dry period between about mid-May and mid-October 1987, the lead electrodes showed little daily variation and a long-term negative drift of about 25 mV. Their DC value appeared to be relatively constant at about +75 mV for the final 3 months of this period. The CCS electrodes showed somewhat greater daily variation than the lead electrodes during this period, with occasional large (50-70 mV) positive excursions lasting for a few days. The DC level of the copper sulfate electrodes was stable within a few mV of its initial value from the time of its installation through mid-August, when the electrolyte solution had leaked out. After being reinstalled with gelled electrolyte, the DC level of these electrodes returned to its previous value and stayed constant through mid-October.

c. Seasonal rainfall began in mid-October 1987 and continued through the end of the monitoring period in mid-January 1988. This rainfall appeared to produce the following effects:

(1) The DC potential of the lead electrodes dropped from about +75 mV to about +10 mV between mid-October and the end of October, then rose to about +30 MV between the end of November 1987 and mid-January 1988. Day-to-day variations were somewhat greater than those seen during the preceding dry period.

(2) The DC potential of the CCS electrode pair dropped from an average value of about +20 mV during the dry period to about -5 mV following the onset of the rainy season. Day-to-day variations appeared to be somewhat lower during the rainy period, with no consistent response to individual periods of rain. The occasional large positive excursions seen during the dry period were less frequent during the rainy season.

(3) The DC value of the potential between the copper sulfate electrode pair remained within about +/-2 mV of its pre-rainfall mean of about -3 mV. However, individual periods of heavy rain often were followed by negative excursions of about -10 mV, lasting 1-2 days. As the electrode pair was installed on a hillside with the negative electrode at about 4 ft lower elevation than the positive electrode, these excursions have the correct polarity for a streaming potential generated by downslope movement of near-surface ground water. If this is the case, it is not apparent why similar excursions were not seen on the CCS and lead electrode pairs.

Discussion

25. From the results described above, the most significant conclusions of the long-term monitoring study are as follows:

a. Stabilization period: The copper sulfate electrode pair reached a stable DC potential value within a few minutes of installation and remained at that value for the duration of the study. These results are similar to those seen for previous copper sulfate monitoring arrays (Corwin and Morrison 1977). The CCS electrodes showed large potential excursions for a period of about 3 months following installation, after which they remained in a band of about 30 mV with the exception of occasional +50- to +70-mV excursions of a few days duration during the dry season. Additional monitoring would be necessary to determine whether the CCS electrodes have actually attained a stable DC value. The lead electrodes also required a period of about 3 months after installation to settle to a relatively constant value, but drift continued even through the 4-month dry season. Continuing changes of the DC level of these electrodes during the rainy season indicate that a stable DC level was not reached within the 11 months following their installation.

b. Response to external electric fields: The experimental results indicate that all three electrode types have identical response to external electric fields in the earth that have periods of a few seconds to a few minutes.

c. Day-to-day variations: Disregarding the effects of rainfall, the copper sulfate electrodes showed the lowest level of day-to-day variability, with most of the variation due to the difficulty of estimating DC levels in the presence of several millivolts of background noise caused by the BART system. Day-to-day variation of the lead electrodes during the dry season was almost as low as that of the copper sulfate electrodes, probably because their burial below the surface isolated them from direct heating by sunlight.

d. The CCS electrodes showed the highest day-to-day variability, in part due to direct heating effects. It also appears that, especially during dry weather, the CCS electrodes were subject to significant potential excursions, probably caused by the buildup and subsequent decay of periodic corrosion reactions.

e. Reliability: The CCS and lead electrodes needed no maintenance after installation. The copper sulfate electrodes with liquid electrolyte, even though well sealed, leaked out all their electrolyte within 6-1/2 months of installation. Inspection of the gelled copper sulfate electrodes after about 16 months of operation showed no electrolyte loss. Although it should be kept in mind that the soil was saturated during about half of this period, which would tend to retard leakage, the gelled electrodes appear to be capable of long-term, unmaintained burial.

26. Summarizing the findings of previous investigations and the field experiment described above, copper sulfate electrodes appear to stabilize much more rapidly than do CCS or lead electrodes and to be capable of maintaining a stable DC value indefinitely. Lead electrodes made of commercial grade lead and buried at depths practical for multiple electrode arrays appear to perform poorly, showing DC offsets in response to rainfall even after almost 1 year of burial. Although lead is the electrode material of choice for long-term telluric monitoring arrays consisting of a few carefully prepared electrodes constructed of expensive chemically pure material and buried at depths of 4- to 8-ft, it does not appear to be practical for arrays of tens or hundreds of electrodes constructed of affordable commercial grade material to be buried at depths of 2 ft or less.

27. CCS electrodes are considerably noisier and less stable than copper sulfate. If the response of CCS electrodes to SP signals generated by seepage flow is the same as that of copper sulfate, the choice between them would be based on the superior signal-to-noise (S/N) ratio of copper sulfate versus the lower initial cost and possibly lower maintenance costs of CCS. However, there is evidence from WES dam seepage studies using CCS electrodes that SP signal levels as well as noise levels are greater for CCS electrodes as compared with copper sulfate, giving comparable S/N ratios for the two electrode types. In this context, "noise" is any electrical potential variation that is not related to the phenomena of interest, i.e., flow of water (seepage) in the subsurface. A number of the laboratory tests described in the following section were conducted to attempt to determine whether CCS electrodes give greater SP signal levels for a given seepage flow than do copper sulfate electrodes.

Laboratory Measurements

28. The laboratory measurements described in this section were conducted to study the response of CCS and copper sulfate electrodes to environmental variations such as temperature and soil moisture content and to examine the SP response of these electrode types to the flow of water through a porous medium.

Freezing of copper sulfate electrodes

29. Freezing of the liquid or gelled electrolyte of a nonpolarizing electrode could result in damage to the electrode and/or degradation of electrode performance. To examine the results of electrolyte freezing, one of the gelled copper sulfate electrodes described previously was held overnight in a freezer at 8° F.

30. Inspection of the electrode showed that the electrolyte was frozen solid, but that there was no apparent physical damage to the electrode. Values of potential and contact resistance between the frozen electrode and an identical nonfrozen electrode in a bath of copper sulfate solution at various stages in the experiment are tabulated as follows. The negative lead of the digital multimeter used for the measurements was connected to the unfrozen electrode.

Condition	Potential (mV)	Contact Resistance (kohm)
Before freezing	+1.7	1.71
Positive electrode partly frozen	-9.8	86
Positive electrode fully frozen	-16.1	770
Positive electrode fully thawed	+1.1	1.50

After conclusion of the freezing experiment, the electrodes were reinstalled in the earth. Their performance after reinstallation appeared to be identical to that before freezing.

31. These results indicate that freezing and subsequent thawing of this type of electrode do not appear to damage the electrode or affect its performance. However, the field measuring system must be designed with high enough input impedance to handle the increased contact resistance for frozen electrodes. Alternatively, the gel could include a percentage of antifreeze solution (such as glycol) to retard freezing at the cost of somewhat greater unfrozen resistance.

32. The 18-mV-negative potential change for the 60° F temperature drop is typical for copper sulfate electrodes. In a field installation, maximum temperature differences would be considerably less, and maximum temperature effects probably would be limited to a few millivolts. Temperature effects are discussed in more detail in later sections.

Streaming potential measurements

33. The streaming potential cell shown in Plate 6 was designed to examine the SP response of CCS and copper sulfate electrodes to water flow. The cell was made from thin-walled plastic tubing, and all fittings and connections also were of plastic to eliminate possible corrosion potentials from metal components. The cell was filled with medium-grained sand of mixed mineralogy and saturated with tap water of about 300-ohm-ft resistivity.

34. The CCS electrodes were 6-in. lengths of the same 1/2-in. diameter copper-clad steel grounding rods described previously, and the copper sulfate electrodes were Tinker & Rasor Model 2A "pocket cell" electrodes (3/8-in. outside diameter) filled with gelled copper sulfate solution as described above. The CCS electrodes were allowed to equilibrate in the saturated sand for about 1 week prior to beginning the experiment.

35. Flow rates for the test runs were kept low (0.008 to 0.396 gpm) in an effort to maintain laminar flow. The relationship between flow rate and pressure drop across the electrodes was determined by replacing the electrodes with a pair of manometer tubes and measuring the water height difference in the tubes at a known flow rate.

36. The first test run was made using the CCS electrodes in the configuration shown in Plate 6, with the electrodes extending to within 1/4 in. of the opposite wall of the tube. For the second set of runs, both CCS and copper sulfate electrodes were installed with their lower (inner) ends approximately flush with the bottoms of the plastic fittings. For the final set of test runs, both electrode types were completely isolated from the water flow by means of a small plug of clay inside the plastic fitting. The purpose of these successive removals of the electrodes from the flow was to attempt to separate effects caused by interaction between the moving water and the electrode surface (so-called "flow potentials") from those due to streaming potentials generated by flow through the porous medium.

37. Results are tabulated below. Each listed value of measured potential is the average of several runs at different flow rates. Because the zero values of the measured potentials for the CCS electrodes were not stable, reproducibility of the listed values probably is about ±25 percent. Copper sulfate values probably are reproducible within about ±10 percent.

Condition	Measured potential (mV/atm) CCS	Copper Sulfate
Electrodes in flow	4,670	--
Electrodes at bottom of fitting	1,260	420
Electrodes isolated by clay plug	510	380

38. Potentials measured by the two electrode types isolated from the flow by the clay plug were not significantly different. The magnitude of about 400 mV/atm is similar to that measured by other investigators for similar test configurations (e.g., Ogilvy, Ayed, and Bogoslovsky 1969; Tuman 1963). When the electrodes were partially isolated from the flow, the potential change for the copper sulfate electrodes was not significant, but the CCS electrode reading increased by a factor of about 2.5. When the CCS electrodes were arranged to span nearly the full width of the tube, exposing them to the maximum flow, their potential increased to a value about nine times greater than that for the isolated condition.

39. The value of about 4,670 mV/atm for the CCS electrodes is much greater than that expected for a true streaming potential. This discrepancy, along with the large potential differences between isolated and nonisolated flow, imply that the CCS electrodes are subject to significant "flow potentials" caused by the movement of water along the electrode surface. These flow potentials for metal electrodes have been observed in previous studies (Ogilvy, Ayed, and Bogoslovsky 1969). Conversely, nonpolarizing electrodes appear to be free from flow potential effects (Ogilvy, Ayed, and Bogoslovsky 1969; Corwin and Conti 1973).

40. With the electrodes isolated from the flow, as would be the case for a typical field SP measurement, streaming potential response appears to be about the same for CCS and copper sulfate electrodes. This raises the question of the origin of the large-amplitude anomalies (greater than 100 mV) observed on CCS electrode arrays that appear to be related to subsurface seepage flow but are not seen on measurements taken at the same stations with copper sulfate electrodes (see Part III).

41. One possibility is that some of these anomalies may be generated by flow potentials caused by movement of water through surface soils, with this movement related in turn to the presence of faults or fractures that extend from the surface to the zone of seepage. As discussed below, soil property

variations associated with surface expression of subsurface features also could generate anomalies on CCS electrodes that are indicative of seepage zones.

Temperature effects

42. Diurnal SP variations on a CCS electrode pair that appeared to be related to electrode temperature differences were described above. While such variations probably would tend to average out during the course of long-term monitoring, they could generate spurious anomalies in day-to-day measurements. Therefore, it is useful to have some idea of the magnitude of SP changes generated by electrode temperature differences.

43. The temperature response of nonpolarizing electrodes can be derived analytically (Ives and Janz 1961; MacInnes 1961), and has been measured for a number of different electrode types. Such measurements have been performed for copper sulfate electrodes by Semenov (1974), Ewing (1939), and Morrison et al. (1979a). For a variety of experimental conditions, the temperature coefficient of copper sulfate electrodes was found to average about +0.5 mV per degree F (i.e., heating the positive electrode caused a positive SP change). It should be noted that temperatures do not refer to the soil around the electrode, but to the metallic element of the nonpolarizing electrode. Thus, there is a time lag between heating of the soil and appearance of an SP change due to heating of the electrode element.

44. Because no such measurements appear to have been made for CCS electrodes, a laboratory study was performed to determine their temperature coefficient. The electrode pair used for the streaming potential measurement described above was installed in a plastic container filled with the same saturated sand used in the streaming potential cell. The electrodes were immersed to a depth of 3 in. in the sand and separated by 7 in. As for the streaming potential cell, a digital multimeter and strip chart recorder were connected across the electrode pair, with their positive terminals to the heated electrode.

45. Thermometers were strapped to the two electrodes to measure their temperature while one of the electrodes was heated with a hot air gun. Response to temperature changes was almost immediate, and averaged about +1 mV per degree F for a series of temperature differences ranging up to 77° F.

46. This coefficient is about twice that measured for copper sulfate electrodes. Because the maximum diurnal difference in surface soil

temperature between any two electrodes in a monitoring array may be of the order of several degrees, soil temperature differences would be expected to produce diurnal SP variations of only a few millivolts for electrodes not exposed to direct sunlight, as would be the case for buried electrodes.

47. For CCS stake electrodes exposed to direct sunlight, however, diurnal temperature differences between exposed and shaded stakes, and consequent diurnal SP variations, could be much greater. Examples of such variations are seen in Plate 4. Their magnitude is large enough that they could produce significant spurious long-period anomalies by aliasing of daily readings under conditions of changing solar electrode heating. Therefore, for arrays of metal stakes exposed to solar heating, care must be taken that temperature effects are accounted for. Results of the long-term monitoring experiment described above indicate that temperature effects for either metal or nonpolarizing electrodes buried more than a few inches beneath the surface are small and generally can be ignored.

Soil moisture variations

48. A series of laboratory and field studies performed by Morrison et al. (1978, 1979a, 1979b) indicated that the most significant soil property affecting field SP readings taken with nonpolarizing electrodes was the moisture content of the soil at the electrode measurement station. Changes in moisture content were found to have a greater effect than variations of soil type or of soil moisture salinity, pH, or Eh. For copper sulfate electrodes in a variety of soil types, the average response to soil moisture changes was about +1 mV per percent increase in soil moisture content (i.e., the electrode in the wetter soil became more positive with respect to that in the dryer soil).

49. Because similar measurements do not appear to have been made for CCS electrodes, a laboratory study of the response of CCS electrodes to soil moisture variations was performed. The electrodes used were those described above for the streaming potential and temperature measurements, and the soil was a silty clay obtained from the Beaver Lake Dam site described in Part III (the sample is representative of the soil in which most of the CCS electrodes were installed).

50. Samples of nominal (in situ moisture content) and wet soil were placed in contact in a small plastic container. (Water from exit 6 at Beaver Dam was added to the nominal soil to obtain the wet sample.) Moisture content

for the two samples was determined by weighing the wet samples, drying them over low heat, and reweighing. Moisture contents by weight for the wet and dry samples were about 34 and 30 percent, respectively. The value for the wet sample may be a few percent low due to the presence of some gravel in the sample.

51. A digital multimeter and strip chart recorder were connected to the electrodes, which were allowed to equilibrate in the nominal soil. The positive electrode then was moved to the wet soil, and SP values allowed to equilibrate. The positive electrode then was moved back to the nominal soil and the process repeated several times. For comparison, this same procedure also was carried out with copper sulfate electrodes.

52. It proved impossible to obtain a reproducible response from the CCS electrodes for the first few trials. Zero levels changed up to 100 mV each time the positive electrode was reinstalled in the nominal soil, and the response to placement in the wet soil drifted for hours without reaching a steady value. Quasi-steady values ranged from within a few mV of the value with both electrodes in the nominal soil to +/-100 mV of this value. After several trials, however, somewhat more reproducible readings could be obtained, for which the quasi-steady potential appeared to be about 50 mV more negative with the positive electrodes in the nominal soil.

53. In contrast, the copper sulfate electrodes exhibited a reproducible response of +6-mV difference between the wet and nominal soils (i.e., the electrode in the wet soil was positive with respect to that in the dry soil). This value is reasonably consistent with the measured change in soil moisture content (given that, as discussed above, this change may actually be somewhat greater than 4 percent).

54. The results of this experiment indicate that CCS electrodes are extremely sensitive to surface effects caused by movement of the electrode within the soil (it was observed that even slight disturbance of one of the electrodes often produced SP changes of several tens of mV or more). These surface effects may be related to formation and removal of corrosion reaction products. The results also indicate that steady-state response of CCS electrodes to soil moisture changes may be of the order of about -10 mV per percent moisture change.

55. In a clay-rich soil such as that from the Beaver Dam site moisture content may vary by as much as about 10 to 15 percent between very wet and

very dry stations. Thus, SP variations measured by CCS electrodes due to changes in moisture content in such soils may be as much as 100 or 150 mV. However, it does not appear that moisture content effects alone are the source of station-to-station SP variations of a few hundred mV or more.

Conclusions of Electrode Study

56. Of the three electrode types studied, electrodes of commercial-grade metallic lead appear to be the least suitable for long-term monitoring of SP variations related to seepage flow. Buried at a depth of less than 1 ft, lead electrodes do not appear to achieve a stable potential during dry weather, and exhibit unstable DC shifts in response to rainfall even after a year of burial.

57. Copper sulfate electrodes with gelled electrolyte appear to be capable of surviving at least a few years of burial without maintenance or significant deterioration of physical properties or performance. Response of these electrodes to changes of environmental parameters such as temperature or soil moisture content is relatively small, consistent, and reversible. These responses are of the order of a few mV, compared with typical streaming potential anomalies at dam sites of a few tens of mV.

58. Thus, copper sulfate electrodes appear to be technically acceptable for SP monitoring applications. Their major drawback in comparison with CCS electrodes is their considerably higher initial cost (about $20 to $30 each compared with a few dollars for a CCS stake) and additional effort involved in installation (burial and careful insulation of connections).

59. For conventional streaming potential measurements, CCS electrodes appear to have a S/N ratio considerably lower than that of copper sulfate electrodes. Field and laboratory measurements indicate that responses of CCS electrodes to environmental disturbances are one or two orders of magnitude greater than those for copper sulfate electrodes. This higher noise level is due both to the direct exposure of the metal electrode to the soil (as opposed to the isolation provided by the construction of a nonpolarizing electrode) as well as the exposure of the unburied portion of the stake to solar heating and rainfall.

60. As streaming potential response for CCS electrodes isolated from direct contact with flowing fluid is about the same as that for copper

sulfate, there would appear to be no technical advantage to using CCS electrodes for SP monitoring. However, the apparent correlations between subsurface seepage flow and SP anomalies of more than 100 mV measured by field arrays of CCS electrodes imply that some secondary mechanism may generate these large-amplitude SP anomalies. Such mechanisms might include soil property variations and/or surface water movement associated with faults or fractures that extend from the surface to a seepage path at depth. Additional research, possibly including field measurements of soil properties at electrode stations for a CCS installation, would be necessary to determine whether such mechanisms exist.

PART III: SELF-POTENTIAL INVESTIGATIONS AT BEAVER LAKE DAM, ARKANSAS

Introduction

61. This section describes results of geophysical investigations performed at Beaver Lake Dam, Arkansas, at pool elevations of 1,116 ft (August 1986) and 1,120 ft (February 1987). The geotechnical problem at the Beaver Dam site is anomalous underseepage in the foundation of Dike 1. The dike is constructed across a graben with vertical displacements of 200 ft (61 m). A detailed description of the site and the geotechnical problem is presented in Appendix C. The purposes of the present investigations were (a) to determine the relationship between SP readings and seepage flow rates and patterns; and (b) to study the performance of copper-copper sulfate and copper-clad steel electrodes.

62. Investigations performed at the field site included:

a. Measurement of SP on permanently installed copper-clad steel (CCS) stake electrodes (referenced to the CCS base electrode at the north end of line B). Note that no measurements were made for line A, on which the electrodes were installed under water, on the floor of the reservoir.

b. Measurement of SP profiles using copper sulfate electrodes along stake lines B, C, D, and E, as well as additional stations in areas of interest.

c. Acquisition of electrical resistivity data at three stations along line C (February 1987) for comparison with previous data.

d. Monitoring of SP noise levels between CCS stake and copper sulfate electrode pairs over periods of several days to obtain information on time variation of SP readings unrelated to seepage flow.

e. Field and laboratory measurements of water and soil resistivities to determine their effect on the SP readings.

Results of these investigations are described in the following sections.

Summary of Results

63. SP contours from data measured at low pool (1,116 ft) in August 1986 and at high pool (1,120 ft) in February 1987 showed negative anomalies associated with subsurface seepage flow paths and positive anomalies associated with areas of seepage outflow. SP anomaly patterns were influenced by

topographic variations, but topographic effects do not appear to make major contribution to the observed SP anomalies.

64. Changes between the low and high pool measurements included a reduction of most anomaly amplitudes at high pool and significant shifts of anomaly patterns at several locations. The reduced anomaly amplitudes probably were associated with reduced subsurface resistivity at high pool caused by increased poor water saturation levels. The shifted SP anomaly patterns appear to be associated with changes in seepage flow patterns.

65. Studies of electrode performance and background noise levels at the Beaver Dam site indicate that buried nonpolarizing electrodes give satisfactory S/N levels for long-term monitoring of SP variations associated with seepage flow. As discussed in Part II, less expensive CCS stake electrodes also may prove satisfactory for this purpose if their possible greater response to SP seepage anomalies offsets their observed higher noise level caused by variations in environmental conditions such as temperature and soil moisture content.

66. Measured S/N ratios for CCS electrodes appear to be lower than those for copper sulfate electrodes, and the two electrode types measured differing SP profiles along the same survey lines. The CCS data profiles were not simply "amplified" versions of the copper sulfate data profiles, but, instead, the two electrode types appear to be responding to different input parameters.

Results of Field Measurements

Self-potential measurements on copper stake electrodes

67. A network of CCS was installed at the site by WES and Little Rock District (LRD) personnel in March 1985. Installation details and the subsequent measurement program for these stake electrodes are described in the Dam Safety Assurance Program Reconnaissance Report, Supplement No. 1, of April 1986; the Feature Design Memorandum (FDM) of September 1987, and a thesis by Llopis (1987).

68. As part of the present program, SP measurements were made on the CCS stake electrodes on 15 February 1987. Because previous construction at the site had resulted in considerable damage to the permanently installed

connecting cables, measurements were made using a reel of insulated wire connected between the stake base electrode at the north end of line B and the stake to be measured. Readings were taken using a Fluke Model 8020A digital multimeter. Results are summarized in Table 1 and are discussed in the following sections.

Self-potential measurements using copper-copper sulfate electrodes

69. Results of measurements performed at low pool (1,116 ft) in August 1986 are described in the final report for Phase I of this study.* Field procedures and equipment for these measurements and for those taken at high pool are described in Appendix B.

70. The measuring stations used for the August 1986 survey were reoccupied in February 1987 (with some minor changes of station locations in the southeastern portion of the survey area). Station locations and contoured data for the August 1986 and February 1987 surveys are shown in Plates 7 and 8, respectively.

71. In later discussions, line S-1-S-3 refers to a north-south SP profile that runs through the locations of Piezometers S-1 and S-3, extending from about 150-ft north of S-1 and a similar distance south of S-3. Line E4.5 refers to a profile that begins at sta E5 and extends about 450 ft to the south (Plate 8). Portions of both of these lines were measured in August 1986, and complete data profiles were taken in February 1987.

72. SP profiles for the two copper sulfate electrode surveys, together with topography along each north-south survey line, are shown in Plate 9; and Plate 10 shows the differences between the readings for the two surveys (February 1987 values minus August 1986 values) along each north-south survey line.

Measurement of time variations of self-potential readings

73. The report for Phase I of this study described measurements of time variations across selected pairs of CCS stake and copper sulfate electrodes

---

* Corwin, Robert F., 1986, "Development of Self Potential Interpretation Techniques for Seepage Detection," Phase I Final Letter Report, Contract DACW39-86-C-0059, US Army Engineer Waterways Experiment Station, Vicksburg, MS.

Table 1

Self-Potential Measurements on Copper-Clad Steel Stake Electrodes

15 February 1987

Pool Level 1,120 ft

Line B		Line C		Line C		Line D		Line E	
Station	(mV)	Station	(mV)	Station	(mV)	Station	(mV)	Station	(mV)
1	-361	1	+13	36	-256	1	+9	1	*
2	-555	2	+32	37	-18	2	*	2	*
3	-478	3	-12	38	-148	3	-17	3	*
4	-522	4	+11	39	-33	4	-90	4	*
5	-544	5	+34	40	-66	5	*	5	-8
6	*	6	-116	41	-136	6	-90	6	*
7	-544	7	+18	42	-137	7	-58	7	-86
8	-561	8	-170	43	-37	8	-69	8	+42
9	-532	9	-93	44	-441	9	*		
10	-599	10	-26	45	-497	10	+14		
11	-567	11	-18	46	-324	11	-84		
12	-6	12	-12	47	-7	12	+6		
13	-513	13	-56	48	-471	13	-10		
14	-217	14	-381	49	-207	14	+24		
15	*	15	-17	50	+16	15	*		
16	-555	16	-392	51	-31	16	*		
17	-509	17	*	52	+21	17	*		
18	-409	18	-279	53	-27				
19	-318	19	-24	54	-578				
20	-477	20	-423	55	-314				
21	-414	21	-232	56	-93				
22	-443	22	-317	57	-8				
23	-520	23	*	58	-34				
24	-442	24	-367	59	*				
25	-244	25	-436	60	*				
26	-85	26	-489	61	-26				
27	-8	27	-85	62	+10				
28	-28	28	-306						
29	-32	29	-39						
30	-34	30	-306						
31	-23	31	-226						
		32	-239						
		33	-476						
		34	-354						
		35	-596						

Note: Reference at stake base electrode at north end of line B.
* Indicates missing stake.

performed in August 1986. The readings across the CCS stake electrode were made using the permanent cable installed for those electrodes, and there was some question as to whether observed variations associated with rainfall might have been due to grounding of the cable. Therefore, similar measurements were made in February 1987 using an independent insulated cable between stakes C42 and C62.

74. The potential between these stakes was monitored continuously on a strip chart recorder from 1,000 on 15 February 1987 to 2,000 on 18 February 1987. The strip chart record is shown in Plate 11. The significance of the recorded data is discussed below.

Electrical resistivity soundings

75. During the course of the field investigation, it became apparent that information about possible changes of subsurface electrical resistivity vales would be needed to properly interpret the SP data. Resistivity data had been obtained by WES personnel in August of 1986 at sta C21, sta C27, and sta C33. For comparison with these data, vertical electric soundings were taken at sta C21, sta C28, and sta C33 in February 1987 (C27 could not be reoccupied due to piezometer installation).

76. The data were taken using a Soiltest "Strata Scout" Model R-40C resistivity meter (20 mA maximum output). The Schlumberger array was used at sta C28 and the Wenner array at sta C21 and sta C33.

77. Observed data and interpreted layering, determined with an automated computer inversion program, are summarized in Table 2. Because the instrument signal level was marginal for the desired depth of investigation, interpreted layering should be considered approximate. Interpreted layering for the August 1986 and February 1987 measurements are compared in Plate 12. The significance of the observed resistivity variations is discussed below. For a discussion of the electrical method, see Department of the Army (1979) and Butler et al. (1982).

Measurements of
ground-water resistivity

78. Because soil resistivity and SP anomaly source strength both depend strongly on the resistivity of ground water, both in situ and laboratory measurements of ground-water resistivity were performed. Measurements of temperature and resistivity for reservoir surface water and seepage flow water

Table 2

Measured Data and Interpreted Layering for Vertical Electric Soundings, February 1987

Measured Data					
Station C21 (Wenner Array)		Station C28 (Schlumberger Array)		Station C33 (Wenner Array)	
a (ft)	ρa (ohm-ft)	AB/2 (ft)	ρa (ohm-ft)	a (ft)	ρa (ohm-ft)
5	213	4.64	189	5	116
10	181	6.81	234	10	147
20	152	10.0	284	16	190
30	171	14.7	329	20	214
50	195	21.5	391	30	294
100	185	31.6	454	50	390
		46.4	484	64	373
		68.1	426	100	520
		100.0	247		
		147.0	122		

Interpreted Layering			
	C21	C28	C33
ρ_1 (ohm ft)	230.0	173.0	110.0
t_1 (ft)	8.1	4.6	10.2
d_1 (ft)	8.1	4.6	10.2
ρ_2 (ohm-ft)	41.6	728.0	916.0
t_2 (ft)	5.0	31.8	20.7
d_2 (ft)	13.1	46.4	30.9
ρ_3 (ohm-ft)	773.0	22.8	144.0
t_3 (ft)	11.0		26.1
d_3 (ft)	24.1		57.0
ρ_4 (ohm-ft)	136.0		5,000.0

from exit 6 were taken on 19 February 1987 for comparison with previous data taken by WES personnel. Samples of each of these waters were taken and laboratory measurements of conductivity (the inverse of resistivity) as a function of temperature were performed using a Yellow Springs Model 33 S-CT temperature-conductivity meter. Plots of measured conductivity versus temperature are shown in Plate 13. These data are discussed below.

Interpretation of SP Data Taken with Copper Sulfate Electrodes

79. For purposes of this discussion, we will refer to the data taken in August 1986 (pool level 1,116 ft) as "low pool" data, and the February 1987 data (pool level 1,120 ft) as "high pool" data.

80. Comparison between SP profiles (Plates 9 and 10) and contours (Plates 7 and 8) taken at low and high pool indicates that, although the general SP pattern is similar at low and high pool levels, significant detail changes have taken place.

a. The general level of SP activity appears to be somewhat less at high pool than at low pool. This effect is most clearly seen in line D (Plate 9), where the SP anomaly profile shapes are similar at high and low pool, but peak-to-peak amplitude is about 100 mV at low pool and about 50 mV at high pool. This effect also is seen at the south end of line B, as well as in the seepage areas around and to the east of exit 6, where maximum anomaly amplitudes are about +60 mV at low pool and about +40 mV at high pool (exit 6 is located about 100-ft south of sta D14-D17).

b. From theoretical considerations, we would expect the amplitude of seepage-related SP anomalies to increase with increasing seepage flow rates at high pool level. Such increases in SP anomaly levels have been observed at other dams where measurements were made at low and high pool level. Therefore, the observed apparent general decrease in SP activity level at high pool must be explained to understand the true relationship between seepage rates and SP anomaly amplitude at Beaver Dam. Possible reasons for this observed decrease are discussed in later sections.

c. Significant shifts in locations of major anomaly features are seen. For example, the negative closure centered near sta C45 at low pool appears to have migrated about 100 ft to the north at high pool, and the negative closure centered near sta D5 at low pool shows a considerable change of orientation at high pool. A further change is seen in the northern portions of lines B and C, where high pool anomaly levels are more positive

on this portion of line B, but more negative in the same area of line C. This results in a significant shift of the contour pattern in this area.

81. In an effort to interpret the observed profiles and changes in terms of seepage flow, several aspects of the observed data were investigated. These aspects included the relation between SP anomalies and observed seepage patterns and geology, the effects of topography on the SP readings, and the relation between SP anomaly amplitudes and soil and ground-water resistivity.

Relation between SP anomalies, geology, and observed seepage

82. In the absence of preferred seepage paths, the SP pattern around an impoundment structure such as a dam or dike generally will show maximum negative values on the crest of the structure, with values becoming uniformly more positive in the downstream direction. This positive downstream gradient is due to the uniform seepage flow beneath the structure. This same "negative summit" effect also is seen in areas of topographic relief, where downhill flow of ground water often generates SP signals that mirror image the topography.

83. In areas where uniform seepage is interrupted by channeling along preferential flow paths, negative anomalies are seen to follow along the subsurface seepage flow paths, and positive anomalies form in areas where the seepage flow is upward toward the surface. The presence of subsurface features such as faults, dikes, contacts, or artificial drainage structures also will have a characteristic effect on the SP pattern.

84. The Beaver Dam data at both high and low pool exhibit the behavior discussed above. Negative anomalies along the southern fault zone correlate with known subsurface seepage flow paths and positive anomalies are seen in the vicinity of the seepage exits in the southeastern portion of the survey area. A negative anomaly centered near sta D5 may indicate seepage along a fault zone inferred from seismic, radar, and resistivity data, with positive anomalies corresponding to the emergence of seepage water in the south ravine. Although data coverage in the vicinity of sta 64+00 on line C is not sufficient to allow reliable contouring, a strong SP gradient apparent both in the contours and in the profiles of Plates 9 and 10 in this area appears to be related to seepage flow along the southern boundary of the northern fault zone.

85. Soil conditions for the August 1986 survey ranged from very dry over most of the survey area to saturated in the seep areas. Because previous studies have shown that SP readings made with copper sulfate electrodes often become more positive as soil moisture content increases (see Part II), there was some concern that the positive SP anomalies seen at the seep areas could be caused primarily by the higher soil moisture content in those areas.

86. For the February 1987 survey, previous rainfall had uniformly saturated the surface soil throughout the survey area. Therefore, the positive SP anomalies at the seepage exit areas appear to be related mainly to seepage flow rather than to variations in soil moisture content.

87. Results of a brief study of the source depths for the SP anomalies along line C are shown in Plates 14 and 15. The study was conducted using computer program SP1.BAS, discussed in Part IV and included in Appendix A.

88. Plate 14 shows the original SP field data for line C, taken in August 1986. In Plate 15, the data have been "reduced" for interpretation purposes by removing a least-squares trend line and subtracting a constant shift of 10 mV. This allowed a better visual fit between the field data and the calculated model curve.

89. The model parameters are listed in Plate 15. The model consisted of four negative line sources and one positive line source, all trending east-west and 100 ft in length. The source at x = 6,398 ft is at a depth of 2 ft, representing a near-surface effect that may be one of the boundaries of the northern fault zone. The negative sources at x = 6,900, 7,250, and 7,650 ft appear to represent zones of horizontal seepage flow, while the positive source at x = 7,458 ft could represent a zone of upward water flow. The maximum depth of about 50 ft for these four sources places them close to or somewhat above the high-velocity bedrock shown in Figure 31 of Llopis (1987).

90. The locations of these SP sources are in good general agreement with high-resistivity peaks shown in Figure 18 of Llopis (1987) and with the locations of fracture zones inferred from seismic and radar data discussed in Appendix A of the Feature Design Memorandum (FDM) of September 1987. As discussed in Part IV of this report, a more detailed SP modeling effort using program SPXCPL presently is being conducted.

91. Thus, regardless of the relations between SP anomaly amplitude and seepage flow rate, and between SP patterns and topography as discussed below,

the contoured SP data at Beaver Dam appear to be strongly correlated with know seepage flow paths. These correlations are discussed in more detail in Appendix A of the September 1987 FDM.

Topographic effects

92. The effects of topography on SP readings are discussed briefly above. Inspection of Plate 9 shows the mirror image effect between SP and topographic profiles along lines D and S1-S3, and between sta 7300 and sta 7500 on line C. However, it is of considerable interest that the opposite effect is seen at the southern ends of lines C and E4.5 and at the northern ends of lines B and C.

93. Close inspection of the profiles for lines D and S1-S3 indicates that the peaks of the topographic and SP profiles are offset from each other. Cross-plots of SP versus elevation on these lines (Plates 16 and 17) indicate the expected negative correlation between SP and elevation, but the correlation is not as strong as would be expected if the observed anomalies were due only to topographic effects.

94. This weak correlation, along with the positive correlation seen on other lines, suggests that although topographic effects contribute to observed SP anomalies at Beaver Dam, they are not necessarily the major source of anomalies even where the topography is steep.

Effect of ground-water resistivity

95. The magnitude of the streaming potential generated by seepage flow is directly proportional to the resistivity of the flowing ground water. Therefore, with other conditions equal, SP anomaly amplitudes will increase linearly as ground-water resistivity increases. Also, for a given source amplitude, SP anomalies measured at the surface will increase linearly with the resistivity of the soil between the seepage zone and the surface.

96. The soil and water resistivity measurements described previously were made to determine whether these resistivity values had changed between low and high pool levels. As shown in Plate 12, earth resistivity values changed significantly between the low pool measurements in August 1986 and the high pool measurements in February 1987. At depths of less than 5 to 10 ft, resistivities generally were somewhat less at low pool than at high pool. At greater depths, there is considerable variability in the observed resistivity changes. Particularly significant are the decreases at high pool from 12,700

to 136 ohm-ft for the basement resistivity value at sta C21 and from 3,700- to 22.8-ohm-ft at sta C27-C28.

97. Previous repeated earth resistivity measurements in other areas show little seasonal variation (Morrison, Corwin, and Chang 1977). Therefore, it appears that the observed resistivity variations at Beaver Dam are related to the seepage flow at depths of about 30- to 50-ft. Note that sta C33 and C27-C28, where the greatest resistivity decreases at depth were observed, are just upstream of the large negative SP anomaly that was previously interpreted as related to seepage flow along a fault inferred by seismic reflection, radar, and resistivity data. Also, this is an area where a significant change in the SP anomaly contour pattern was observed between low and high pool.

98. There are two possible explanations for the generally lower observed resistivities at high pool: increased pore saturation due to the greater seepage flow, and decreased pore water resistivity due to changes in the temperature of the seepage water. To investigate the effect of temperature changes on pore water resistivity, laboratory measurements as described previously were performed.

99. The data shown in Plate 13 indicate that, as expected from theoretical considerations, water conductivity increases with increasing temperature. (Note that resistivity is the inverse of conductivity, and resistivity in ohm-ft is equal to 32,800 divided by conductivity in micromhos/cm.) Thus, from the data in Plate 13, seepage water resistivity at a typical winter temperature of 10° C is about 300 ohm-ft, and decreases to about 230 ohm-ft at a typical summer water temperature of 20° C.

100. As this effect is opposite from the observed general decrease in soil resistivity during the winter, and as the observed soil resistivity changes are considerably greater than the 100-ohm-ft range expected from temperature changes, our conclusion is that the observed soil resistivity changes are due primarily to changes in levels of pore water saturation caused by infiltration of surface precipitation and by changes in seepage flow rates.

101. Considerable work remains to be done in relating the observed resistivity variations between low and high pool to piezometric profiles and seepage patterns. However, the observed resistivity variations have two important implications. First, it appears that periodic measurements of resistivity variations could provide a useful technique for monitoring pore

saturation levels and seepage patterns. Second, the observed resistivity decreases are large enough to readily account for the observed general decrease in SP anomaly amplitude at high pool levels. Even though SP anomaly source amplitudes would increase due to the higher seepage flow rates at high pool and the higher water resistivity during the winter, the effect of greatly reduced soil resistivity caused by increased pore water saturation could cause a reduction in the SP anomaly amplitude measured at the earth's surface.

Data Acquisition

102. In the previous discussions it was assumed that the measured SP data represented the actual electric field at the surface of the earth. This is strictly true only if no errors are contributed by the measuring electrodes, and if short-period SP variations unrelated to seepage flow either are insignificant relative to seepage anomalies or can be corrected as part of the data reduction process. Investigations of both of these possible error sources are discussed below.

Short-period variations of the earth's electric field

103. Because seepage-related SP anomalies would be expected to vary over periods of several days or more, any SP variation occurring over a period of a few days or less would be considered as short-period for the purposes of this study. Also defined as short-period variations are those not related to the electrode effects discussed below, but instead to actual variations of the earth's electric field. Understanding of short-period variations is important for SP seepage monitoring studies because such variations are superimposed on the anomalous SP field generated by seepage flow, and thus are a source of noise during the measuring process.

104. Short-period variations have two sources: natural and artificial. Natural variations are caused by time fluctuations of the earth's magnetic field that generate electric currents in the earth through electromagnetic coupling. These currents in turn generate electric potentials in the earth that are called telluric voltages. Periods of these telluric voltages range from less than 1 sec up to hours or days. The magnitude of the telluric voltage field depends on the resistivity of the earth beneath the measuring

point as well as the magnitude of the magnetic field fluctuations. Telluric voltages in a uniform earth will increase linearly with increasing separation between the measuring points.

105. The measurements at Beaver Dam indicate that telluric variations with periods of about 10 sec to several minutes can range up to about ±10 mV per 1,000 ft of electrode separation. Examples of such variations are seen in Plate 11 between 0830 and 1200 on 16 February, and at about 1800 on 18 February. A longer-period telluric variation of about 1-hr duration and 10-mV amplitude is seen between 0300 and 0400 on 18 February. Information such as that shown in Plate 11 allows selection of appropriate measurement procedures and data reduction methods to remove the effects of short-term variations and allow measurement of the true steady-state SP field.

106. It should be noted that lightning strikes, even when located several hundred miles from the measuring site, can cause very large short-period fluctuations. However, the period of such fluctuations is so short (less than 1 sec) that they rarely will affect the SP measurements. Many examples of voltage "spikes" generated by lightning strikes are seen in the data of Plates 5 and 6 of the Phase I report.

107. Short-period SP variations also can be generated by artificial sources, particularly overhead power lines and grounds of electrical machinery. Overhead powerlines induce 60-Hz noise into SP measuring systems, often causing drift and irregular fluctuations of the measured values. This problem was present at Beaver Dam, where it was found that 60-Hz noise severely affected the strip chart recorders used for long-term monitoring. Installation of capacitors across the chart recorder inputs greatly reduced the 60-Hz noise. This implies that appropriate input filtering should be part of any future SP monitoring system installed at electrically noisy sites such as Beaver Dam.

108. An example of short-period noise generated by electrical machinery is shown in the upper illustration of Plate 18. As described in more detail in Part II, the measurements were made across CCS stake and copper sulfate electrode pairs separated by 28 ft and located about 1 mile from an electrical substation for the electrically operated Bay Area Rapid Transit (BART) system in the San Francisco Bay Area of California.

109. The noise level ranges from about 1- to 5-mV over the 28-ft electrode separation, which extrapolates to about 40- to 200-mV per 1,000 ft.

The association of the noise with operation of the BART system is shown in the lower illustration of Plate 18, Noise levels during the nonoperational period from about 1 a.m. to 4 a.m. are much lower than those during the day. Even with this very high noise level, average daily potentials for both electrode pairs are stable (during good weather conditions) and with appropriate filtering of short-period variations it would be possible to monitor long-term seepage potentials even under such noisy conditions.

110. Note that in Plate 18, the response of both the copper sulfate and the CCS stake electrodes to short-period variations is virtually identical. This contrasts with their differing response to changes in environmental conditions below and in Part II.

Electrode effects

111. General discussion. The steady-state potential measured between an electrode pair in the earth is the sum of four major contributions:

a. Polarization potentials caused by electrochemical differences between the two electrodes (this potential may be constant or may change with time).

b. Environmental effects caused by different temperature or soil conditions (moisture content, chemistry, etc.) at the two electrode locations.

c. Artificial sources.

d. The anomaly, if present, that is to be measured.

Additionally, installation defects such as a grounded connecting cable or poor contact between an electrode and the soil can contribute large offsets to the measured potentials.

112. Electrode effects for "nonpolarizing" electrodes (in which the metal sensing element is isolated from the soil in a bath of solution containing a salt of the metal element; e.g., CCS) have been studied extensively (see Part II). Results of these studies indicate that long-term variations between pairs of nonpolarizing electrodes buried in the earth are only a few mV, and generally do not exceed 10 mV. A sample record between a pair of copper sulfate electrodes installed at Beaver Dam is shown in Plate 5 of the Phase I report. Maximum long-period drift between these electrodes was about 5 mV.

113. Electrode effects for CCS stake electrodes have not previously been studied in detail. It is known that the magnitude of point-to-point potential variations measured with CCS stake electrodes is much larger than that measured by nonpolarizing electrodes (for example, see Plates 7 and 8 of

the Phase I report). The contribution of electrode effects to these variations is discussed in Part II.

114. Long-term measurements (over periods of several hours to a few days) between pairs of CCS stake electrodes at Beaver Dam are described in the Phase I report. Results of the studies of Part II indicate that much of the observed variation was caused by diurnal temperature effects. As discussed in Part II, rainfall appears to have a very significant effect on the potential between a pair of CCS stake electrodes. Plate 6 of the Phase I report shows an offset of more than 50 mV between stakes at sta E1 and sta E8 that appears to be related to rainfall. Because this offset could possibly have been caused by grounding of the connecting cable between the electrodes, a similar measurement was made in February 1987, using an independent insulated connecting cable.

115. Results of this measurement are shown in Plate 11 of this report. A strip chart recorder connected between stakes at sta C42 and sta C62 showed a change from about -120 mV to about -200 mV occurring at 2200, 15 February. The change followed a moderate 1-day rainstorm that ended a few hours before the variation. Following the offset, the potential slowly drifted back to about -140 mV over a period of about 3 days, when the measurement was terminated.

116. Similar rainfall-related variations have been observed on a CCS stake pair installed as part of a long-term monitoring experiment (the experimental installation also includes pairs of copper sulfate and buried metallic lead (Pb) electrodes). The results of this monitoring experiment are described in Part II.

117. These results indicate that electrode effects due to temperature and soil moisture variations are considerably larger for CCS stake electrodes than for copper sulfate electrodes. However, there is some evidence that signal levels (generated by seepage flow) may also be greater for CCS electrodes (see Plates 7 and 8 of the Phase I report). A field study of this possible "amplification" effect is discussed below.

118. Comparison of copper sulfate and CCS data. A major consideration in the selection of electrodes for long-term seepage monitoring installations is the question of whether CCS electrodes measure a greater SP signal level for a given seepage flow than do nonpolarizing electrodes such as copper sulfate. Laboratory studies of this question are described in Part II. Below

are compared in detail some of the data for copper sulfate and CCS electrodes obtained from the Beaver Dam survey of February 1987. As described previously in this section, both the copper sulfate and the CCS data for this survey were taken using the same field procedure. Therefore, differences between the data sets should be due only to electrode effects.

119. Plate 19 shows unsmoothed copper sulfate and CCS data for line C. It is apparent that the total range of SP activity is about 10 times greater for the CCS electrodes than for the copper sulfate electrodes (about 700 mV versus about 50 mV); and that the magnitude of point-to-point variations as a percentage of total range is greater for the CCS electrodes (i.e., the standard deviation for the CCS data profile is greater). There appear to be some areas of correlation between the two profiles, but the variability of the data makes it difficult to be certain of this.

120. In an effort to make visual comparison between the two profiles easier, the field data were smoothed using a three-point running mean. The smoothed profiles are shown in Plate 20. In general, the profiles appear to be correlated poorly, if at all. The CCS profile shows a generally negative central area that is not apparent on the copper sulfate profile, and the locations of individual positive and negative peaks on the two profiles are not coincident. The major apparent similarity between the two smoothed profiles is the predominant spatial wavelength of about 200 ft in the central portion of the profiles. However, the negative anomalies of this wavelength for the CCS profile are more sharply peaked, even after smoothing, than those for the copper sulfate profile. This suggests a shallower source depth for the CCS variations, since the source depth is directly related to the width of the anomaly at half its maximum value.

121. Comparison of unsmoothed data profiles for line B is shown in Plate 21. Because the data for this line generally were less noisy than those for line C, smoothing did not affect the visual correlation of the profiles. Although some apparent correlations are seen between the two profiles (e.g., the positive trend at the right side and the relative low centered near sta 7200), in general the data do not appear to be significantly correlated.

122. Based on these comparisons, the CCS profiles do not appear to represent an "amplified" version of the copper sulfate profiles. This conclusion is in agreement with the results discussed in Part II, which indicate that streaming potential response for CCS electrodes is no greater than that

for copper sulfate electrodes. Because these results also indicate that the geologic noise level is considerably greater for CCS electrodes, it is concluded that the S/N ratio for copper sulfate electrodes is greater than that of CCS electrodes for seepage monitoring applications.

123. However, the successful results of previous studies by WES and by Erchul (1986) using CCS electrodes for seepage monitoring indicate that useful data regarding seepage flow can be obtained from CCS electrode arrays. Therefore, it is possible that some mechanism not apparent from the present studies actually does amplify the field response of CCS electrodes to streaming potentials. As discussed in Part II, more detailed laboratory studies, along with careful long-term monitoring of coincident arrays of CCS and nonpolarizing electrodes under known seepage conditions, would be necessary to determine any such mechanism.

Conclusions of Beaver Dam Study

124. The SP contours taken with copper sulfate electrodes at the site are strongly related to seepage flow patterns. Even though the SP data are affected to some extent by topography and by seasonal changes of soil and pore water resistivity, it appears that negative SP anomalies are associated with subsurface seepage flow paths and that positive SP anomalies are associated with areas of seepage outflow.

125. Although the effects of seasonal subsurface resistivity variations complicate the interpretation of SP changes due to pool level variations, there appear to be some significant SP variations between pool levels of 1,116 and 1,120 ft that could be related to changes in seepage flow patterns. The most important of these are the variations measured in the northern portions of lines B and C, seen in the contours of Plates 7 and 8 and the profiles of Plates 9 and 10. The proximity of these variations to the northern fault zone indicate that significant seepage flow variations between high and low pool levels may have occurred along this fault zone or its boundaries. This interpretation is supported by the possible appearance of fines in the seepage flow from this area in February 1987.

126. Other significant changes in SP patterns appear to be shifts in the locations of the negative SP anomalies centered near sta C45 and sta D5.

Comparison of these shifts in SP anomaly locations with piezometer data should establish whether they are related to changes in seepage flow patterns.

127. Survey results indicate that monitoring of subsurface resistivity data is necessary for complete interpretation of SP data. The resistivity data also should prove very useful for monitoring of soil saturation changes due to surface infiltration and seepage flow.

128. Measurements made during the two field studies have established the nature and magnitude of SP noise due to telluric, artificial, and environmental sources at the Beaver Dam site. The S/N level for copper sulfate electrodes clearly is large enough to permit reliable monitoring of long-term SP variations having magnitudes of greater than a few millivolts. As both anomaly amplitudes and variations related to pool level appear to exceed 10 mV, copper sulfate or similar nonpolarizing electrodes should be suitable for long-term monitoring of seepage-related SP anomalies.

129. CCS stake electrodes are less expensive to purchase, install, and maintain than are nonpolarizing electrodes. Although their noise response to environmental changes such as temperature or rainfall is greater than that of nonpolarizing electrodes, they have been used successfully for seepage-related SP measurements. However, results from this study indicate that the two electrode types may be responding to different input parameters. Factors that determine which electrode type is more suitable from both economic and technical considerations for long-term SP monitoring are discussed in more detail in Part II.

PART IV: METHODS FOR INTERPRETATION OF SEEPAGE-RELATED SP DATA

Introduction

130. In this section, a catalog and description techniques are presented for interpretation of SP data for seepage investigations. It is assumed that the field data are of good quality, and that the effects of geologic, artificial, topographic, time-varying, and other noise sources have been accounted for.

131. SP data may be interpreted qualitatively, geometrically, or quantitatively. The interpretation procedure selected will depend on the desired goals of the investigation, the quality of the field data, the amount of available additional geological, geophysical, and hydrologic data, and the time and computer resources available for the interpretation phase of the investigation.

132. Qualitative interpretation involves preparation of data profiles and contours and visual inspection of these to look for patterns known or thought to be characteristic of seepage flow paths. The results of many previous investigations cited in Part V (as well as the Beaver Lake Dam study described in Part III) and of quantitative studies using the techniques described below indicate that negative SP anomalies often are seen at areas where seepage flow is entering the dam and above seepage paths where flow is horizontal or descending; and that positive anomalies often are seen above areas where flow is ascending toward the surface or where surface seepage is occurring.

133. Such qualitative interpretation has proved useful in many cases where the SP data were used primarily to indicate locations for more intensive hydrologic or geophysical investigations. However, the use of geometric interpretation techniques, which require minimal additional effort, can help to provide information about flow path depth and configuration as well as location.

134. Geometric interpretation involves the use of calculated curves and contours generated by relatively simple SP source models to match the observed field data. The available models include polarized points, lines, cylinders, spheres, sheets, and other geometric forms. Matching of field data to the

curves generated by these sources can provide useful preliminary information about the form, depth, and orientation of inferred seepage paths.

135. Although no quantitative information about seepage flow rates is provided by these techniques, they are useful not only for the source parameters they provide but also for helping to eliminate SP anomalies caused by sources for which depth or configuration is inconsistent with known geologic or hydrologic information. Also, the preliminary models derived from these techniques are useful as input to the quantitative modeling programs discussed below.

136. The listing in the following section summarizes a number of source models selected from the geophysical literature. Because most of the algorithms are relatively simple, they may be programmed on a calculator or personal computer. Appendix A includes computer program SP1.BAS, written for the IBM-PC and compatible computers for the calculation of anomalies generated by the geometric source models described below, as well as a user's manual, sample output, and the program listing. SP1.BAS can be used directly for field SP data interpretation using geometric source models.

137. Quantitative interpretation of SP data may be done using techniques described in the references of Nourbehecht, Madden, Fitterman, Sill, and others cited in the following sections. These techniques involve the use of computer programs adapted from algorithms originally developed for calculation of potentials and apparent resistivities for two- and three-dimensional resistivity distributions in the earth. Input to these programs include the electrical resistivity structure of the region to be modeled, values of streaming potential coupling coefficients and permeability for the region, and the location and intensity of pressure sources and sinks representing areas of seepage inflow and outflow.

138. These computer programs are complex to use and require considerable memory and execution time compared with the relatively simple geometric source models discussed above. In many cases resistivity, coupling coefficient, or permeability values may not be available and must be estimated. Nevertheless, these quantitative techniques can provide a powerful tool for interpretation of seepage-related SP data. Unlike the simpler techniques discussed above, they can (a) account for complex geologic, electrical, and hydrogeologic structure; (b) distinguish between pressure sources and sinks, and (c) provide quantitative estimates of seepage flow rates and velocities.

139. Very little information has been published regarding the use of these computer programs (which originally were developed for interpretation of geothermal SP data) for analysis of seepage-related SP data. The subsequent section on quantitative modeling briefly discusses the derivation and use of one such program. The following tabulation lists references for each source model.

References for SP Source Models

1. Point current sources (single and multiple)

Alfano 1962
Broughton, Edge, and Laby 1931
Corwin 1976
Corwin et al. 1981
DeMoully and Corwin 1980
Heiland 1940
Merkel 1971
Morrison et al. 1978
Morrison et al. 1979a
Morrison et al. 1979b
Paul et al. 1965
Paul and Banerjee 1970
Semenov 1974
Stern 1945
Telford et al. 1976
Van Nostrand and Cook 1976

2. Horizontal lines sources (including polarized sheet sources modeled as dipolar line pairs)

Banerjee 1970
Broughton, Edge, and Laby 1931
Laxman et al. 1986
Meiser 1962
Murty et al. 1985
Paul 1965
Rao et al. 1970
Rao et al. 1983
Roy and Chowdhury 1959
Semenov 1974

3. Spherical sources

Bhattacharya and Roy 1981
de Witte 1948
Heiland 1940
Iakubovskii and Liajov 1980
Muoi and Quynh 1988
Petrowsky 1928

Rao et al. 1970
Semenov 1974
Telford et al. 1976
Yungul 1945
Yungul 1950

4. Cylindrical sources

Bhattacharya and Roy 1981
Murty et al. 1985
Semenov 1974

5. Dipolar sheet source

Fitterman 1979a
Fitterman and Corwin 1982
Fitterman 1984

6. Quantitative modeling

a. Specific for SP interpretation

Fitterman 1976
Fitterman 1978
Fitterman 1979a
Fitterman 1979b
Fitterman 1979c
Fitterman 1982a
Fitterman and Corwin 1982
Fitterman 1983a
Fitterman 1984
Harding 1981
Hulse 1978
Ishido and Mizutani 1981
Nourbehecht 1963
Nourbehecht and Madden 1970
Sill and Johng 1979
Sill 1981a
Sill and Killpack 1982
Sill 1982a
Sill 1982b
Sill 1982c
Sill 1983a
Sill 1983b

b. Fundamental theory for quantitative modeling

Denbigh 1951
Marshall and Madden 1959
Mitchell 1976
Onsager 1931
Pourbaix 1949
Prigogine 1955

Geometric SP Source Models

140. This section summarized SP source models for a variety of source geometries. Model geometry and equations for calculating SP fields are shown in Plates A1 through A5 of Appendix A. For metric calculations the most convenient units are milliamps (mA) for current I, millivolts (mV) for potential voltage V, ohm-meters (ohm-m) for resistivity ρ , and meters (m) for length. Corresponding English units are mA, mV, ohm-feet (ohm-ft), and feet. The equations used for the algorithms of the computer program SP1.BAS included in this report are those of Plates A1 through A5. A summary of selected references for each geometric source type, as well as for quantitative modeling of SP data , is given in the preceding section.

141. It should be noted that the references cited above for geometric modeling usually include not only derivations and equations fro calculating model curves but also interpretation schemes based on the use of anomaly wavelengths and shapes, characteristic curves, nomograms, and a variety of other methods. In many cases use of these interpretation schemes prior to curve matching using computer program SP1.BAS in Appendix A can save considerable time by providing reasonable first estimates of source parameters; and, in some cases, these easily obtained estimates may be sufficient for the degree of interpretation desired.

Point current sources

142. The geometry and modeling equation for a point source of current in a uniform half-space is shown in Plate A1 (a current sink is defined as a negative source). A point source or sink or multiple combinations of point sources and sinks provide a powerful and flexible geometry for modeling of SP anomalies. Any arbitrary source configuration, with any arbitrary charge distribution, can be expressed as an appropriate spatial distribution of point sources and sinks.

143. A particularly useful application of a single point source or sink model is to provide a first estimate of the depth to the source of a circular or nearly circular SP anomaly. Because a point source represents the minimum possible source size, the source depth of the anomaly can be no greater than that which provides a reasonable fit to a point source model. Thus, fitting a point source to the observed data can quickly indicate the maximum source

depth. The size of the source region then must increase as its depth decreases from this maximum value.

144. The half-wavelength XH (the distance from the origin at which the anomaly is one-half of its maximum value) of an anomaly generated by a point source buried at depth d is given by

$$XH = 3\sqrt{d}$$

This equation is helpful for quickly estimating the depth of a point source.

145. As numerous analytical equations have been developed for calculating the fields generated by point sources in inhomogeneous media, the use of single or multiple point sources allowed relatively simple calculation of SP fields in the presence of geologic structure such as layers, contacts, faults, dikes, etc. More complex two- or three-dimensional structure may be modeled using algorithms developed for resistivity interpretation.

146. Examples of the use of multiple point sources to model complex source geometry are given in DeMoully and Corwin (1980) and Corwin et al. (1981). Morrison et al. (1978) present a computer program for calculating the SP field generated by an arbitrary array of point sources and sinks in the presence of a vertical resistivity contact. The computer program SP1.BAS included in Appendix A presently calculates point source fields only for a uniform half-space but could be adapted relatively easily to handle more complex resistivity structure.

Horizontal line sources

147. The geometry and modeling equation for a horizontal line source of current are shown in Plate A2. The source is parallel to the y-axis, has a constant current I per unit length, and is located in a uniform half-space.

148. The line source represents the simplest geometry for modeling elongated SP anomalies. As for a point source, the depth to a line source that fits the field data represents the maximum possible source depth for an elongated anomaly.

149. More complex elongated source geometries may be modeled as distributions of multiple line sources and sinks. In the literature, many models described as sheet sources actually are dipolar line pairs located along the top and bottom edges of the "sheet". Such models are widely used for interpreting SP fields generated by thin, elongated mineral deposits. For this

study, a sheet model is considered as one having uniform charge on the faces of the sheet rather than charge concentrated along the upper and lower edges.

150. The analytical equation in Plate A2 is valid only for horizontal lines having constant current per unit length. A series of closely spaced point sources may be used to approximate lines for which the current distribution is not constant or for which the lines are not horizontal or for use in areas of nonuniform resistivity.

Spherical sources

151. The geometry and modeling equation for a spherical source are shown in Plate A3. The axis of polarization of the sphere is inclined at an angle α to the vertical, and the potential along the surface of the sphere decreases cosinusoidally from its "equator" (where the charge is maximum) toward the axis of polarization. The sphere is located in a half-space of uniform resistivity. This is a rather restrictive model but is one of the few spherical models that can be handled analytically with a simple closed form solution.

152. This model has proved useful in interpreting SP data for mineral deposits that have similar dimensions along all three axes. For seepage problems, this type of dipolar sphere might in some cases represent flow through a roughly spherical cavity. The sphere model also could be useful for initial interpretation of approximately circular field anomalies, to check whether the model curve shapes are more characteristic of a point source (indicative of a large ratio of source depth to source size) or a spherical source (indicative of shallower burial depth).

153. To approximate a charge distribution other than the sinusoidal dipole of this model, a closely spaced distribution of point sources and/or sinks may be placed on a spherical surface. As noted in some of the references, at burial depths that are large relative to the radius of the sphere, the SP field of this spherical model approaches that of a simple dipole consisting of a point current source and sink. For example, the SP field generated by a sphere having an inclination angle α of 30 deg and a depth/diameter ratio of 5 deviates by no more than 1.5 percent from the field of a point dipole having the same inclination angle.

Cylindrical sources

154. The source geometry and modeling equation for a horizontal cylinder of infinite strike extent are shown in Plate A4. The cylinder

carries a uniform dipolar charge around its circumference, and the angle of polarization β is measured from the vertical axis. The cylinder is located in a half-space of uniform resistivity. As for the sphere above, this restrictive model is one that has an analytical solution in closed form.

155. The relation of the cylindrical model to the line source is analogous to that of the sphere to the point source. Cylindrical models having other than constant dipolar charge may be approximated by a series of line sources placed around a cylindrical circumference, and line sources also can be used to approximate a cylinder of finite length. At burial depths that are large relative to the radius of the cylinder, the SP field of the cylinder approaches that of a line dipole having the same inclination as the angle of polarization of the cylinder and a separation equal to the diameter of the cylinder.

Vertical dipolar sheet source

156. Plate A5 shows the geometry and modeling equation for a vertical rectangular sheet source having a constant positive charge per unit area on one face and an equal and opposite charge on the other face. The resistivity of the earth on the two sides of the sheet (in the x- or y-direction) may be different.

157. This model is particularly useful because it has been observed that ground-water flow in the vicinity of vertical discontinuities of resistivity and/or electrokinetic coupling coefficient often generates dipolar charge distributions of this type, and anomalies fitting this model have been observed in a number of field studies. Although most of these anomalies were related to the movement of geothermal fluids in the vicinity of fault or fracture zones, similar anomalies also have been observed above vertical or nearly vertical geologic features in the vicinity of flows of nonthermal ground water.

158. More complex source distributions can be modeled using techniques discussed by Fitterman (1979a,b,c) or by approximating the sheet with a distribution of point or line sources and sinks. Sheets that are not vertical also can be modeled using either techniques described by Fitterman (1984) or by using approximations with point or line sources.

Quantitative Modeling Techniques

159. The quantitative SP modeling techniques discussed previously are based on concepts of irreversible thermodynamics and coupled flows of fluids, heat, electrical current, and chemical diffusion as described by Onsager (1931), Pourbaix (1949), Denbigh (1951), Prigogine (1955), and others. Application of these concepts to flow in soils is discussed by Mitchell (1976).

160. Specific application of these concepts to interpretation of SP data was first studied by Nourbehecht (1963), followed by the work of Fitterman, Sill, and other investigators listed in the previous section. Of particular interest are publications by Sill (1983a) and Sill and Killpack (1982). The first of these summarizes previous work, presents a number of useful type curves, and shows a field example for which quantitative techniques were used to interpret SP data for a geothermal area in terms of heat and fluid flow. The 1982 publication describes a computer program (SPXCPL) for quantitative two-dimensional modeling of SP data generated by the flow of fluid and/or heat in the earth.

161. Efforts presently are underway by M. Wilt of the Engineering Geoscience group at the University of California, Berkeley, to adapt and document SPXCPL for use on personal computers and to use the program to model SP anomalies generated by dam seepage. Plate 22 shows results of a preliminary run of SPXCPL to determine the general SP pattern associated with dam seepage flow. A relatively negative anomaly is seen over the seepage inflow area and a relatively positive anomaly is seen over the seepage outflow area. As discussed previously, this general pattern agrees with that often seen in field data.

162. A specific effort presently is being made to use SPXCPL to help interpret the SP data from Beaver Lake Dam, Arkansas (Part III). Results of this study are expected to be presented at a symposium to be held at Karlsruhe University, West Germany, in the spring of 1988.

PART V: SUMMARY OF FINDINGS AND RECOMMENDED PROCEDURES

Summary

163. Conclusions of the electrode and Beaver Lake Dam studies are included in Parts II and III of this report. The paragraphs below briefly summarize findings for the entire research effort and present recommended technical procedures for the use of self-potential methods for dam seepage investigations.

164. Nonpolarizing copper-copper sulfate electrodes using a gelled electrolyte appear to be technically suitable for monitoring of self-potential (SP) signals generated by water flow associated with dam seepage. Noise levels generated by sources such as rainfall and temperature variations are predictable and are considerably lower in amplitude than expected signal levels. Less expensive electrodes of CCS appear to have signal levels comparable to copper-copper sulfate electrodes, but considerably higher noise levels. Electrodes of commercial-grade metallic lead installed at depths comparable to the copper-copper sulfate or CCS electrodes do not appear to be suitable for long-term SP monitoring.

165. The most important results of the field investigation at Beaver Lake Dam, Arkansas, included furnishing of data for the electrode studies described above; providing information about the relation between SP, hydrologic, geologic, and other geophysical data; establishment of baseline data on natural and artificial noise sources at a typical dam site; and indicating the need for electrical resistivity data as a component of any long-term SP monitoring program.

166. Comparison of SP data with the extensive information obtained from other investigations at this site indicated that significant SP anomalies were associated with the seepage flow, with negative anomalies seen above downward or horizontal flow and positive anomalies above areas of upward flow. Variations of the areal SP anomaly pattern between high and low pool levels occurred at fault or fracture zones inferred as seepage flow paths by hydrologic or other geophysical data, and these SP variations indicate significant spatial variations in the flow pattern between high and low pool, i.e., changes in flow paths. SP magnitude variations correlated to flow rate variations are complicated and masked by the changes in subsurface resistivity.

167. The computer program developed as part of this study provides a rapid technique for estimating the depth and configuration of seepage flow paths determined from SP data. A preliminary study using a recently developed quantitative modeling program indicated that quantitative SP modeling methods based on concepts of irreversible thermodynamics and coupled flows can be very useful for more detailed interpretation of seepage-related SP data.

168. The bibliography and data base included as part of this report summarizes much of the published information available on the use of SP techniques for seepage and other flow-related investigations. This data base should provide a useful starting point for future studies or applications.

Conclusions and Recommendations

169. Based on the findings of this research effort and of the references cited in the bibliography, the self-potential method can provide useful, and sometimes unique, information about dam seepage flow. Selection of appropriate data acquisition and interpretation techniques is important for effective use of the SP method for this application. A recommended field and data reduction procedure for simple SP surveys is presented in Appendix B, and some recommended techniques for SP seepage detection and monitoring networks are discussed below.

170. The recommended method of acquiring SP data for seepage monitoring is the use of a permanently installed array of buried copper-copper sulfate electrodes with gelled electrolyte. All the electrodes should be hard-wired to a common station having weather protection and power available to run a small computer system. The installation also should include permanently installed arrays of resistivity monitoring electrodes with cables running to a transmitter-receiver unit at the common station. Measurement of resistivity along with SP is necessary if SP magnitudes are to be correlated to flow rates.

171. As described in the body of the report, appropriate filtering of the SP readings is required to minimize the effects of high-frequency noise such as natural tellurics and that due to 60-Hz sources. Each SP reading should be averaged over a period of 1 or 2 min to account for the effects of longer-period telluric variations. Rainfall, temperature, pool level,

seepage flow rates, and other important data should be recorded along with the SP and resistivity values.

172. The computer system would be used to acquire, reduce, store, and plot the SP and resistivity data. The entire procedure could be done automatically, on a daily or weekly schedule. Once such a system is installed, the only labor needed would be periodic collection and interpretation of the data. If desired, the data could be transmitted via telephone lines to a location remote from the installation. This type of computer system is well within the present state of the art, and could be assembled using available personal computers, data acquisition systems, and other commercial components.

173. There are two major technical advantages of such a system. First is the ease of acquiring and processing data, which allows frequent measurements, reduced the probability of missing a significant seepage event, and allows developing events to be intensively monitored. Second, the data quality obtained from a permanently installed array will be considerably better than that obtained from repeated conventional field surveys. Even using the most careful field procedures as described in Appendix B, a certain amount of irreproducible error is accumulated each time an electrode is put into the soil. This error is minimized by one-time installation of a permanent array.

174. The initial cost of the system described above could be reduced by employing manual rather than computer acquisition of the data. However, the cost of the computer system is small relative to that of the electrodes, cables, and installation labor, and the initial savings would be less than the increased labor costs for acquisition and reduction of data (especially if reading frequency is increased to follow a developing event).

175. Initial costs can be eliminated entirely by employing repeated conventional field surveys rather than a permanently installed array. This would require mobilizing and transporting personnel and equipment to the field site each time a measurement is made. As discussed above, the disadvantages of such an arrangement include reduced data quality, the possibility of missing seepage events due to increased sampling intervals, and the difficulty of monitoring developing events. Also, because successful SP field data acquisition requires considerable training and experience, it could be difficult to maintain data continuity and quality over a period of several years.

176. Data reduction and interpretation techniques would be similar however the data were acquired. The SP data would be referred to a common base

station and plots along each profile line would be prepared. The entire data set would be contoured, and profiles and contours of differences between successive data sets also would be prepared.

177. Using the computer program developed as part of this study, along with all available supplemental hydrologic and geophysical data, the profiles and contours would be interpreted in terms of seepage flow paths and changes in these paths with time. If more intensive interpretation in terms of seepage flow rates and path locations is warranted, a quantitative interpretation program such as that described in the body of this report could be used.

PART VI: BIBLIOGRAPHY AND DATA BASE

178. This section presents a bibliography and data base of references related to the acquisition and interpretation of seepage-related SP data. Topics covered include theoretical and laboratory studies of streaming potential phenomena, field studies of seepage problems, studies of electrode performance, and modeling and interpretation of SP data. A list of key letters for retrieval of specific topics is given below. Each of the listed references includes one or more of these key letters indicating the main topic(s) of the reference.

List of Key Letters

B	Extensive bibliography
E	Electrode studies
DS	Dam seepage investigation
F	In-field seepage investigation
G	Geothermal investigation
L	Laboratory measurement of streaming potentials
M	Modeling or interpretation of SP data
T	Streaming potential theory
TM	Telluric current measurement
O	Other

REFERENCES

Abaza, M. M. I., and Clyde, C. G. 1969. Evaluation of the Rate of Flow Through Porous Media Using Electrokinetic Phenomena: Water Resources Research, Vol 5, No. 2, pp 470-483.

L,T

Abaza, M. M. I. 1966. Streaming Current and Streaming Potential Induced by Water Flow Through Porous Media: Ph.D. Thesis, Utah State University, Logan.

L,T

Ahmad, M. U. 1964. A Laboratory Study of Streaming Potentials: Geophysical Prospecting, Vol 12, No. 1, pp 49-54.

L,T

Alfano, L. 1962. Geoelectrical Prospecting with Underground Electrodes: Geophysical Prospecting, Vol 10, No. 3, pp 290-303.

M

Banerjee, B. 1970. Interpretation of Self Potential Data for Vertical and Nearly Vertical Sheets of Infinite Horizontal Extension: Pageoph., Vol 82, No. 8, pp 588-591.

M

Bhattacharya, B. B., and Roy, N. 1981. A Note on the use of a Nomogram for Self-Potential Anomalies: Geophysical Prospecting, Vol 29, pp 102-107.

M

Bhattacharya, B. B. 1986. Reply to Comment by N. S. Rajan, N. L. Mohan, and M. Narasimha Chary: Geophysical Prospecting, Vol 34, pp 1294-1295.

M

Bogoslovsky, V. A., and Ogilvy, A. A. 1970. Natural Potential Anomalies as a Quantitative Index of the Rate of Seepage from Water Reservoirs: Geophysical Prospecting, Vol 18, pp 261-268.

DS,F

_____. 1970. Application of Geophysical Methods for Studying the Technical Status of Earth Dams: Geophysical Prospecting, Vol 18, pp 758-773.

DS,F,M

_____. 1972. The Study of Streaming Potentials on Fissured Media Models: Geophysical Prospecting, Vol 20, pp 109-117.

L,T

_____. 1973. Deformations of Natural Electric Fields Near Drainage Structures: Geophysical Prospecting, Vol 21, pp 716-723.

DS,F

_____. 1974. Detailed Electrometric and Thermometric Observations in Offshore Areas: Geophysical Prospecting, Vol 22, pp 381-392.

F

Bogoslovsky, V. A., Ogilvy, A. A., and Strakhova, N. A. 1977. Magnetometric and Electrometric Methods for the Investigation of the Dynamics of Landslide Processes: Geophysical Prospecting, Vol 25, pp 280-291.

F

Bogoslovsky, V. A., and Ogilvy, A. A. 1977. Geophysical Methods for the Investigation of Landslides: Geophysics, Vol 42, No. 3, pp 562-571.

F

Bogoslovsky, V. A., Kuzmina, E. N., Ogilvy, A. A., and Strakhova, N. A. 1979. Geophysical Methods for Controlling the Seepage Regime in Earth Dams: International Association Eng. Geol. Bull., No. 20, pp 249-251.

DS,F

Broughton Edge, A. B., and Laby, T. H. 1931. The Principles and Practice of Geophysical Prospecting: Cambridge University Press, p 372.

M

Butler, D. K., Gangi, A. F, Wahl, R. E., Yule, D. E., and Barnes, D. E. 1982. "Analytical and Data Processing Techniques for Interpretation of Geophysical Survey Data with Special Application to Cavity Detection," Miscellaneous Paper GL-82-16, US Army Engineer Waterways Experiment Station, Vicksburg, MS.

O

Chadwick, D. G., and Jensen, L. 1971. The Detection of Magnetic Fields Caused by Groundwater and the Correlation of Such Fields with Dowsing: Report PRWG78-1, Utah Water Research Laboratory, College of Engineering, Utah State University, Logan, p 57.

F,M

Cooper, S. S., Koester, J. P., and Franklin, A. G. 1983. Geophysical Investigation at Gathright Dam: US Army Corps of Engineers Miscellaneous Paper GL-82-2.

DS,F

Corwin, R. F. 1973. Offshore Application of Self-Potential Prospecting: Ph.D. Thesis, University of California, Berkeley, p 303.

B,E,M

Corwin, R. F., and Morrison, H. F. 1977. Self-Potential Variations Preceding Earthquakes in Central California: Geophysical Research Letters, Vol 4, No. 4, pp 171-174.

E

Corwin, R. F., and Conti, U. 1973. A Rugged Silver-Silver Chloride Electrode for Field Use: Rev. Sci. Instrum., Vol 44, No. 6, pp 708-711.

E

Corwin, R. F. 1976. Offshore Use of the Self-Potential Method: Geophysical Prospecting, Vol 24, No. 1, pp 79-90.

M

Corwin, R. F., and Hoover, D. B. 1979. The Self-Potential Method in Geothermal Exploration: Geophysics, Vol 44, No. 2, pp 226-245.

B,G,M,T

Corwin, R. F., de Moully, G. T., and Morrison, H. F. 1981. Interpretation of Self-Potential Survey Results from the East Mesa Geothermal Field: Journal of Geophysical Research, Vol 86, No. B3, pp 1841-1848.

G,M

Davenport, G. C., Hadley, L. M., and Randall, J. A. 1983. The Use of Seismic Refraction and Self-Potential Surveys to Evaluate Existing Embankments: Paper presented at Rocky Mt. Regional AIME Mtng., Vail, CO.

DS,F

Denbigh, K. G. 1951. The Thermodynamics of the Steady State: Wiley, New York, p 103.

M,T

De Moully, G. T., and Corwin, R. F. 1980. Self-Potential Survey Results from the Beowawe KGRA, Nevada: Trans. Geothermal Resources Council, Vol 4, pp 33-36.

G,M

Department of the Army 1979. Geophysical Exploration, Engineer Manual EM 1110-1-1802, Office of the Chief of Engineers, Washington, D.C.

O

de Witte, L. 1948. A New Method of Interpretation of Self-Potential Field Data: Geophysics, Vol 13, No. 4, pp 600-608.

M

Dobson, J. V., Firman, R. E., and Thrisk, H. R. 1971. The Behavior of Cells Using Silver/Silver Chloride and Skin-Calomel Electrodes at Temperatures from 25° C to 200° C and 1 bar to 2 kbar Pressure: Electrochemica Acta, Vol 16, No. 6, pp 793-809.

E

Erchul, R. A. 1986. The Evaluation of Spontaneous Potential in the Detection of Sinkhole Drainage Patterns: Final Report, Project DACW-39-86-K-0006, US Army Engineer Waterways Experiment Station, Vicksburg, MS.

F

_____. 1988. Geotechnical Applications of the Self-Potential (SP) Method, Report 1, the Use of Self-Potential in the Detection of Subsurface Flow Patterns in and Around Sinkholes: Technical Report REMR-GT-6, US Army Engineer Waterways Experiment Station, Vicksburg, MS.

F

Erchul, R. A., and Slifer, D. W. 1989. Geotechnical Applications of the Self Potential (SP) Method, Report 2, the Use of Self Potential to Detect Ground Water Flow in Karst: Technical Report REMR-GT, (in review), US Army Engineer Waterways Experiment Station, Vicksburg, MS.

F

Ernstson, K., and Scherer, H. U. 1986. Self-Potential Variations with Time and Their Relation to Hydrogeologic and Meteorological Parameters: Geophysics, Vol 51, No. 10, pp 1967-1977.

E,F

Ewing, S. 1939. The Copper-Copper Sulfate Half-Cell for Measuring Potentials in the Earth: Tech. Section, American Gas Association Distribution Conferences.

E

Faraday, M. 1932. Terrestrial Magnetoelectric Induction: Philos. Trans. Royal Soc. of London, Vol 122, pp 163-176.

E

Fitterman, D. V. 1976. Calculation of Self-Potential Anomalies Generated by Eh Potential Gradients: US Geology Survey Open-File Report 76-98.

M

_____. 1978. Electrokinetic and Magnetic Anomalies Associated with Dilatant Regions in a Layered Earth: Journal Geophyics Research, Vol 83, No. B12, pp 5923-5928.

M

_____. 1979a. Calculations of Self-Potential Anomalies Near Vertical Contacts: Geophysics, Vol 44, No. 2, pp 195-205.

M

_____. 1979b. Relationship of the Self-Potential Green's Function to Solutions of Controlled-Source Directed-Current Potential Problems (Short Note): Geophysics, Vol 44, No. 11, pp 1879-1881.

M

_____. 1979c. Theory of Electrokinetic-Magnetic Anomalies in a Faulted Half-Space: Journal Geophys. Research, Vol 85, No. B11, pp 6031-6040.

M

_____. 1982a. Computer Program SPDIKE for Calculation of Self-Potential Anomalies Near Vertical Dikes: US Geology Survey Open-File Report 82-470.

M

_____. 1982b. Self-Potential Measurements and Interpretation at Riviere Langevin and Cirque de Salazie, Ile de la Reunion: US Geological Survey Open-File Report 82-580.

F,G,M

Fitterman, D. V., and Corwin, R. F. 1982. Inversion of Self-Potential Data from the Cerro Prieto Geothermal Field, Mexico: Geophysics, Vol 47, No. 6, pp 938-945.

G,M

Fitterman, D. V. 1983a. Modeling of Self-Potential Anomalies Near Vertical Dikes: Geophysical, Vol 48, No. 2, pp 171-180.

M

Fitterman, D. V. 1983b. Self-Potential Surveys Near Several Denver Water Department Dams: US Geological Survey Open-File Report 83-302.

DS,F

_____. 1984. Thermoelectrical Self-Potential Anomalies and Their Relationship to the Solid Angle Subtended by the Source Region: Geophysics, Vol 49, No. 2, pp 165-170.

F,G,M

Fox, R. W. 1830. On the Electro-Magnetic Properties of Metalliferous Veins in the Mines of Cornwall: Philos. Trans. Royal Soc. of London, Part 2, pp 399-414.

E

Frohlick, R. K. 1971. The Influence of Industrial Stray Currents on the Measurement of Earth Potentials and Their Elimination: Geophysical Prospecting, Vol 19, pp 118-132.

E

Gex, P. 1980. Phenomenes d'electrofiltration lies a quelques sites de barrages (in French) [Electrofiltration Phenomena Associated with Several Dam Sites]: Bull. Soc. Vaud Sc. Nat. No. 357, Vol 75, pp 39-50.

DS,F

Gish, O. H. 1923. General Description of the Earth-Currents Measuring System at the Watheroo Magnetic Observatory: Terrestrial Magnetism Atmos. Electricity, Vol 28, pp 89-108.

E,TM

_____. 1924. Natural Electric Currents in the Earth's Crust: Carnegie Institute Washington Year Book, No. 23, pp 178-179.

E,TM

_____. 1926. Improved Equipment for Measuring Earth-Current Potentials and Earth Resistivity: National Research Council Bulletin, Vol 11, Part 2, No. 56, pp 86-91.

E,TM

_____. 1936a. Electrical Messages from the Earth: Their Reception and Interpretation: Washington Acad. Sci. Jour., Vol 26, pp 267-289.

E,TM

_____. 1936b. The Natural Electric Currents in the Earth: Sci. Monthly, Vol 43, pp 47-57.

E,TM

Gorelik, A. M., and Nesterenko, I. P. 1956. Electrofiltration Potential Method in the Determination of the Radius of the Depression Hollow During a Pumping Test from a Borehole [in Russian]: Izv. Ahad. Nauk SSSR, Ser. Geofiz. No. 11, pp 1361-1363.

F

Green, E. 1963. Streaming Potential Measurements: Unpublished Report, MIT Project DSR 9017, Report 9017-2, Geophysical Laboratory Mass. Inst. Technol.

L

Haase, R., and Schonert, H. 1960. Untersuchungen an thermoketten, IV.messungen: Zeitschr. fur Phys. Chemie Neue Folge, Vol 25, No. 34, pp 193-204 (in German).

E

Haines, B. M. 1978. The Detection of Water Leakage from Dams Using Streaming Potentials: SPWLA 19th Ann. Logging Symposium, El Paso, TX.

DS,F

Harding, R. S., Jr. 1981. A Study of the Streaming Potential Mechanism in the Earth: Unpublished Report, Eng. Geoscience, University of California, Berkeley.

M,T

Heiland, C. A. 1940. Geophysical Exploration: New York, Prentice-Hall, p 1013.

M

Hoogervorst, G. H. T. C. 1975. Fundamental Noise Affecting Signal-to-Noise Ratio of Resistivity Surveys: Geophysical Prospecting, Vol 23, pp 380-390.

E

Hulse, S. E. 1978. An Investigation into the Causes of Steady State Electrical Potential Differences Occurring Naturally on the Surface of the Earth: MS Thesis, Department of Geosciences, University of Arizona, p 220.

B,E,M

Hurd, C. O. 1944. Topography's Effect in the Equipotential Line Method: The Mines Magazine, CO School of Mines, pp 15-18, 39, 41.

L

Iakubovskii, Iu. V., y Liajov, L. L. 1980. Exploration electrica, version espanola de la 3ra edition rusa (in Spanish): Editorial Reverte, S. A.-Barcelona, Espana, p 421.

F,M

Ishido, T., and Mizutani, H. 1981. Experimental and Theoretical Basis of Electrokinetic Phenomena in Rock-Water Systems and its Applications to Geophysics: Jour. Geophys. Research, Vol 86, No. B3, pp 1763-1775.

L,M

Ishido, T. 1981. Streaming Potential Associated with Hydrothermal Convection in the Crust: A Possible Mechanism of Self-Potential Anomalies in Geothermal Areas (in Japanese): Journal of the Geothermal Research Society of Japan, Vol 3, No. 2, pp 87-100.

F,G,M

Ishido, T., Mizutani, H., and Baba K. 1982. Streaming Potential Observations Using Geothermal Wells and in Situ Electrokinetic Coupling Coefficients Under High Temperature.

F,G,M

Ives, D. J. G., and Janz, G. J. 1961. Reference Electrodes: Academic Press, New York, p 651.

E

Johnson, G. R. 1983. Rock Property Measurements and Analysis of Selected Igneous, Sedimentary, and Metamorphic Rocks from World-Wide Localities: US Geological Survey Open-File Report 83-736.

L

Kermabon, A. J. 1956. A Study of Some Electrokinetic Properties of Rocks: MS Thesis, Mass. Inst. of Technol., Cambridge.

L

Kilty, K. T. 1984. On the Origin and Interpretation of Self-Potential Anomalies: Geophysical Prospecting, Vol 32, pp 51-52.

M

Koester, J. P., Butler, D. K., and Cooper, S. S. 1982. Geophysical Investigation of Hazardous Waste Management Lagoons at Radford Army Ammunition Plant: Final Report to Huntsville Division, US Army Corps of Engineers.

F

Koester, J. P., Butler, D. K., Cooper, S. S., and Llopis, J. L. 1984. Geophysical Investigations in Support of Clearwater Dam Comprehensive Seepage Analysis: US Army Engineer Waterways Experiment Station, Miscellaneous Paper GL-84-3.

DS,F

Korotayev, A. M. 1979. Electrokinetic Fields of Submarine Sources: Izvestia, Earth Physics, Vol 15, No. 8, pp 592-594.

M

Laxman, G., Sundararajan, N., and Mohan, N. L. 1986. Interpretation of S.P. Anomalies Due to Sheet Like Structures--a Derivative Technique: Submitted to Geophysics.

M

Llopis, J. L. 1987. Geophysical Investigation in Support of Beaver Dam Comprehensive Seepage Investigation: MS Thesis, Department of Civil Engineering, MS State University, Mississippi State, MS, p 138.

DS,F

Llopis, J. L., Butler, D. K. 1988. Geophysical Investigation in Support of Beaver Dam Comprehensive Seepage Investigation: Technical Report GL-88-6, US Army Engineer Waterways Experiment Station, Vicksburg, MS.

DS,F,O

MacInnes, D. A. 1961. The Principles of Electrochemistry: Dover, New York.

E

Madden, T. R. 1961. Electrical Measurements as Stress-Strain Monitors: Unpublished Report, Department of Earth and Planetary Scis., Mass. Inst. of Technol., Cambridge.

L,M,T

Madden, T. R. 1962. Effects of Porosity and Fluids on Physical Properties of Rocks, Electrical Properties of Porous Media: Unpublished Report, Department of Earth and Planetary Science, Mass. Inst. of Technol., Cambridge, p 75.

L,M,T

Matteucci, M. C. 1867. Sur les courants electriques de la terre (On the Electric Currents of the Earth): Annales Chimie et Physique, ser. 4, Vol 10, pp 148-159.

E,TM

Mauchly, S. J. 1918. A Study of Pressure and Temperature Effects in Earth-Current Measurements: Terrestrial Magnetism Atmos. Electricity, Vol 23, pp 73-91.

E,T,M

Marshall, D. J., and Madden, T. R. 1959. Induced Polorization: A Study of its Causes: Geophysics, Vol 24, pp 790-816.

T,E

Meiser, P. 1962. A Method for Quantitative Interpretation of Self-Potential Measurements: Geophysical Prospecting, Vol 10, No. 2, pp 203-218.

M

Merkel, R. H. 1971. Resistivity Analysis for Plane-Layer Half-Space Models with Buried Current Sources: Geophysical Prospecting, Vol 19, pp 626-639.

M

Meyer, W. H. 1972. Laboratory Streaming Potential Measurements: Unpublished Report, Civil Engineering, University of California, Berkeley.

L

Mitchell, J. K. 1976. Fundamentals of Soil Behavior: Wiley, New York.

M

Morrison, H. F., Corwin, R. F., and Chang, M. 1977. High-Accuracy Determination of Temporal Variations of Crustal Resistivity, in Geophysical Monograph 20, the Earth's Crust: American Geophys. Union, Washington, DC, pp 593-614.

Morrison, H. F., Corwin, R. F., de Moully, G., and Durand, D. 1978. Interpretation of Self-Potential Data from Geothermal Areas: Semi-Annual Technical Progress Report, October 31, USGS Contract No. 14-08-0001-10545, University of California, Berkeley.

Morrison, H. F., Corwin, R. F., Harding, R., and de Moully, G. 1979a. Interpretation of Self-Potential Data from Geothermal Areas: Semi-Annual Technical Progress Report, April 30, USGS Contract No. 14-08-0001-16546, University of California, Berkeley.

_____. 1979b. Interpretation of Self-Potential Data from Geothermal Areas: Semi-Annual Technical Progress Report, September 30, USGS Contract No. 14-08-0001-16546, University of California, Berkeley.

Muoi, T., and Quynh, Vo T. 1988. A Contribution to the Self-Potential Method: Pageoph, in press.

M

Murty, B. V. Satyanarayana, and Haricharan, P. 1985. Nomogram for the Complete Interpretation of Spontaneous Polarization Profiles Over Sheet-Like and Cylindrical Two-Dimensional Sources: Geophysics, Vol 50, No. 7, pp 1127-1135.

M

Nayak, P. N. 1981. Electromechanical Potential in Surveys for Sulphides: Geoexploration, Vol 18, pp 311-320.

F

Nelson, J. S., and Black, W. E. 1977. Streaming Potential (SP) Techniques Applied to Seepage Investigation, Colstrip Dam, Montana: Paper presented at Annual Mtng., Association of Eng. Geologists, Seattle, WA.

DS,F

Nourbehecht, B., and Madden, T. R. 1970. Irreversible Thermodynamics in Inhomogeneous Media and Geoelectric Application: Unpublished Report, Mass. Inst. Technol., Cambridge, p 54.

F,M

Nourbehecht, B. 1963. Irreversible Thermodynamic Effects in Inhomogeneous Media and Their Applications in Certain Geoelectric Problems: Ph.D. Thesis, Mass. Inst. Technol., Cambridge, p 122.

F,M

Ogilvy, A. A., Ayed, M. A., and Bogoslovsky, V. A. 1969. Geophysical Studies of Water Leakages from Reservoirs: Geophysical Prospecting, Vol 17, No. 1, pp 36-62.

DS,F,L

Ogilvy, A. A., and Bogoslovsky, V. A. 1979. The possibilities of Geophysical Methods Applied for Investigating the Impact of Man on the Geological Medium: Geophysical Prospecting, Vol 27, pp 775-789.

F

Onsager, L. 1931. Reciprocal Relations in Irreversible Processes I: Phys. Rev., Vol 37, pp 405-426.

M

Paul, M. K. 1965. Direct Interpretation of Self-Potential Anomalies Caused by Inclined Sheets of Infinite Horizontal Extensions: Geophysics, Vol 30, No. 3, pp 418-423.

M

Paul, M. K., Datta, S., and Banerjee, B. 1965. Interpretation of Self-Potential Anomalies Due to Localized Causative Bodies: Pageoph., Vol 61, No. 2, pp 95-100.

M

Paul, M. K., and Banerjee, B. 1970. Electrical Potentials Due to a Point Source Upon Models of Continuously Varying Conductivity: Pageoph., Vol 80, No. 3, pp 218-237.

M

Petiau, G., and Dupis, A. 1980. Noise, Temperature Coefficient, and Long-Time Stability of Electrodes for Telluric Observations: Geophysical Prospecting, Vol 28, pp 792-804.

E

Petrowsky, A. 1928. The Problem of a Hidden Polarized Sphere: Philos. Mag., Vol 5, No. 28, pp 334-353; Vol 5, No. 31, pp 914-933.

M

Poldini, E. 1938. Geophysical Exploration by Spontaneous Polarization Methods: The Mining Magazine, Vol 59, pp 278-282; 347-352.

L,M

_____. 1939. Geophysical Exploration by Spontaneous Polarization Methods: The Mining Magazine, Vol 60, pp 22-27; 90-94.

L,M

Pourbaix, M. J. N. 1949. Thermodynamics of Dilute Aqueous Solutions: E. Arnold & Company, London.

M

Prigogine, I. 1955. Thermodynamics of Irreversible Processes: Charles C. Thomas, Springfield, IL.

M

Rajan, N. S., Mohan, N. L., and Narasimha Chary, M. 1986. Comment on "A Note on the Use of a Nomogram for Self-Potential Anomalies" by B. B. Bhattacharya and N. Roy: Geophysical Prospecting, Vol 34, pp 1292-1293.

M

Ram Babu, H. V., and Atchuta Rao, D. 1988. A Rapid Graphical Method for the Interpretation of the Self-Potential Anomaly Over a Two-Dimensional Inclined Sheet of Finite Depth Extent: Submitted to Geophysics.

M

Rao, B. S. R., Marthy, I. V. R., and Reddy, S. J. 1970. Interpretation of Self-Potential Anomalies of Some Geometric Bodies: Pageoph., Vol 78, No. 1, pp 66-77.

M

Rao, D. A., and Babu, H. V. R. 1983. Quantitative Interpretation of Self-Potential Anomalies Due to Two-Dimensional Sheet-Like Bodies: Geophysics, Vol 48, No. 12, pp 1659-1664.

M

Rao, M. B. R. 1953. Self-Potential Anomalies Due to Subsurface Water Flow at Garimenapenta, Madras State, India: Trans. AIME, Mining Engineering, pp 400-403.

F,L,M

Rao, S. V., and Mohan, N. L. 1984. Spectral Interpretation of Self-Potential Anomaly Due to an Inclined Sheet: Current Science, Vol 53, pp 474-477.

Roberts, J. A. R. 1983. Potential Natural (SP) en la busqueda de agua (in Spanish): Unpublished Report, Universidad de Guanajuato (Mexico).

F

Rodriguez, B. D. 1983. A Self-Potential Investigation of a Coal Mine Fire: MS Thesis, CO School of Mines, Golden.

F

Rooney, W. J. 1932. The Significance and Accuracy of Measurements of Earth-Current Potentials: Terrestrial Magnetism Atmos. Electricity, Vol 37, No. 3, pp 363-374.

E,TM

_____. 1937. Earth-Current Variations with Periods Longer than One Day: Terrestrial Magnetism Atmos. Electricity, Vol 42, No. 2, pp 165-172.

E,TM

Roy, A., and Chowdhury, D. K. 1959. Interpretation of Self-Potential Data for Tabular Bodies: Journal of Science and Engineering Research [India], Vol 3, Part 1, pp 35-54.

M

Roy, A. 1963. New Interpretation Techniques for Telluric and Some Direct Current Fields: Geophysics, Vol 28, No. 2, pp 250-261.

M

Sato, M., and Mooney, H. M. 1960. The Electrochemical Mechanism of Sulfide Self-Potentials: Geophysics, Vol 25, No. 1, pp 226-249.

B

Schiavone, D., and Quarto, R. 1984. Self-Potential Prospecting in the Study of Water Movements: Geoexploration, Vol 22, pp 47-58.

F,M

Schriever, W., and Bleil, C. E. 1957. Streaming Potential in Spherical-Grain Sands: Journal of the Electrochemical Society, Vol 104, No. 3, pp 170-176.

L

Scott, B. I. H. 1962. Electricity in Plants: Sci. Am., pp 107-117.

F

Semenov, A. S. 1974. Electrical Prospecting with the Natural Electric Field Method (in Russian): Nedra, Leningrad, p 388.

B,DS,F,M

Sill, W. R., and Johng, D. S. 1979. Self-Potential Survey, Roosevelt Hot Springs, Utah: DOE Report IDO/78-1701.a.2.3, Department of Geology and Geophysics, University of Utah.

F,G,M

Sill, W. R. 1981a. Self Potential Modeling from Primary Flows: DOE/DGE Report No. DOE/ID/12079-42, Department of Geology and Geophysics, University of Utah.

F,G,M

_____. 1981b. Extended Self-Potential Survey, Roosevelt Hot Springs, Utah: Open-File Report, Earth Science Laboratory, University of Utah Research Institute.

F,G,M

Sill, W. R., and Killpack, T. J. 1982. SPXCPL: Two-Dimensional Modeling Program of Self-Potential Effects from Cross-Coupled Fluid and Heat Flow (User's Guide and Documentation for Version 1.0): DOE/DGE Report DOE/ID/12079-60, ESL-74, Earth Science Laboratory, University of Utah Research Institute.

M

Sill, W. R. 1982a. A Model for the Cross Coupling Parameters of Rocks: DOE/DGE Report DOE/ID/12079-69, Department of Geology and Geophysics, University of Utah.

L,M,T

_____. 1982b. Self-Potential Effects Due to Hydrothermal Convection-Velocity Cross Coupling: DOE/DGE Report DOE/ID/12079-68, Department of Geology and Geophysic, University of Utah.

G,M,T

_____. 1982c. Diffusion Coupled (electrochemical) Self-Potential Effects in Geothermal Areas: DOE/DGE Report DOE/ID/12079-73, Department of Geology and Geophysic, University of Utah.

G,M,T

_____. 1983a. Self-Potential Modeling from Primary Flows: Geophysics, Vol 48, No. 1, pp 76-86.

F,G,M

Sill, W. R. 1983b. Interpretation of Self-Potential Measurements During Injection Tests at Raft River, Idaho: Report DOE/ID/12079-103, ESL-120, Earth Science Laboratory University of Utah Research Institute, p 20.

F,G,M

Smith, H. W. 1974. Telluric Current Sensors, in Wolff, E. A., and Mercanti, E. P., Eds.: Geoscience Instrumentation, Wiley, New York, pp 471-483.

E,TM

Stern, W. 1945. Relation Between Spontaneous Polarization Curves and Depth, Size, and Dip of Ore Bodies: Trans. AIME, Vol 164, pp 189-196.

M

Telford, W. M., Geldart, L. P., Sheriff, R. E., and Keys, D. A. 1976. Applied Geophysics: Cambridge University Press, New York.

B,M,O

Tsitsishvili, D. A., and Lashki, A. S. 1955. Electrofiltration Field of Some Phenomena of Hydroelectric Projects in the Georgian SSR: Akad. Nauk, Gruzinskoy, SSR Soobshcheniya, Vol 16, No. 4, pp 269-275.

F,L

Tuman, V. S. 1963. Thermo-telluric Currents Generated by an Underground Explosion and Other Geological Phenomena: Geophysics, Vol 28, No. 1, pp 91-98.

L

US Army Corps of Engineers, Little Rock District. 1987. Beaver Dam, White River, Arkansas, Project Modification for the Rehabilitation Program, Feature Design Memorandum.

DS,F

Van Nostrand, R. G., and Cook, K. L. 1966. Interpretation of Resistivity Data: US Geology Survey Prof. Paper 499, p 310.

B,M

Wilt, M. J., Tsang, C. F., Javandel, I., Lee, S., and Morrison, H. F. 1987. Monitoring of Subsurface Contaminants with Borehole/Surface Resistivity Measurements: Field Results: Unpublished Report, Earth Sciences Division, Lawrence Berkeley Laboratory, Berkeley, CA.

E

Yule, D. E., Llopis, J. L., and Sharp, M. K. 1985. Geophysical Seepage Studies at Center Hill Dam, Tennessee: Miscellaneous Paper GL-85-29, US Army Engineer Waterways Experiment Station, Vicksburg, MS.

DS,F

Yungul, S. 1945. Some Uses of the Spontaneous Polarization Method: Professional Degree Thesis, California Institute Technology, Pasadena, p 70.

M

Yungul, S. 1950. Interpretation of Spontaneous Polarization Anomalies Caused by Spheroidal Orebodies: Geophysics, Vol 15, No. 2, pp 237-246.

M

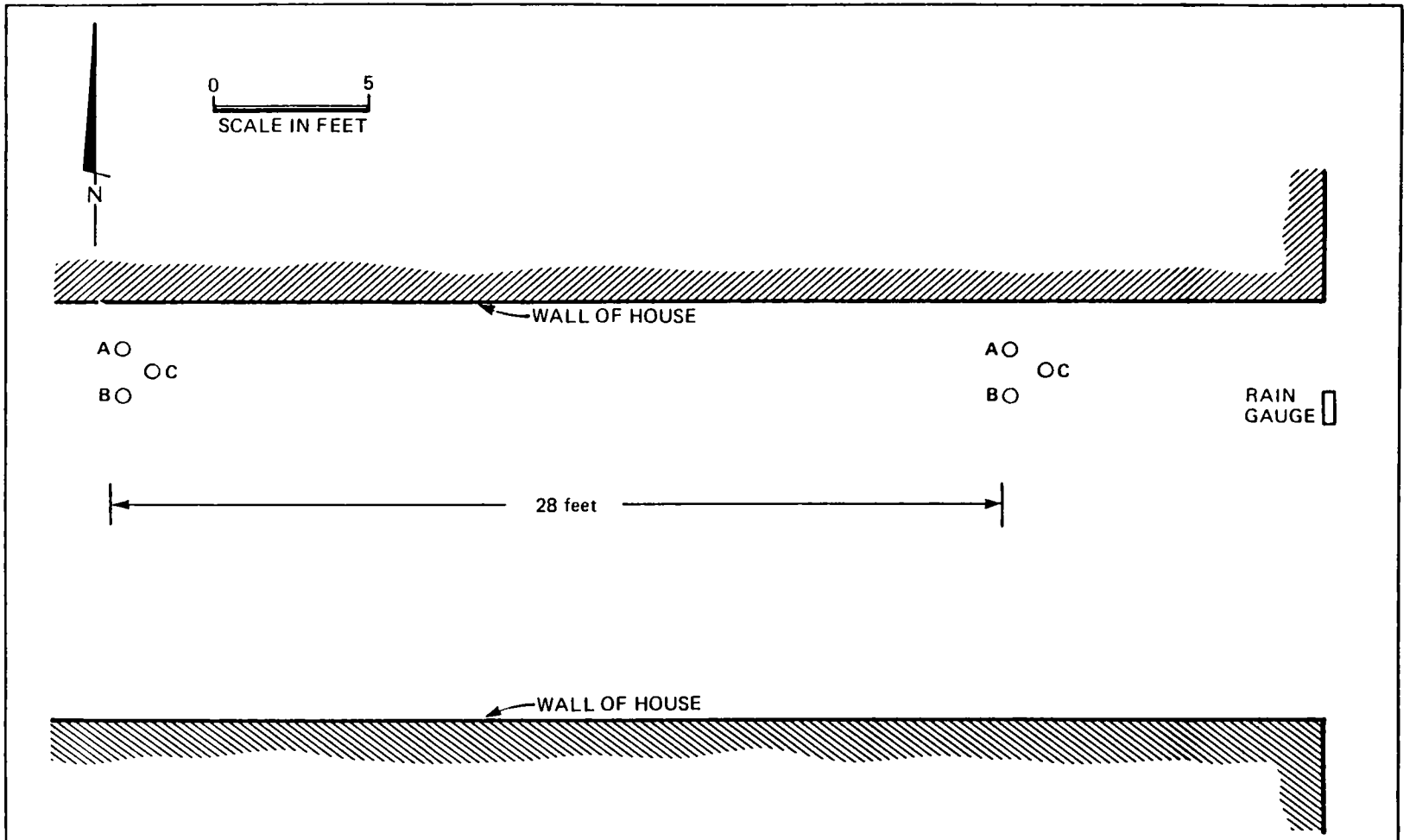

NOTES:

1. Western electrodes are 4 feet lower in elevation than eastern electrodes.
2. Soil type: swelling clay
3. Burial depth: approximately 1 foot
4. The eastern electrodes were connected to the positive terminal and the western electrodes to the negative terminal of the measuring instrument.

EXPLANATION

A – CCS Stakes

B – Copper Sulfate

C – Metallic Lead

Electrode Arrangement

PLATE 1

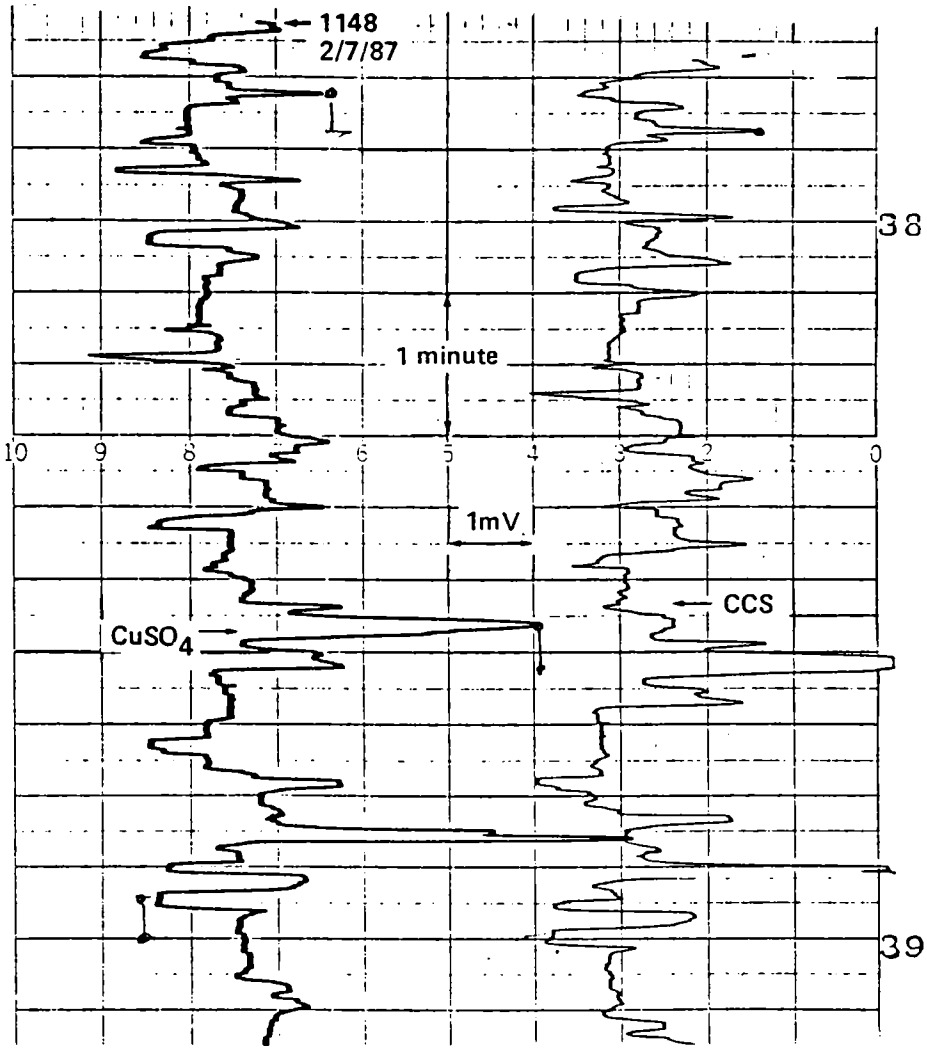

Note: Approximately 15s offset traces due to recording pen offset.

High-Frequency Noise Records

PLATE 2

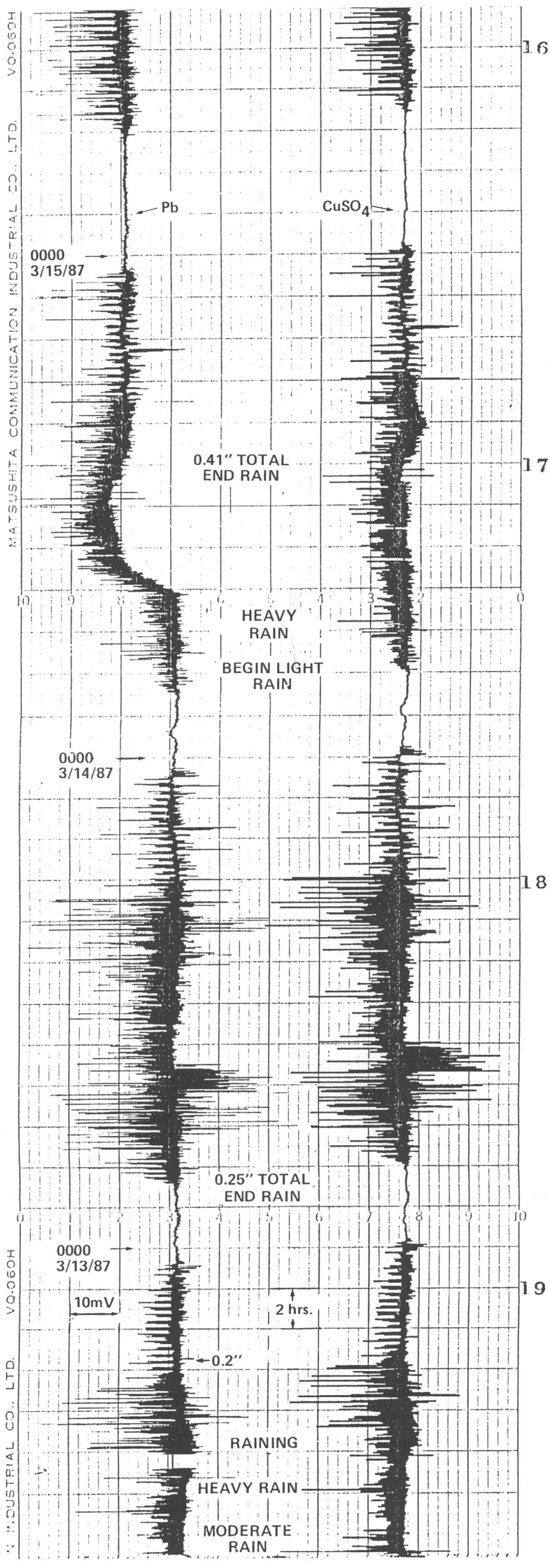

Sample Daily Records for Copper Sulfate and Lead Electrodes

PLATE 3

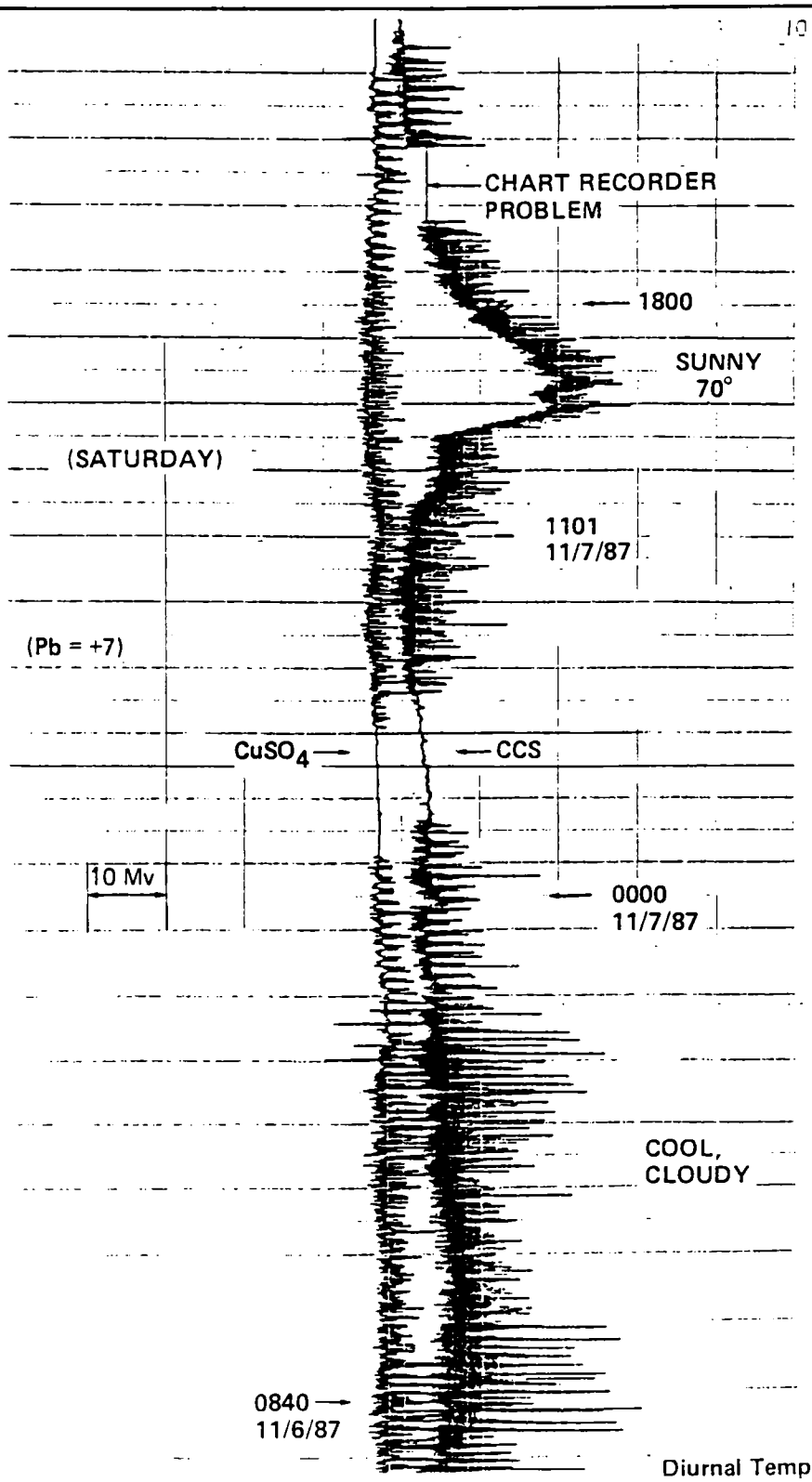

Diurnal Temperature Response

PLATE 4

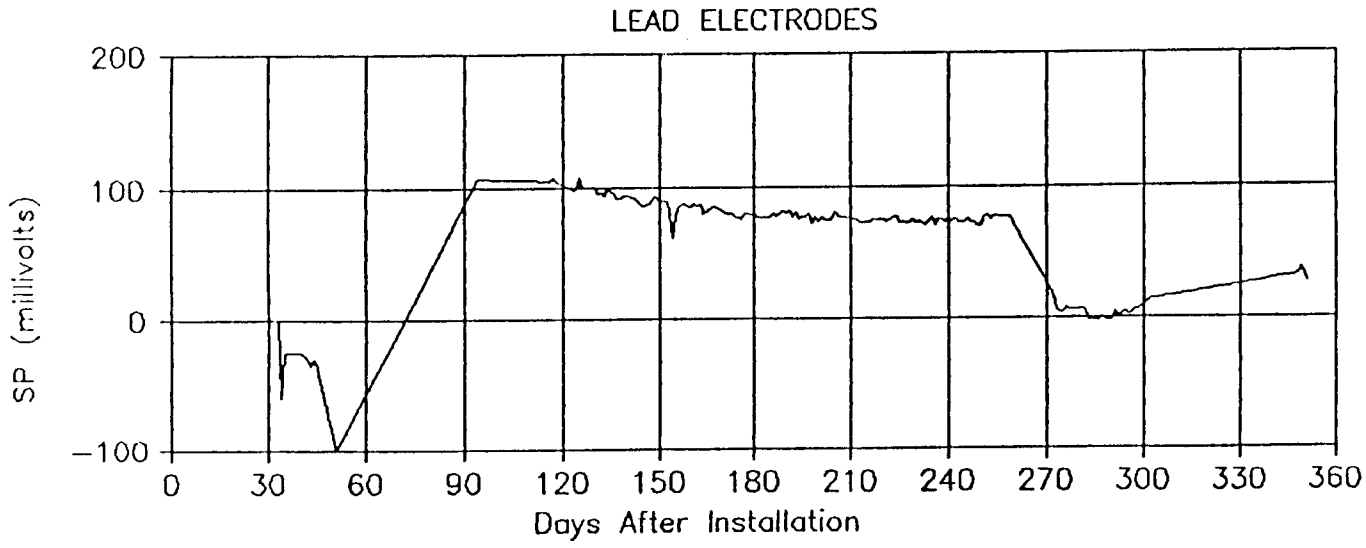

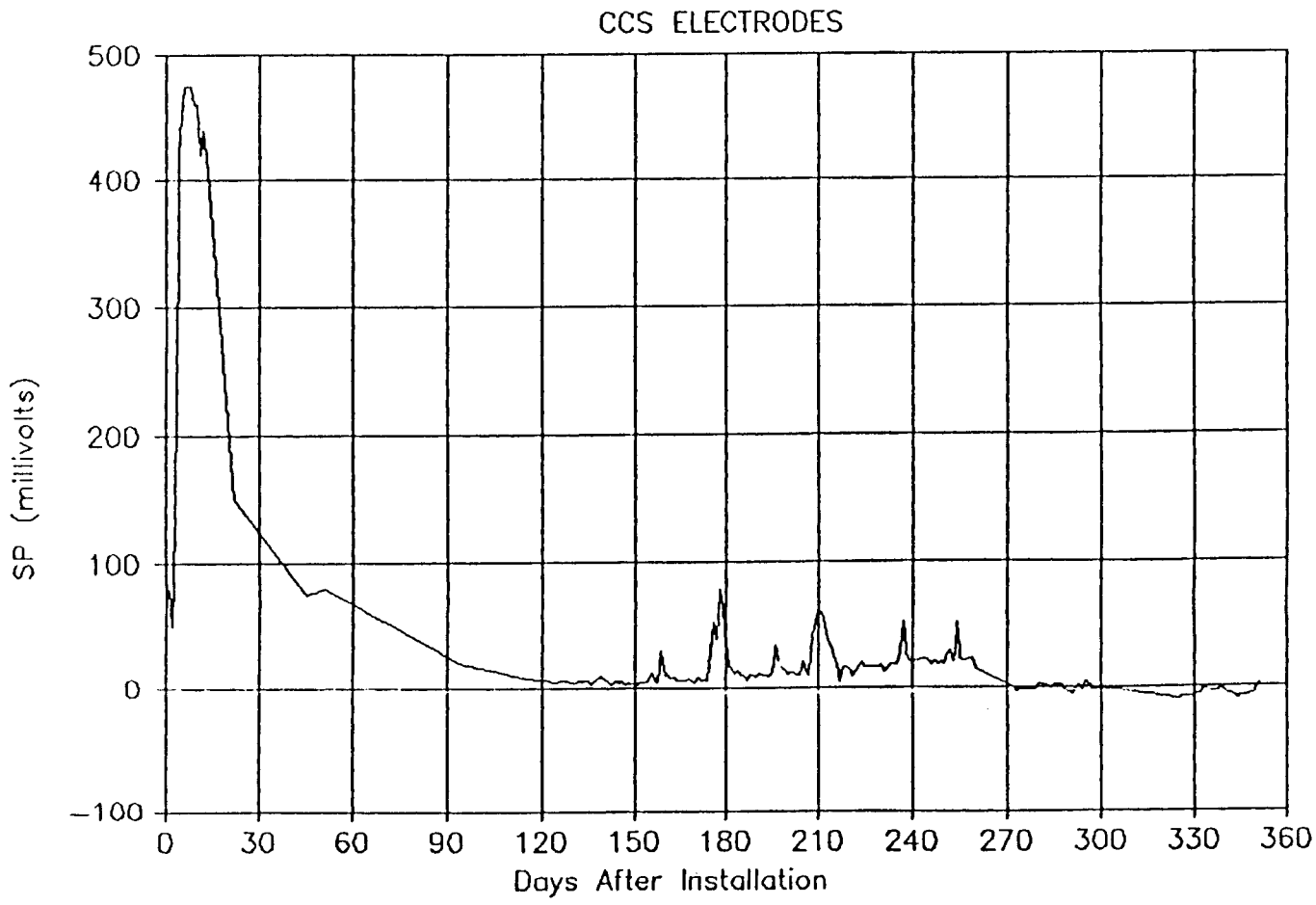

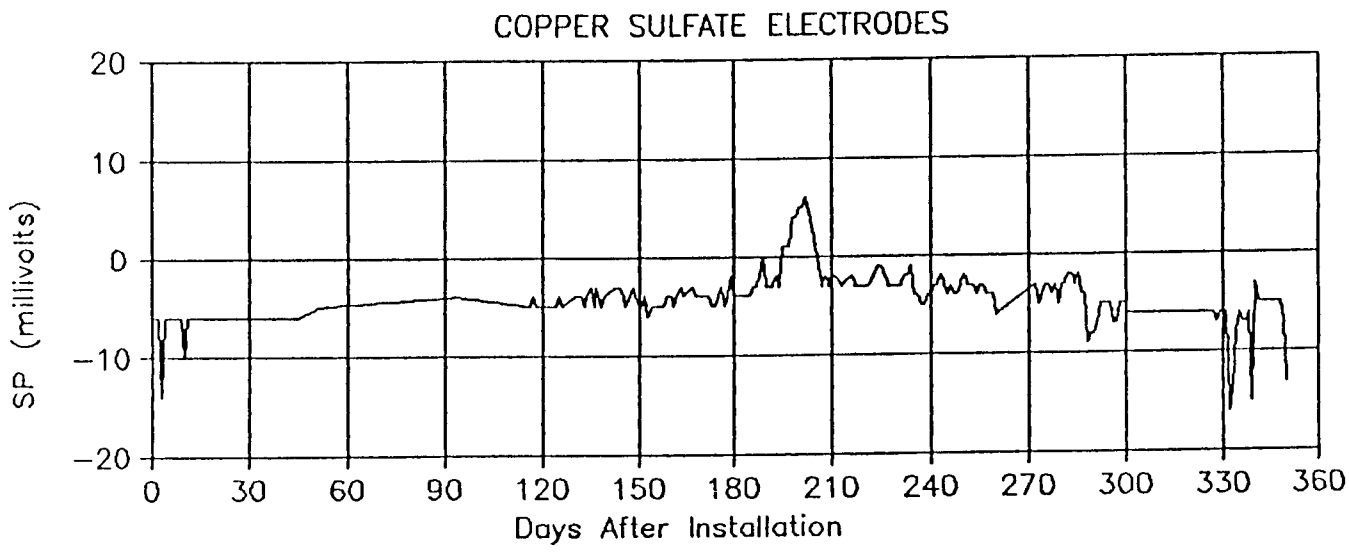

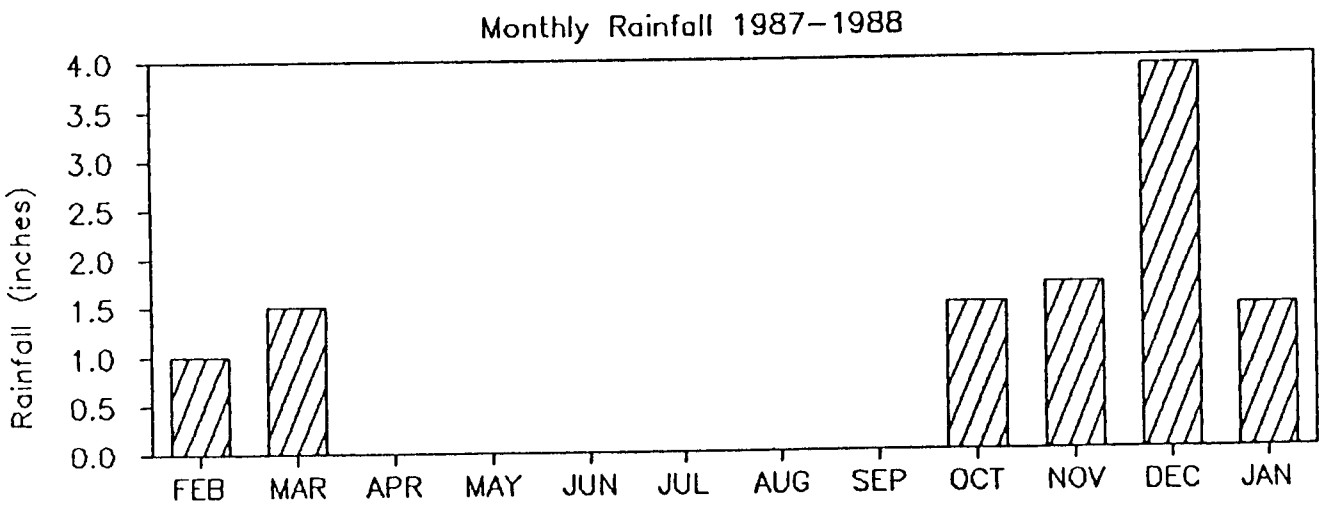

Monthly Monitoring Records

PLATE 5

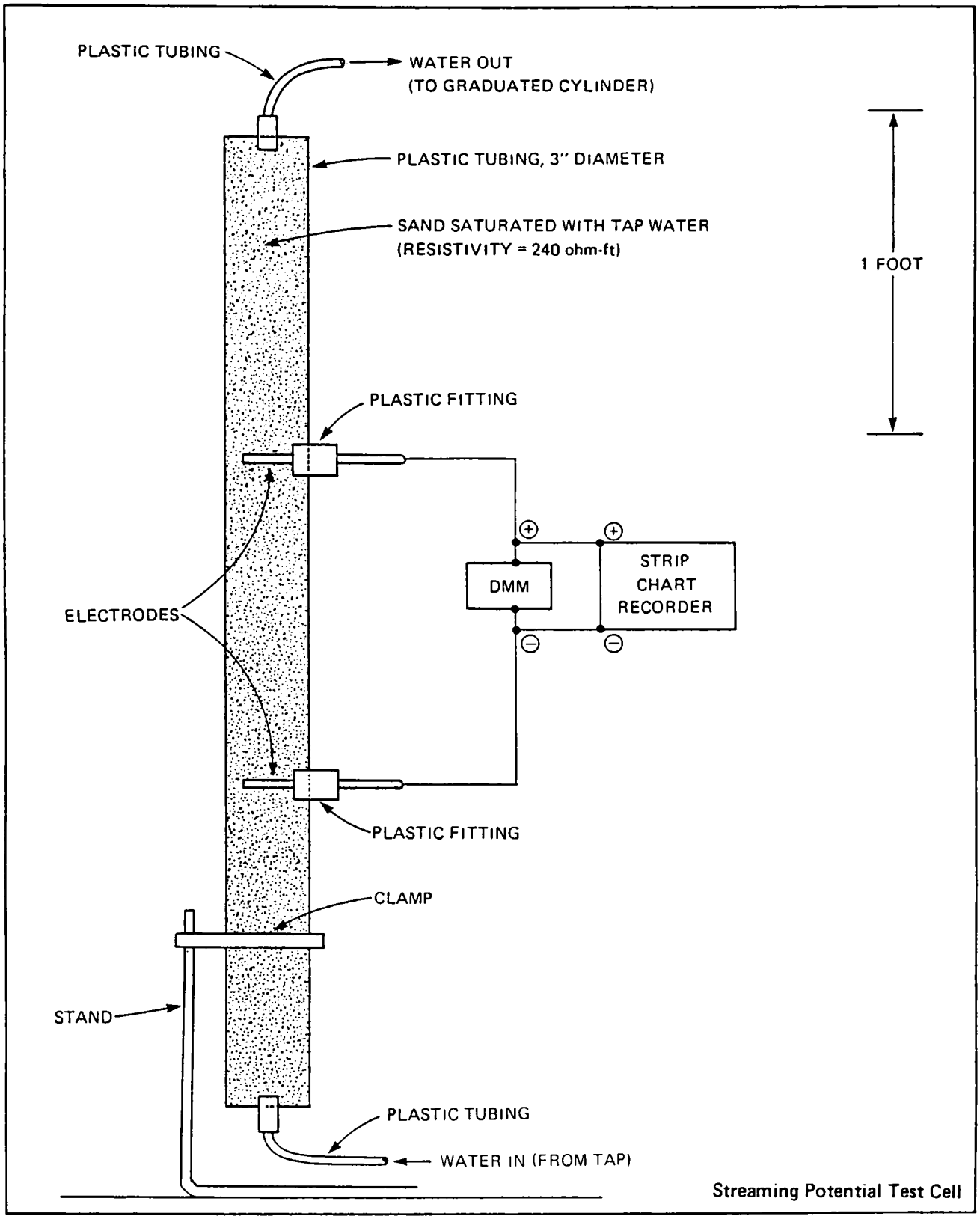

Streaming Potential Test Cell

PLATE 6

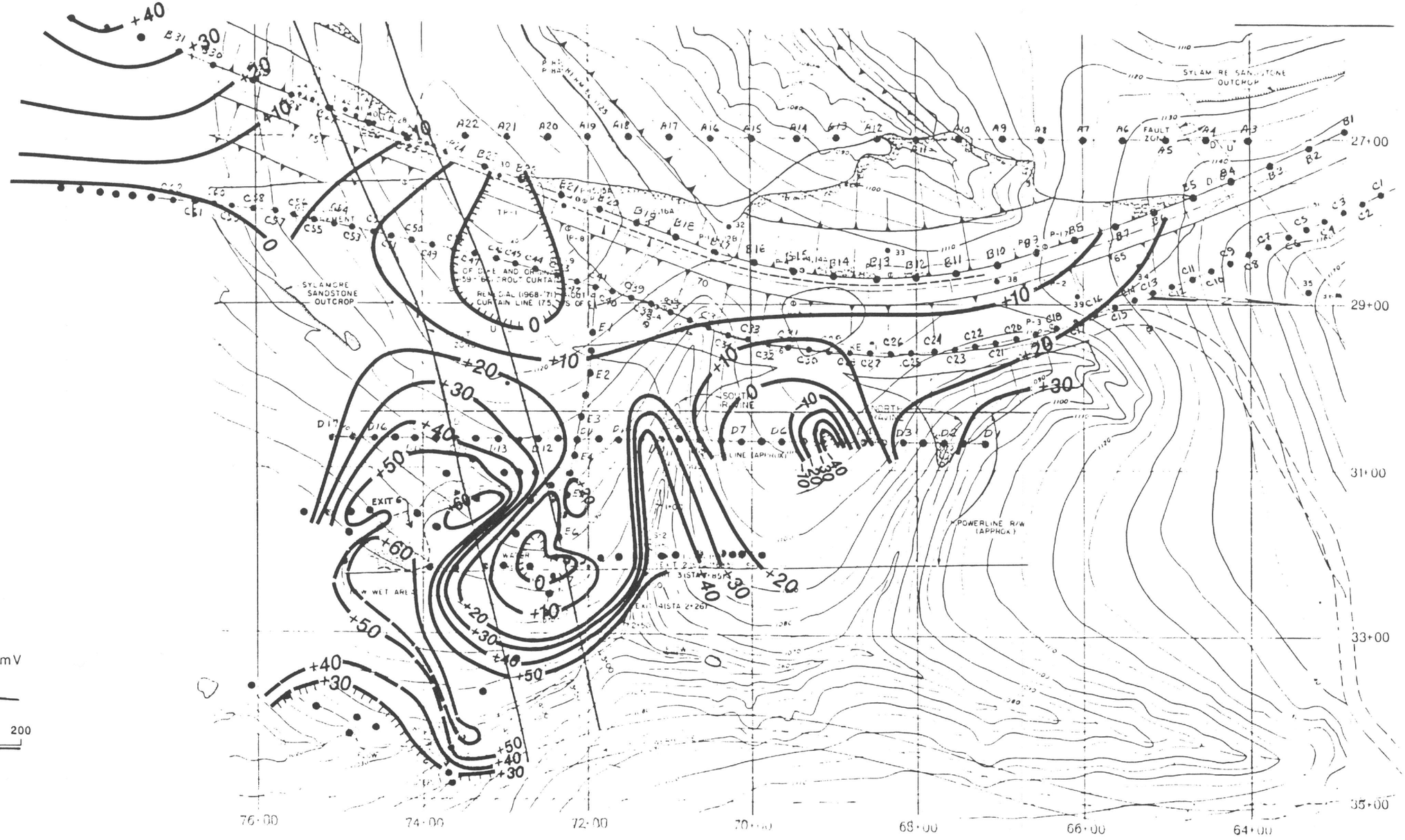

LEGEND

Survey station ●

Contour interval = 10mV

N

0 100 200

SCALE IN FEET

Self-Potential Contours, August 1986

Beaver Dam, Arkansas

PLATE 7

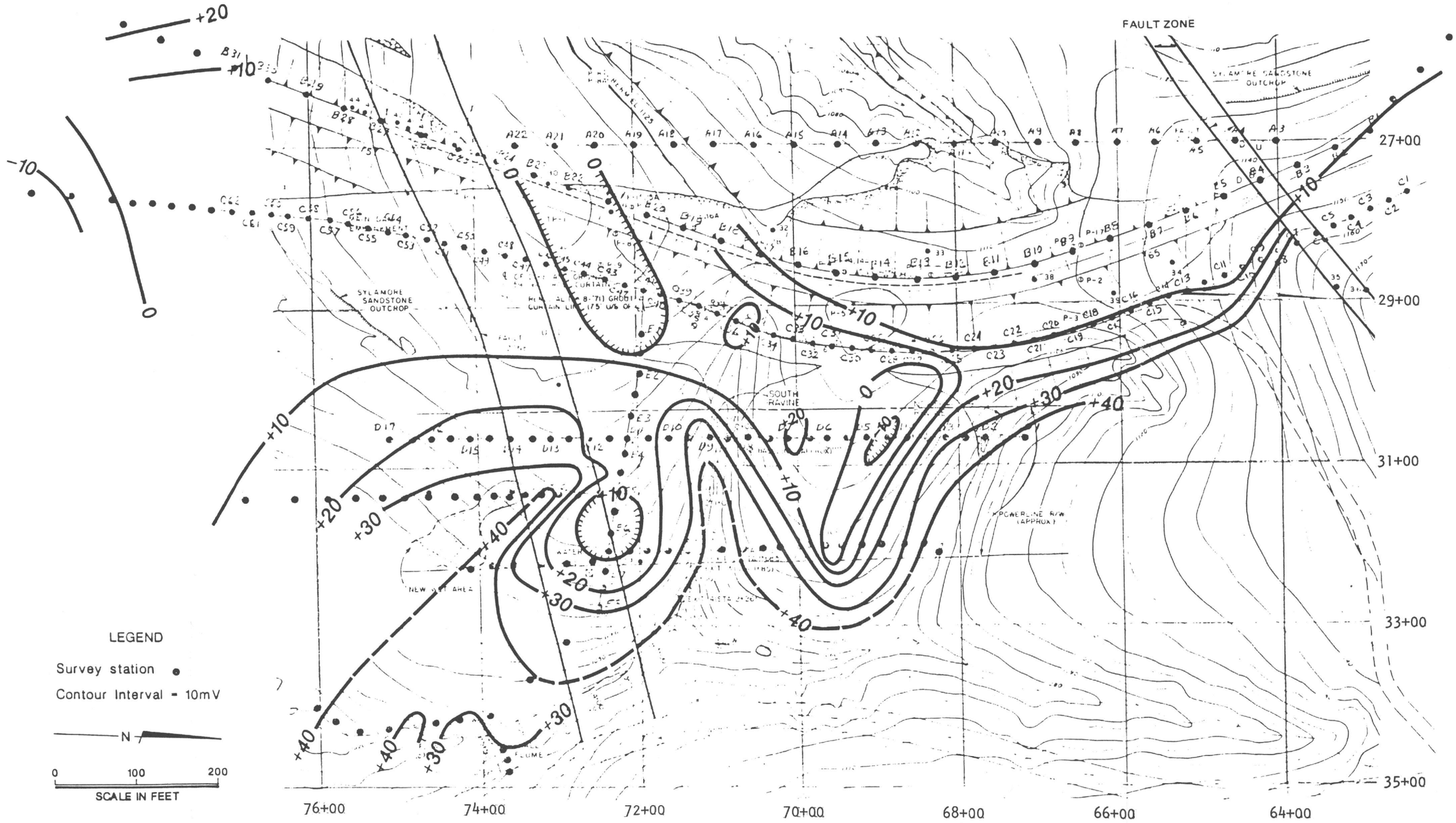

Self-Potential Contours, February 1987
Beaver Dam, Arkansas

PLATE 8

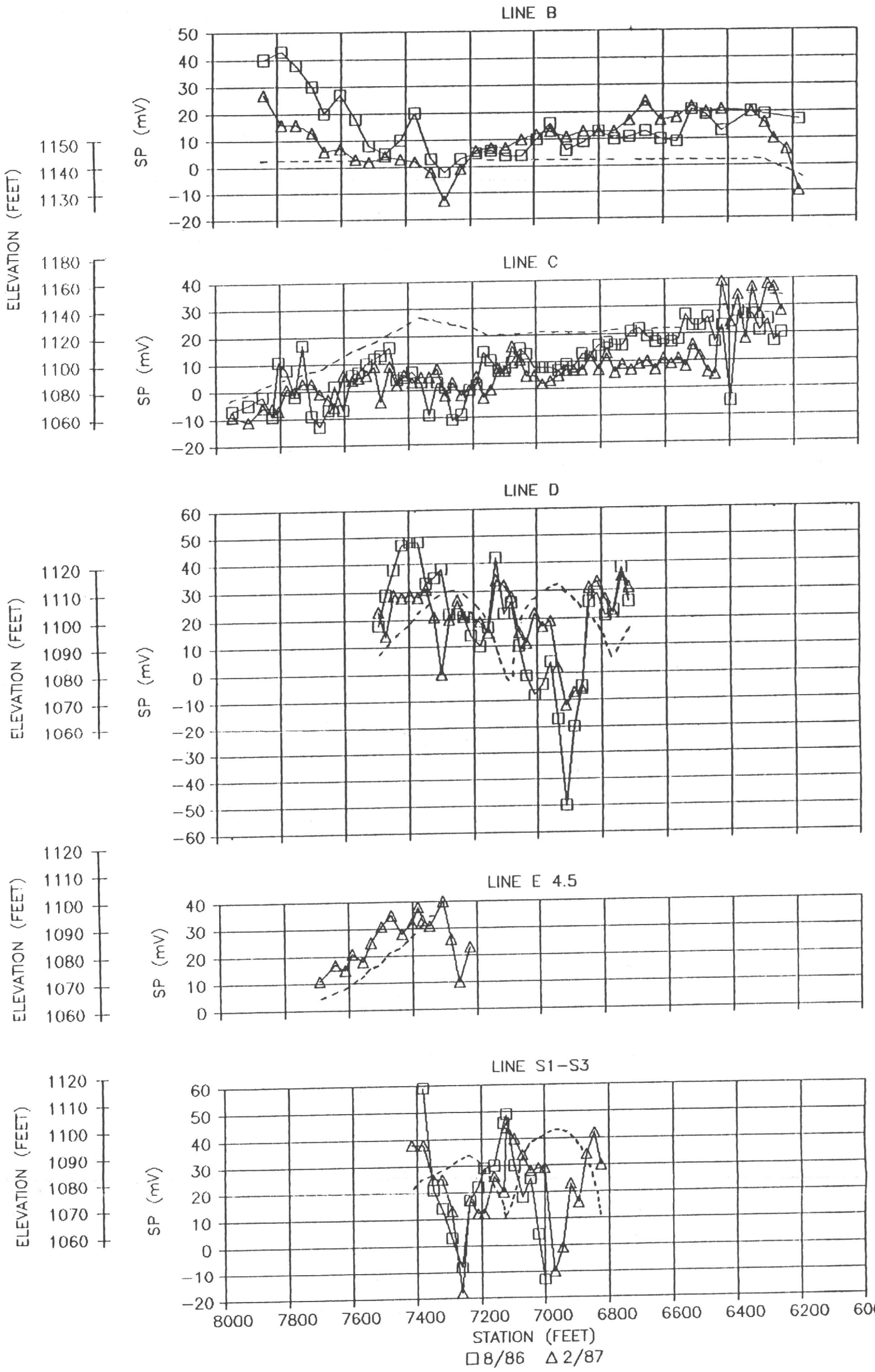

Self-Potential and Topographic Profiles
August 1986 and February 1987
Beaver Dam, Arkansas

PLATE 9

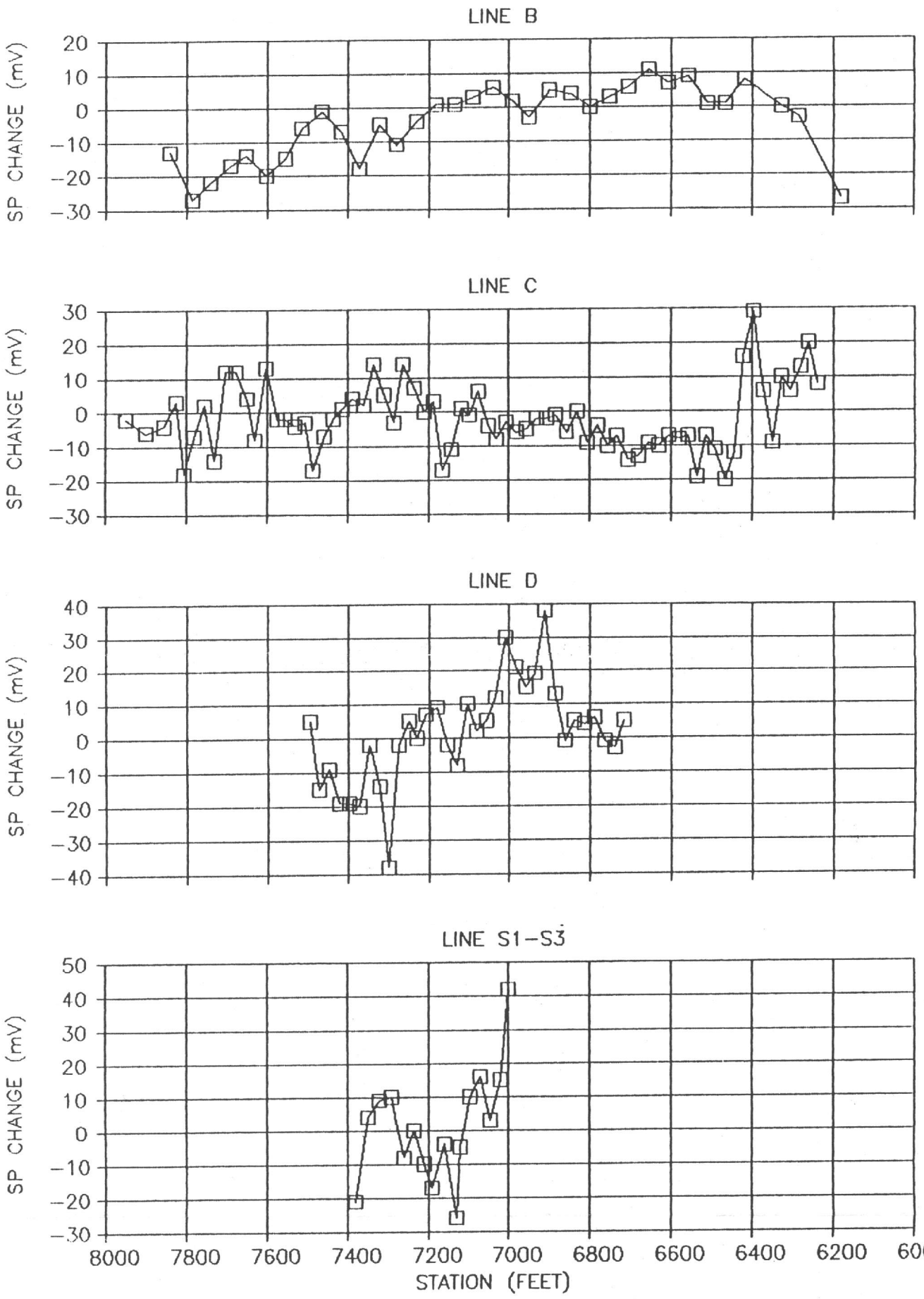

Differences Between Self-Potential Readings, August 1986 and February 1987
Beaver Dam, Arkansas

PLATE 10

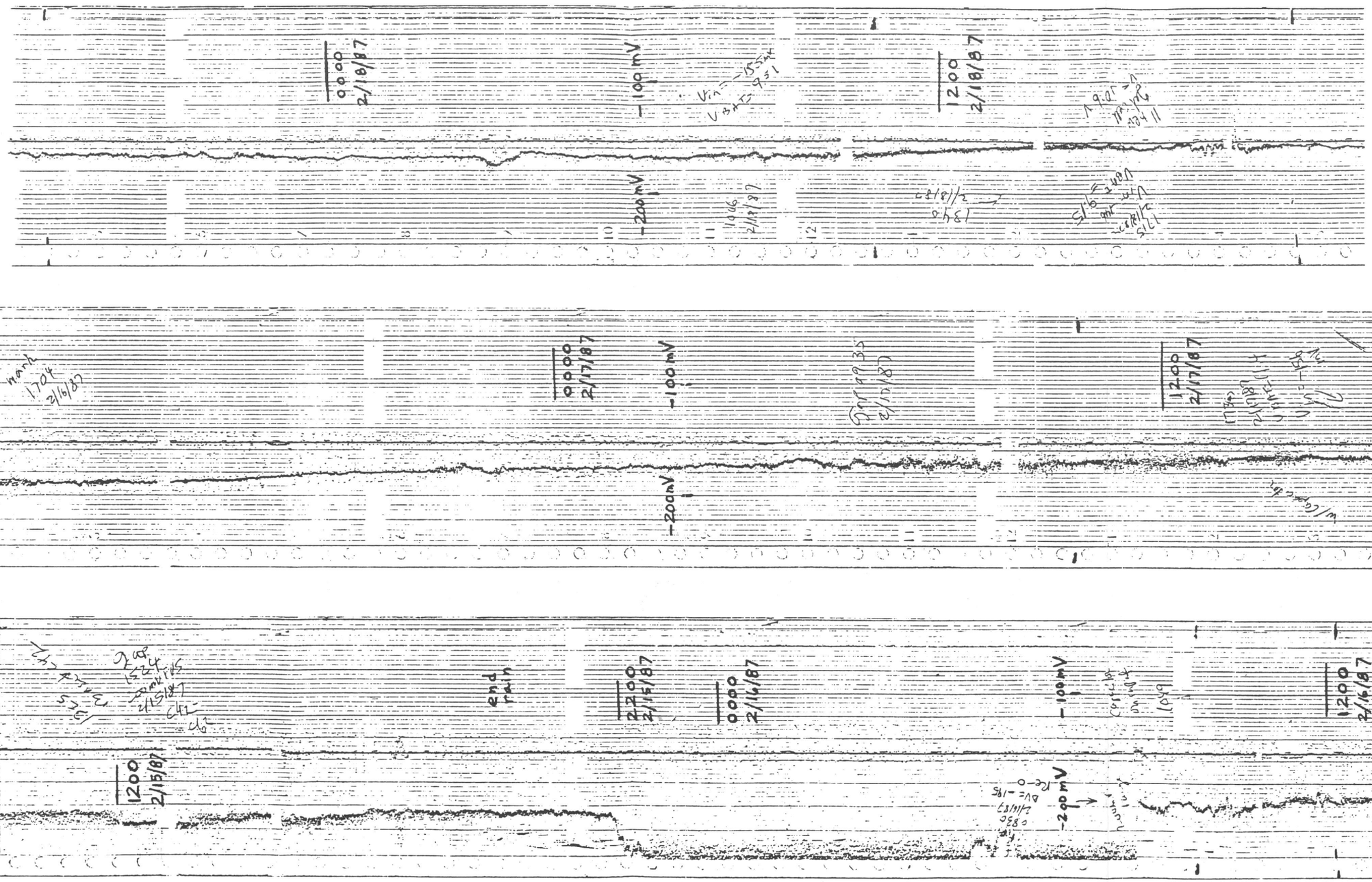

Record of Self-Potential Between Stakes C42 and C62

Beaver Dam, Arkansas

PLATE 11

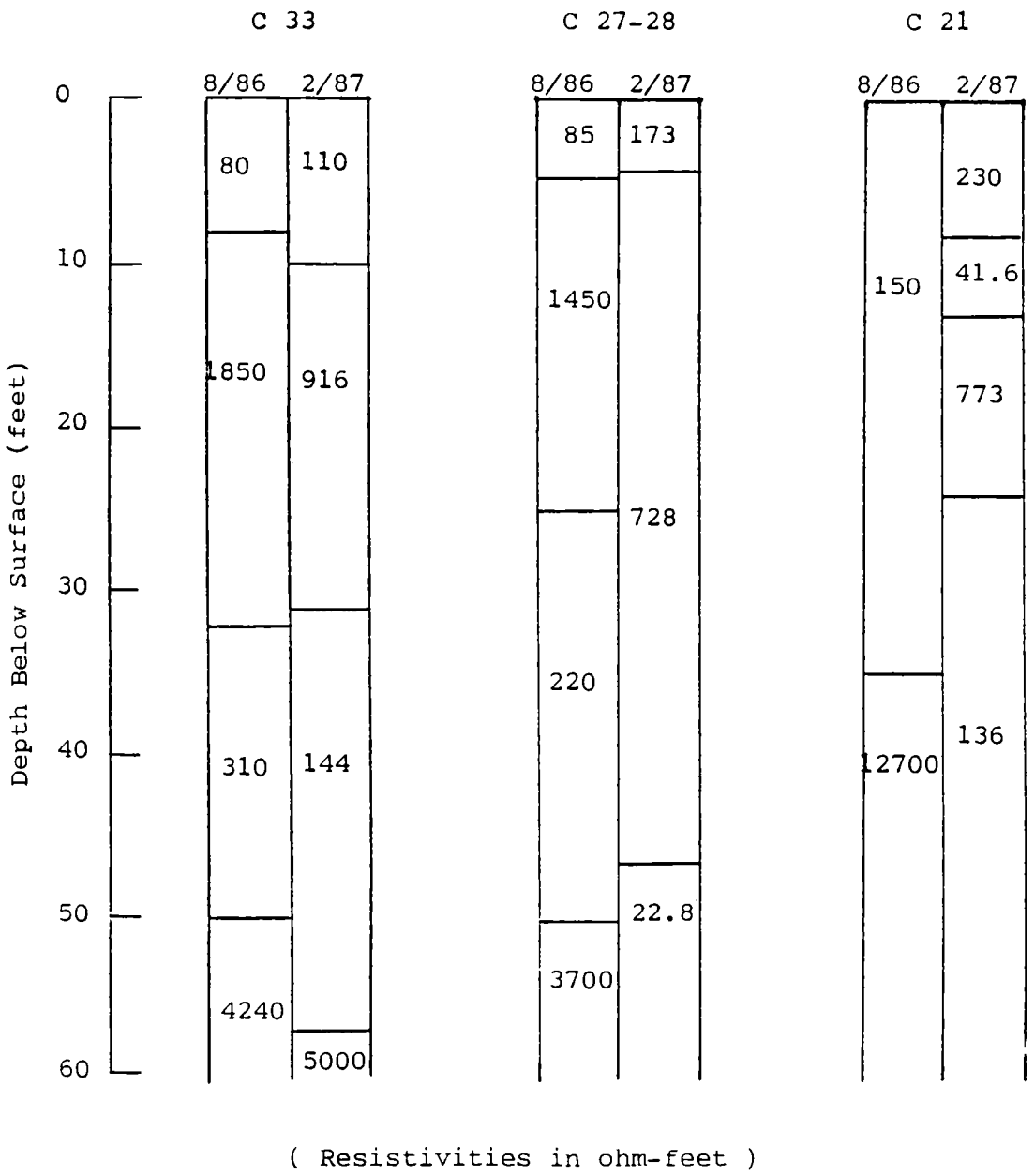

Interpreted Resistivity Layering
Beaver Dam, Arkansas

PLATE 12

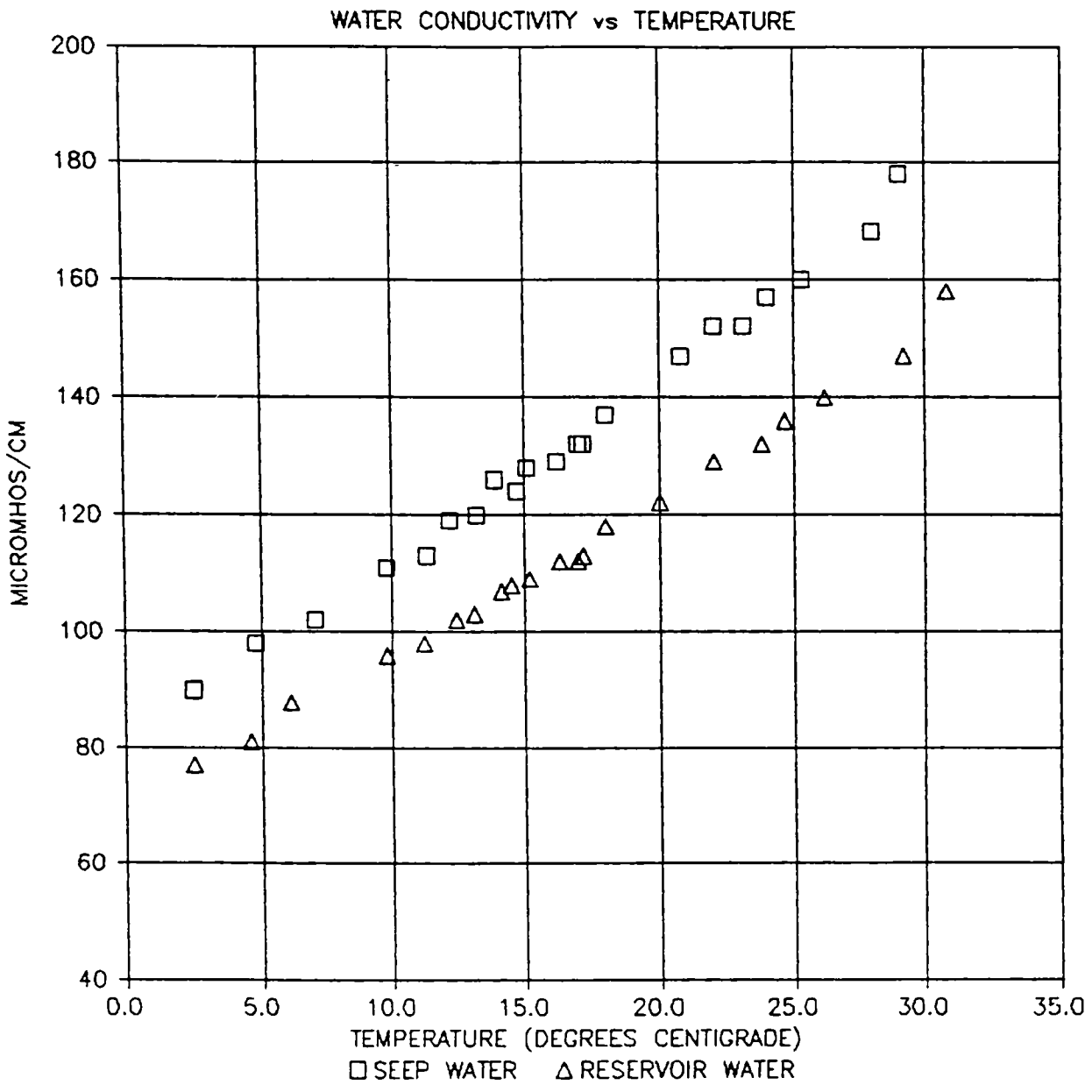

Measured Water Conductivity vs Temperature
Beaver Dam, Arkansas

PLATE 13

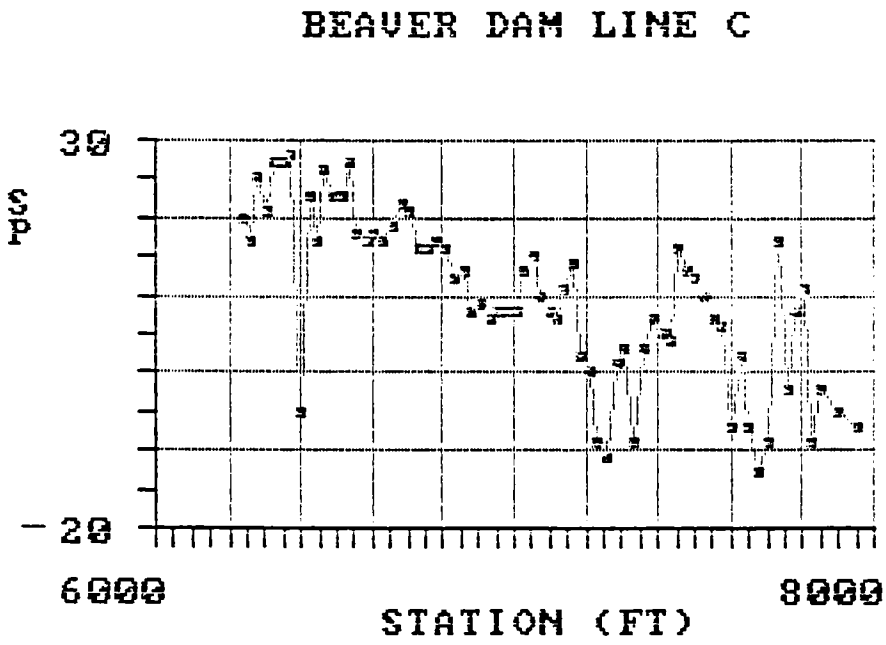

Field Data for Line C, August,1986
Beaver Dam, Arkansas

PLATE 14

```
SELECT SOURCE MODEL TYPE:
    ENTER 1 FOR SPHERICAL SOURCE
    ENTER 2 FOR POINT SOURCE
    ENTER 3 FOR HORIZONTAL LINE SOURCE
    ENTER 4 FOR DIPOLAR SHEET SOURCE
    ENTER 5 FOR HORIZONTAL CYLINDER SOURCE
? 3
LINE SOURCE(S) PARALLEL TO Y-AXIS

Enter resistivity, number of source lines ( <20 ), scale factor
? 100,5,3
Enter source line center point X, Y, depth, current, line half-length
? 6398,2840,2,-.07,50
? 6900,2950,50,-.1,50
? 7250,2850,50,-.2,50
? 7650,2780,50,-.2,50
? 7458,2816,40,.1,50
   SOURCE    X SOURCE   Y SOURCE   Z SOURCE   CURRENT   LENGTH
      1         6398       2840         2       -.07       50
      2         6900       2950        50         -.1       50
      3         7250       2850        50         -.2       50
      4         7650       2780        50         -.2       50
      5         7458       2816        40          .1       50
Strike any key to continue
1LIST   2RUN 3LOAD"  4SAVE"  5CONT6,"LPT1 7TRON8TROFFKEY    0SCREEN
```

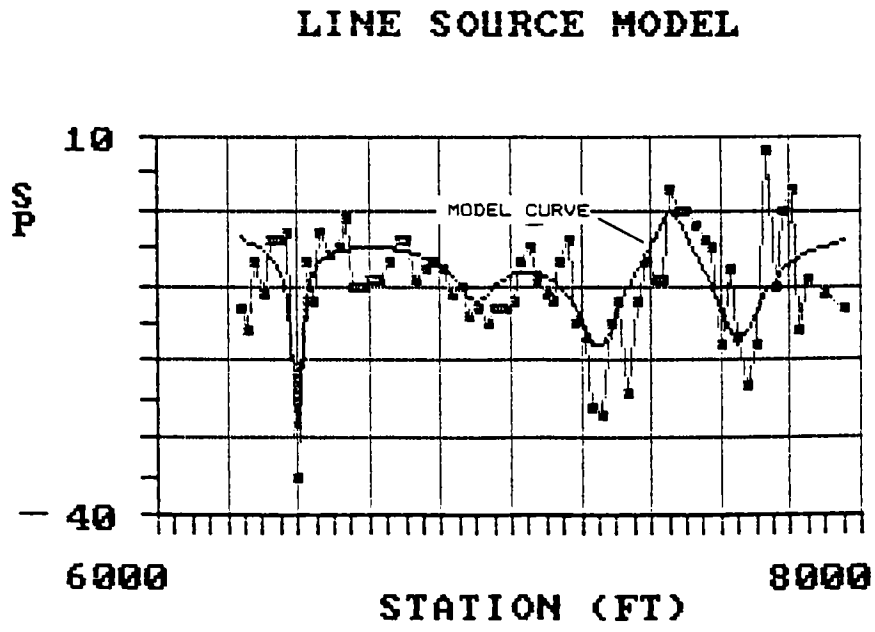

Source Models for Anomalies of Line C, August 1986
Beaver Dam, Arkansas

PLATE 15

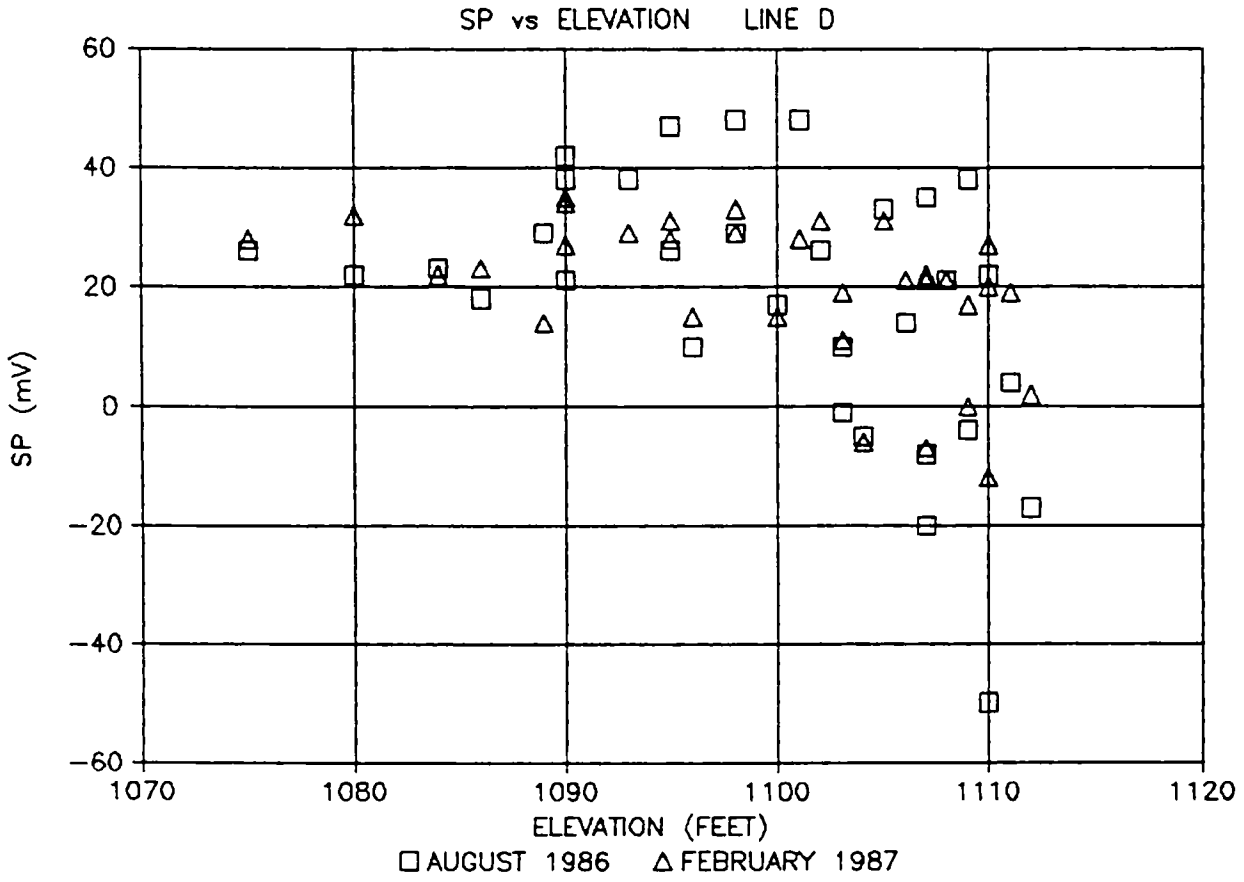

Self-Potential vs. Elevation, Line D
Beaver Dam, Arkansas

PLATE 16

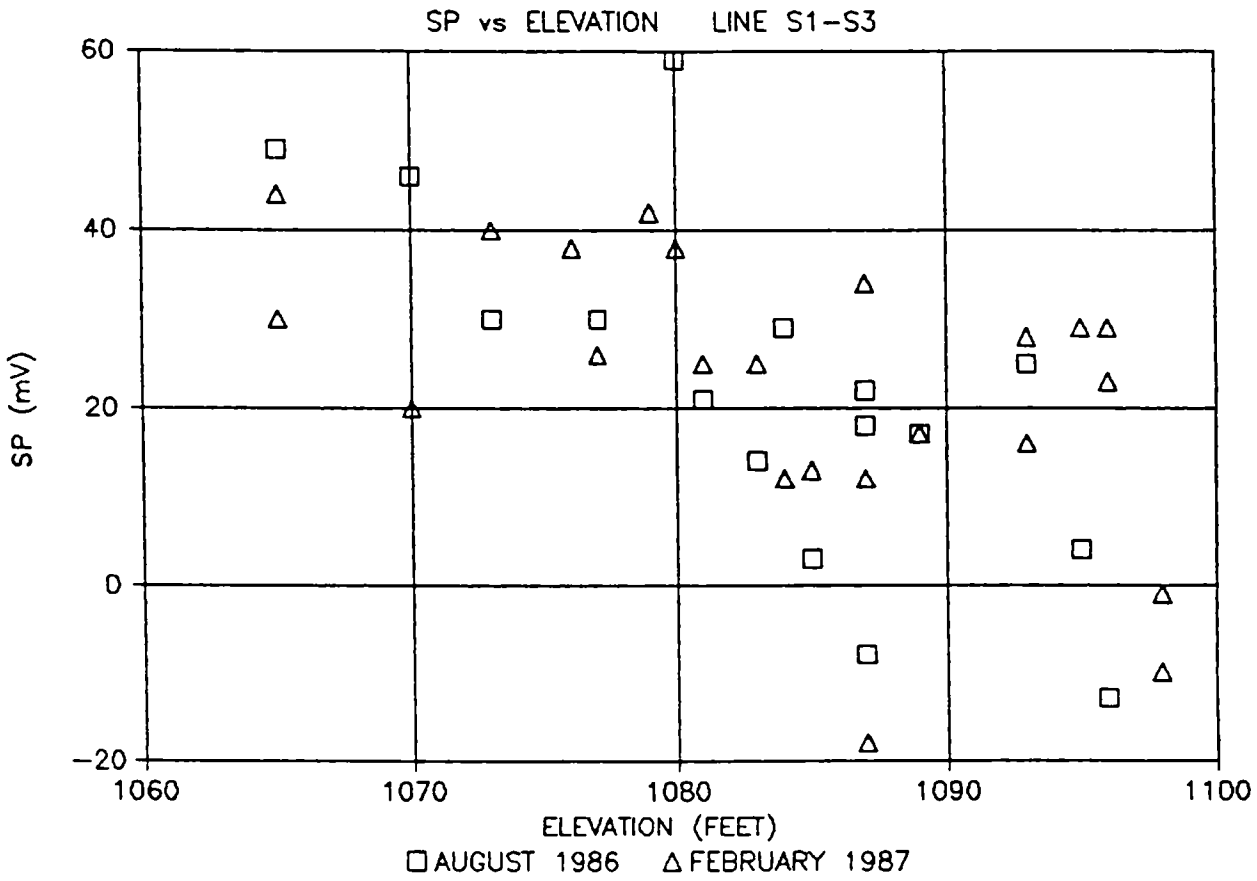

Self-Potential vs. Elevation, Line S1-S3
Beaver Dam, Arkansas

PLATE 17

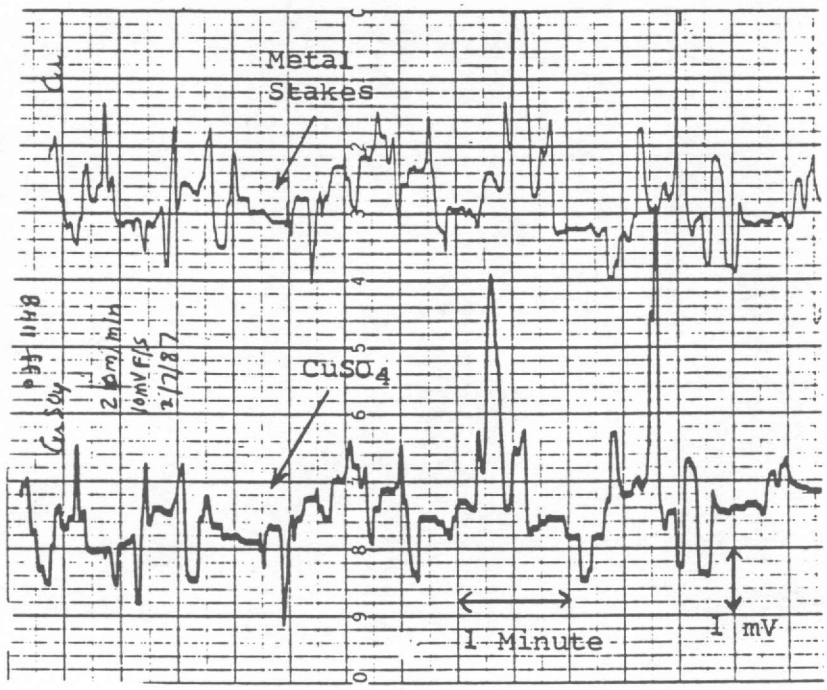

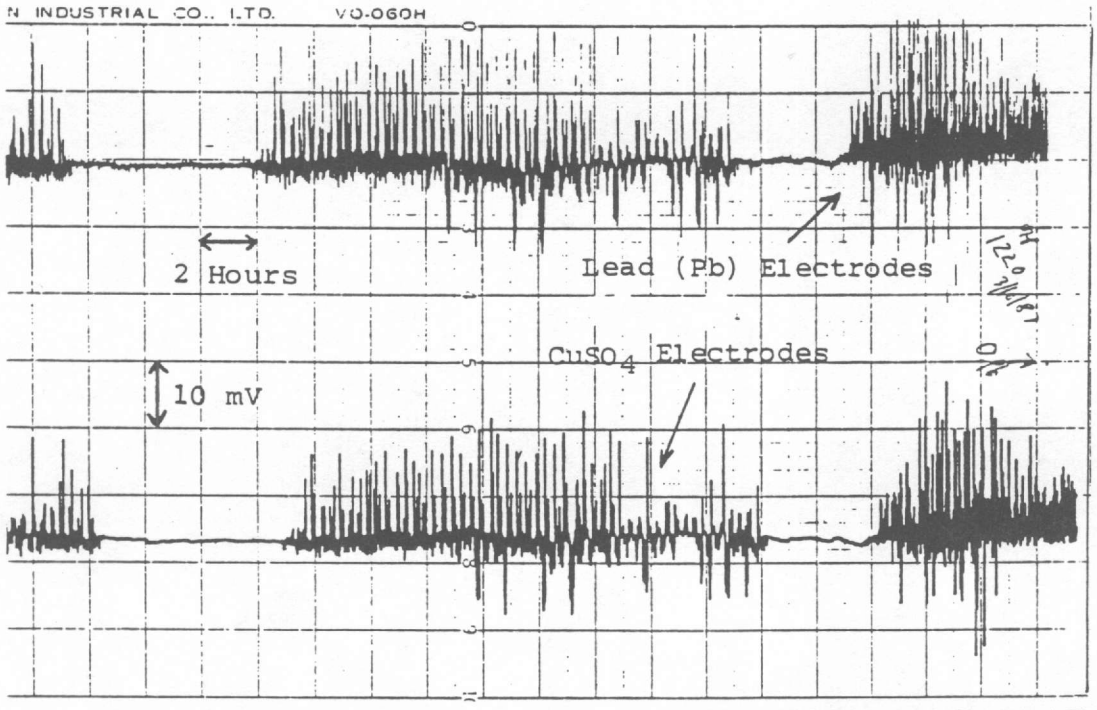

Voltages Generated by Electrical Machinery
San Francisco Bay Area, California

PLATE 18

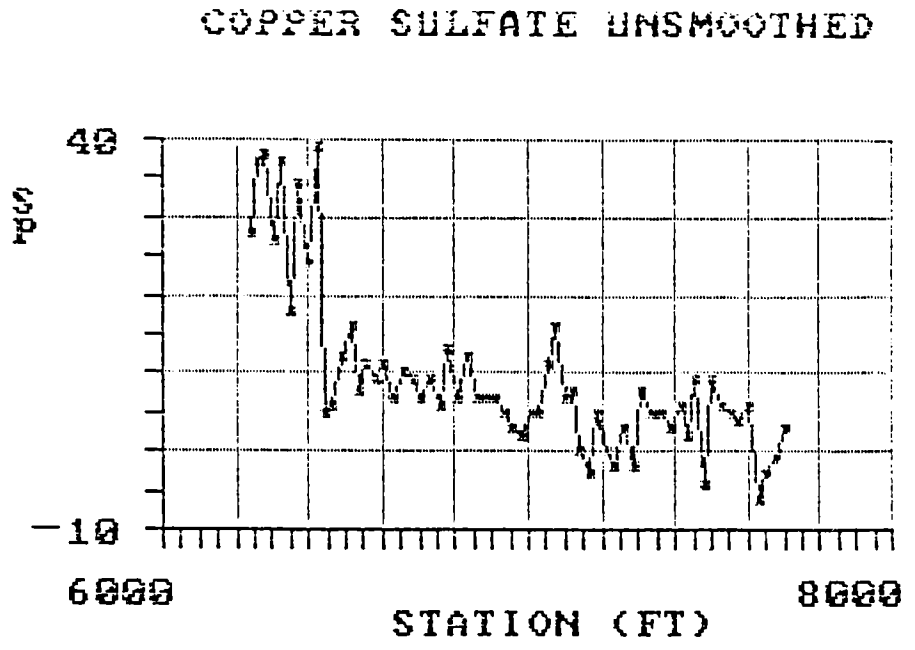

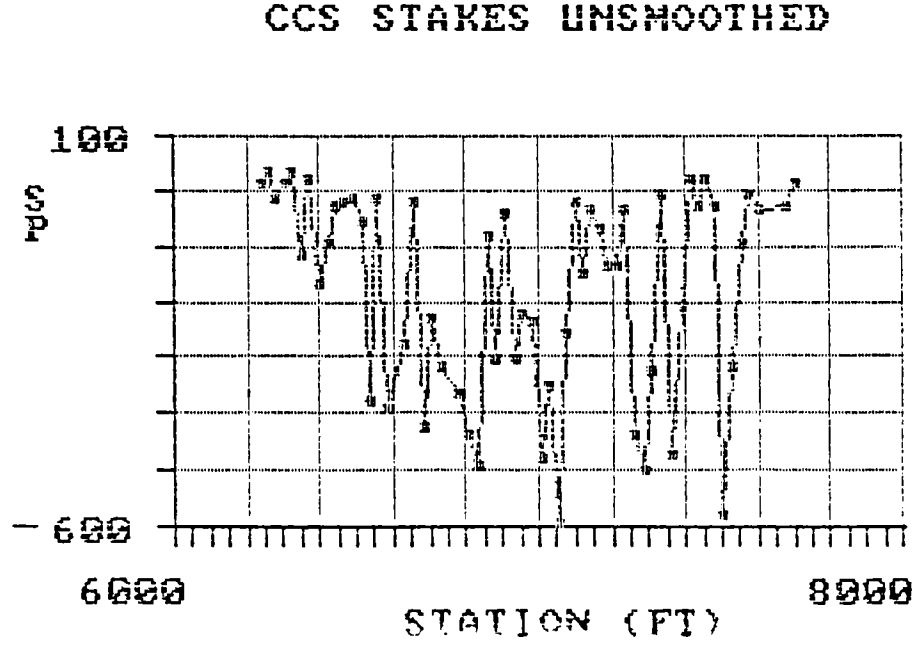

Unsmoothed Data, Line C, February 1987
Beaver Dam, Arkansas

PLATE 19

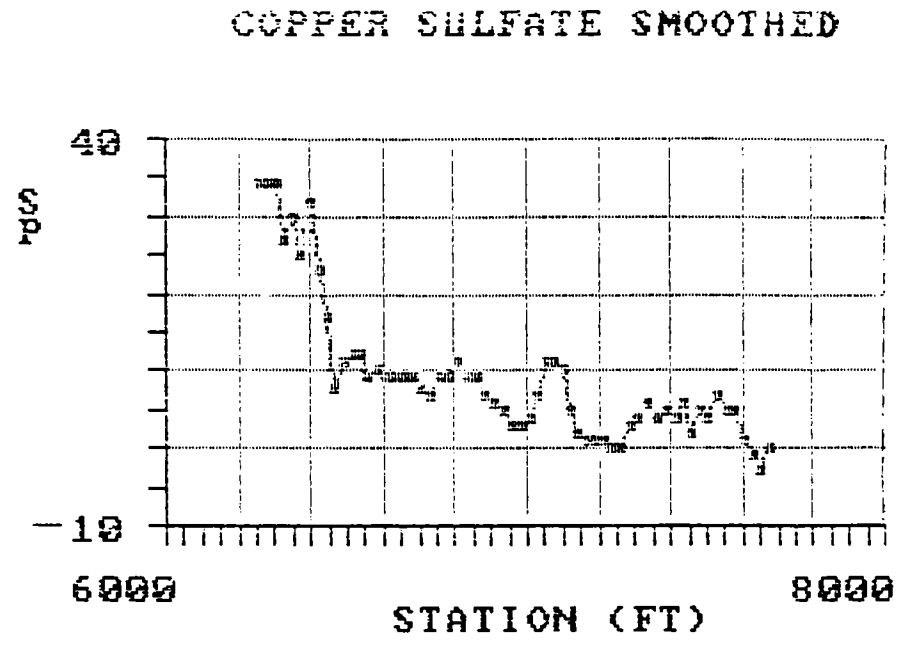

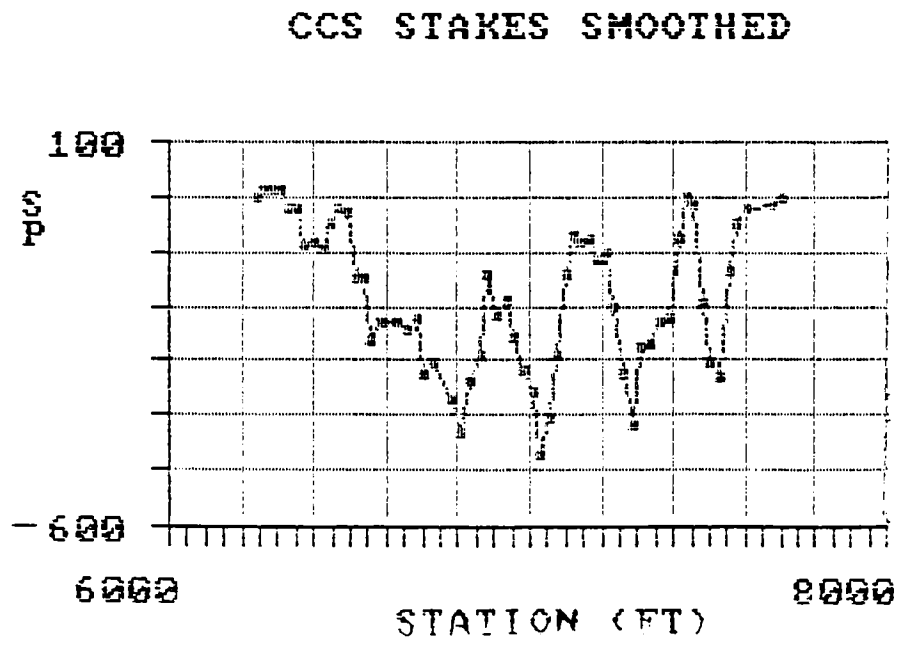

Smoothed Data, Line C, February 1987
Beaver Dam, Arkansas

PLATE 20

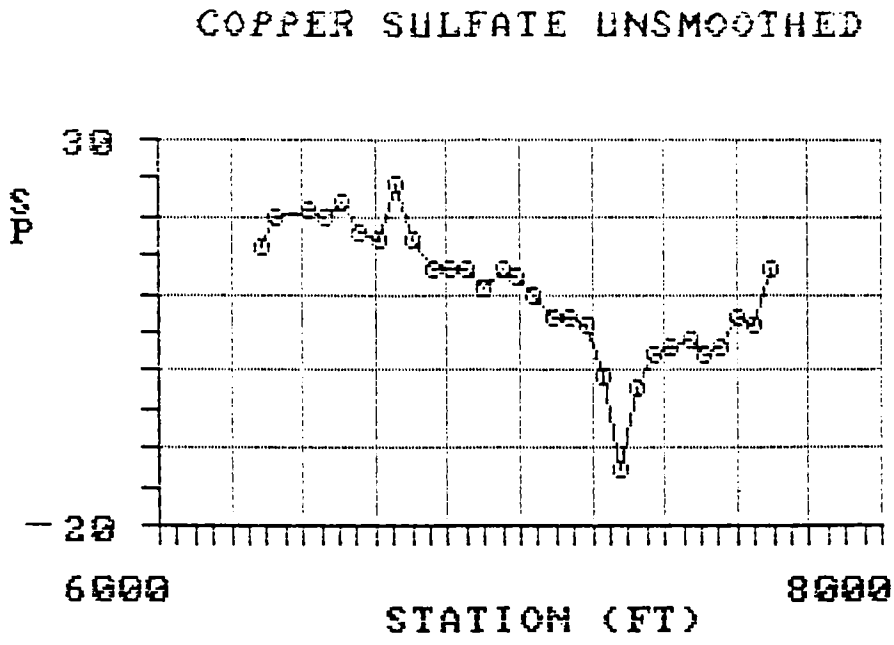

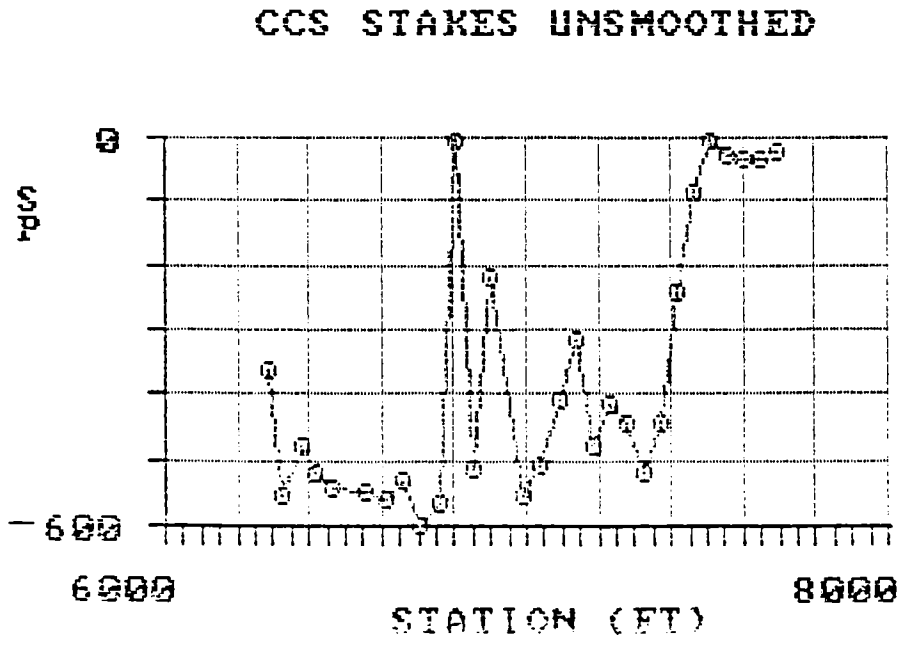

Unsmoothed Data, Line B, February 1987
Beaver Dam, Arkansas

PLATE 21

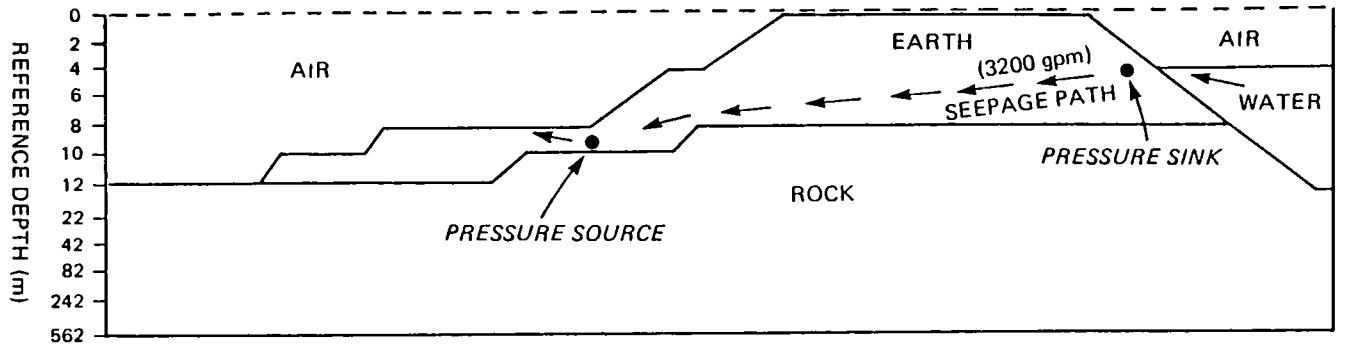

MEDIUM	PERMEA-BILITY (MD)	C (mV/atm)	ρ (ohm-m)
AIR	0	0.1	20000
ROCK	0.1	10	1000
EARTH	10	150	30
WATER	0	0.1	20000

Modeling Done by M. Wilt, University of California, Berkeley.
MD--millidarcies

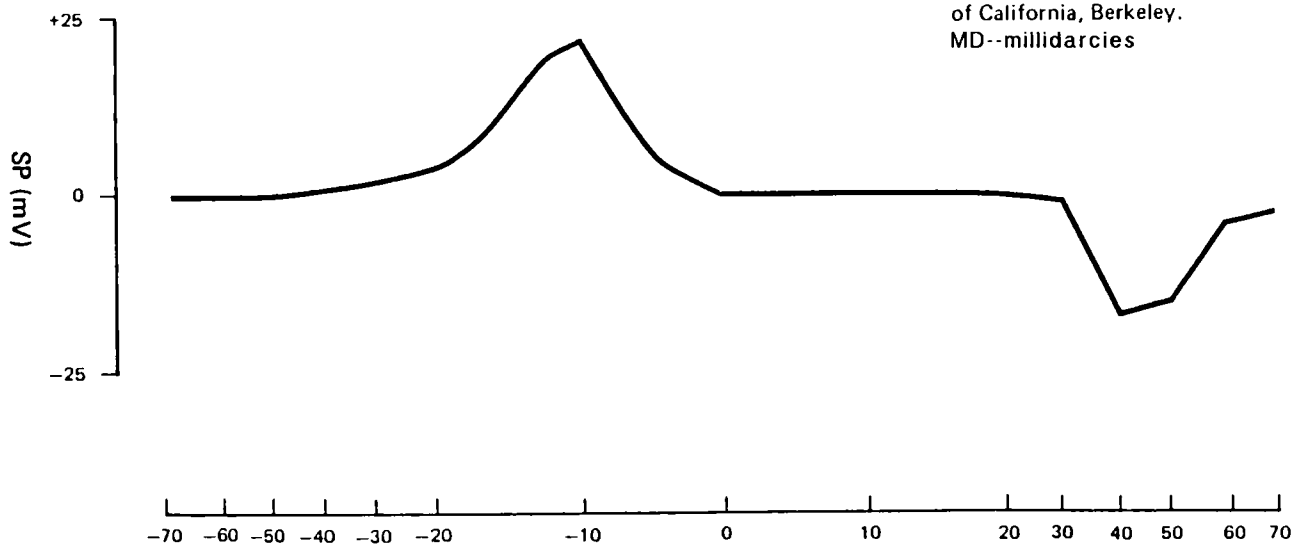

Modeling of Dam Seepage
Using Program SPXCPL

PLATE 22

APPENDIX A: PROGRAM SP1.BAS: INTERPRETATION OF SELF-POTENTIAL DATA USING GEOMETRIC SOURCE MODELS

Program Description

1. Program SP1.BAS is intended to assist in the modeling and interpretation of self-potential (SP) data. The program is written in BASIC for use on IBM-PC and compatible personal computers. Interpretation is done by comparison between field data and calculated curves generated by relatively simple geometric models.

2. The models include charged points, lines, spheres, cylinders, and sheets. Model geometry, algorithms, and references are shown in Plates A1 through A5, and details of individual models are discussed in Part IV of this report. The general interpretation procedure is as follows:

   a. Entry of field data (x and y coordinates of measurement stations, elevations, and measured SP values).

   b. Correction of field data by gradient and/or constant shifts (if desired).

   c. Selection of model type and parameters and calculation of anomaly curve(s).

   d. Comparison between field data profiles and calculated curves using both data listings and graphic displays.

   e. Adjustment of model parameters and recomparison until a satisfactory fit is achieved.

3. As discussed in Part IV, preliminary interpretation procedures using nomograms, characteristic points, half-wavelength comparison, and other techniques are given in the literature. Use of these procedures can be helpful in estimating initial model parameters.

4. Neither the program nor the graphics are highly refined, but because the algorithms are relatively simple the program runs quickly, and the graphics are adequate for visual curve matching. Although the program has been tested extensively, it may contain some "bugs." The authors would appreciate receiving user comments regarding problems and general operation of the program.

5. The program is interactively driven and largely self-explanatory. It is assumed that the user is familiar with the operation of the IBM-PC, general field data entry procedures, and the procedures required to run BASIC programs on the PC. Operating instructions, a sample run, and the program listing are given in the following sections.

6. Before entering BASIC, the "Caps Lock" key must be "on" (i.e., printing capital letters) for the program to run. Also, if it is desired to print graphic output on a dot matrix printer, the computer must be in "GRAPHICS" mode.

7. As discussed previously, the general operating sequence consists of field data entry, data correction (if desired), model entry and curve calculation, and graphic display (if desired). A field data set always must be entered first to create station coordinates for model calculations. If only model curves are desired, a "null" data file with zero SP values at each station may be entered. The program must be rerun to enter a new field data set.

8. The field data may be entered from the keyboard or from a previously generated file. After keyboard data entry, provision is made for writing the data to a disk file if desired. Calculated model output data also may be written to disk files.

9. Up to 14 model curves may be generated for a given field data set, but only four of the curves may be plotted on a single graph. The field data profiles may be omitted from the plots if desired.

10. Additional operating information is listed below. Further operating notes are included as typed comments in the sample run in the following section. The model profiles shown in this sample run were deliberately chosen to be a poor "fit" to the field data so that the curves could be distinguished in the plotted graphs.

a. Selection of x- and y-axis geographic orientation is arbitrary. However, as the cylinder and line models must be parallel to the y-axis, this axis generally would be oriented in the assumed direction of flow. The sheet model may be parallel to either the x- or the y-axis.

b. An output file name always must be entered before a model type is selected. Failure to enter a file name will result in a fatal error.

c. Data may be plotted along either the x- or y-axis of the input coordinate system.

d. The data reduction option is included to allow linear gradient corrections and/or constant shifts to be applied to the field data. Removal of gradients and constant shifts allows the field data to be leveled and centered about the zero millivolt axis for better fits with calculated model profiles. This option also can be used to apply tie-in and electrode drift

corrections to field data. Use of the option is illustrated in the sample run.

e. The point source model includes an option for automatic source input. Inputs include the number of points, initial (x,y,z) and current values, and desired increments for these parameters. This option allows rapid input of multipoint models.

f. Multiple sources may be entered for all models except the dipolar sheet.

g. Model source current or voltage may be varied to adjust calculated model voltages to match field anomaly amplitudes. If it is desired to maintain constant source current or voltage, the "scale factor" included in the model input may be varied instead.

h. After model parameters are entered, there will be a pause after "Strike any key to continue" is displayed while profiles are calculated. Calculation time depends on the number of stations, the number of sources, the type of source model, and computer speed. For a 286-based computer with a math coprocessor, calculation of the models shown in the following section takes a few seconds. For a model having 50 stations and 20 source points, calculation on the same machine requires about 20 sec, and if the points are replaced with line sources the same calculation requires about 30 sec.

Sample Run

11. This section contains a sample run of SP1.BAS. The run illustrates the following operations:

a. Keyboard entry of simulated field data and creation of disk data file TEST.DAT.

b. Reentry of field data from file TEST.DAT.

c. Correction of a portion of the field data using the data reduction option and creation of corrected data file TESTC.DAT.

d. Entry of data file TESTC.DAT into the program.

e. Input of models for point, line, sphere, cylinder, and dipolar sheet sources.

f. Creation of a plot showing the field data and calculated profiles for the point and line sources.

g. Creation of a second plot showing the field data and the calculated profiles for the sphere, cylinder, and dipolar sheet sources.

12. As mentioned previously, fits between the simulated field data and the model profiles were designed to be poor so that the various curves would

be distinguishable on the plots. A few more trials with any of the models would have resulted in much better fits and lower RMS errors.

13. The material on the following pages was printed directly from the screen display. Typewritten comments are intended to help clarify some points and procedures.

SAMPLE RUN

```
                    SP MAIN MENU

          Choose one of the following actions:
                    F1 - Input data
                    F2 - Model data      \ select
                    F3 - Graph data
                    F4 - Reduce data
```

```
          hit the space bar to exit the program.

1LIST   2RUN 3LOAD"  4SAVE"  5CONT6,"LPT1 7TRON8TROFFKEY    0SCREEN
```

This line indicates bottom of screen
except for graphic displays

```
IF YOUR DATA ARE ALREADY IN A DATA FILE THEY MUST BE IN
THE FOLLOWING ORDER IN THE FILE:
```

STATION NUMBER ELEVATION X Y V-MEASURED
(X or Y and V-MEASURED must always be entered; ELEVATION and/or STATION may be omitted)

```
IF THIS IS NOT THE FORMAT OF YOUR DATA THEN ENTER FROM
THE KEYBOARD OR EXIT AND EDIT THE FILE

DO YOU WISH TO INPUT DATA FROM THE KEYBOARD OR FROM A DATAFILE?  (K OR D):  K
```

keyboard entry example

```
WILL YOU BE ENTERING ELEVATIONS?  (Y or N):  Y
                          X's?           :  Y
                          Y's?           :  Y
                    V-MEASURED?          :  Y
ENTER UNITS (F for Ft - M for meters - K for kms):  F
```

```
1LIST   2RUN 3LOAD"  4SAVE"  5CONT6,"LPT1 7TRON8TROFFKEY    0SCREEN
```

KEYBOARD ENTRY SCREEN

Enter a 9999 in X or Y column to quit

STATION	ELEVATION FT	X FT	Y FT	V-MEASURED mV
1	0	-5	0	-20
2	0	-4	0	-50
3	0	-3	0	-70
4	0	-2	0	-90
5	0	-1	0	-95
6	0	0	0	-50
7	0	1	0	0
8	0	2	0	30
9	0	3	0	50
10	0	4	0	50
11	0	5	0	20
12	0	9999		

If you wish to save this data set enter a filename: TEST.DAT

1LIST 2RUN 3LOAD" 4SAVE" 5CONT6,"LPT1 7TRONBTROFFKEY 0SCREEN

SP MAIN MENU

Choose one of the following actions:
F1 - Input data
F2 - Model data
F3 - Graph data
F4 - Reduce data

Space bar was struck to exit program for data file entry example. Program then was re-entered using F2 key or typing RUN

hit the space bar to exit the program.

1LIST 2RUN 3LOAD" 4SAVE" 5CONT6,"LPT1 7TRONBTROFFKEY 0SCREEN

```
IF YOUR DATA ARE ALREADY IN A DATA FILE THEY MUST BE IN
THE FOLLOWING ORDER IN THE FILE:

STATION NUMBER   ELEVATION   X   Y  V-MEASURED
 (STATION, X, and V-MEASURED must always be entered; ELEVATION and/or Y may be
   omitted)

IF THIS IS NOT THE FORMAT OF YOUR DATA THEN ENTER FROM
THE KEYBOARD OR EXIT AND EDIT THE FILE

DO YOU WISH TO INPUT DATA FROM THE KEYBOARD OR FROM A DATAFILE?  (K OR D):  D
                                                  data file entry example
WILL YOU BE ENTERING ELEVATIONS?  (Y or N):  Y
                              X's?        :  Y
                              Y's?        :  Y
                         V-MEASURED?      :  Y
ENTER UNITS (F for Ft - M for meters - K for kms):  F



1LIST   2RUN 3LOAD"  4SAVE"  5CONT6,"LPT1 7TRON8TROFFKEY    0SCREEN

ENTER DATAFILE NAME:  TEST.DAT
ARE THERE STATION NUMBERS IN YOUR DATAFILE? (Y or N): ,Y



1LIST   2RUN 3LOAD"  4SAVE"  5CONT6,"LPT1 7TRON8TROFFKEY    0SCREEN
```

printout of input data

DATA FILE: TEST.DAT

STATION	ELEVATION FT	X FT	Y FT	V-MEASURED mV
1	0	-5	0	-20
2	0	-4	0	-50
3	0	-3	0	-70
4	0	-2	0	-90
5	0	-1	0	-95
6	0	0	0	-50
7	0	1	0	0
8	0	2	0	30
9	0	3	0	50
10	0	4	0	50
11	0	5	0	20

Strike any key to continue. . . .

1LIST 2RUN 3LOAD" 4SAVE" 5CONT6,"LPT1 7TRONBTROFFKEY 0SCREEN

Choose one of the following actions:
F1 - Input data
F2 - Model data
F3 - Graph data
F4 - Reduce data

data reduction example

select ——— F4

hit the space bar to exit the program.
Enter first station number, correction ? 1,5 +5 correction on station 1
Enter last station number, correction ? 6,1 +1 correction on station 6
Enter constant correction ? 8 constant correction +8 on stations 1-6
Correct another set of stations (Y/N)? ? Y
Enter first station number, correction ? 7,0
Enter last station number, correction ? 11,-10
Enter constant correction ? -3
Correct another set of stations (Y/N)? ? N
If you wish to save this data set enter a filename: TESTC.DAT
1LIST 2RUN 3LOAD" 4SAVE" 5CONT6,"LPT1 7TRONBTROFFKEY 0SCREEN

Exit program and re-run to enter data file TESTC.DAT

```
                    SF MAIN MENU

              Choose one of the following actions:
select ———————F1 - Input data
              F2 - Model data
              F3 - Graph data
              F4 - Reduce data
```

hit the space bar to exit the program.

```
1LIST   2RUN 3LOAD"  4SAVE"  5CONT6,"LPT1 7TRONBTROFFKEY    0SCREEN
```

IF YOUR DATA ARE ALREADY IN A DATA FILE THEY MUST BE IN
THE FOLLOWING ORDER IN THE FILE:

STATION NUMBER ELEVATION X Y V-MEASURED
(X or Y and V-MEASURED must always be entered; ELEVATION and/or STATION may be omitted)

IF THIS IS NOT THE FORMAT OF YOUR DATA THEN ENTER FROM
THE KEYBOARD OR EXIT AND EDIT THE FILE

```
DO YOU WISH TO INPUT DATA FROM THE KEYBOARD OR FROM A DATAFILE?  (K OR D):  D

WILL YOU BE ENTERING ELEVATIONS?  (Y or N):  Y
                            X's?          :  Y
                            Y's?          :  Y
                    V-MEASURED?           :  Y
ENTER UNITS (F for Ft - M for meters - K for kms):  F
```

```
1LIST   2RUN 3LOAD"  4SAVE"  5CONT6,"LPT1 7TRONBTROFFKEY    0SCREEN
```

```
ENTER DATAFILE NAME:  TESTC.DAT    input corrected data file TESTC.DAT
ARE THERE STATION NUMBERS IN YOUR DATAFILE? (Y or N):Y
```

DATA FILE: TESTC.DAT

STATION	ELEVATION FT	X FT	Y FT	V-MEASURED mV
1	0	-5	0	-7
2	0	-4	0	-37.80000001192093
3	0	-3	0	-58.60000002384186
4	0	-2	0	-79.40000009536743
5	0	-1	0	-85.20000004768372
6	0	0	0	-41
7	0	1	0	-3
8	0	2	0	24.5
9	0	3	0	42
10	0	4	0	39.5
11	0	5	0	7

Strike any key to continue. . . .

1LIST 2RUN 3LOAD" 4SAVE" 5CONT6,"LPT1 7TRON8TROFFKEY 0SCREEN

Begin input of models

SP MAIN MENU

Choose one of the following actions:
F1 - Input data
select ——— F2 - Model data
F3 - Graph data
F4 - Reduce data

hit the space bar to exit the program.

1LIST 2RUN 3LOAD" 4SAVE" 5CONT6,"LPT1 7TRON8TROFFKEY 0SCREEN

```
                                Point source entry
Enter an output filename:  POINT.OUT  an output file name must be
SELECT SOURCE MODEL TYPE:               entered for each model
    ENTER 1 FOR SPHERICAL SOURCE
    ENTER 2 FOR POINT SOURCE ------ select   Note: enter numbers 1-5,
    ENTER 3 FOR HORIZONTAL LINE SOURCE          not keys F1-F5
    ENTER 4 FOR DIPOLAR SHEET SOURCE
    ENTER 5 FOR HORIZONTAL CYLINDER SOURCE
? 2
  Enter resistivity, no. of source points (<200), scale factor
? 100,2,1
SOURCE COORDINATE ENTRY: MANUAL (1) OR AUTO (2)? 2
ENTER INITIAL X SOURCE, Y SOURCE, Z SOURCE, CURRENT
? 0,0,2,-15
ENTER INCREMENTS FOR X SOURCE, Y SOURCE, Z SOURCE, AND CURRENT
? 3,0,0,35
     SOURCE    X SOURCE   Y SOURCE   Z SOURCE   CURRENT
       1           0          0          2        -15
       2           3          0          2         20
Strike any key to continue
```

AUTO source entry used here for illustration;
usually used only for entry of large number of sources

```
1LIST   2RUN 3LOAD"  4SAVE"  5CONT6,"LPT1 7TRONBTROFFKEY    0SCREEN


    MODEL NUMBER =          1

             STATION       X          Y      V-MEASURED    V-CALCULATED   % ERROR


                 1       -5.0        0.0        -7.0          -5.7        -18.1
                 2       -4.0        0.0       -37.8          -9.7        -74.4
                 3       -3.0        0.0       -58.6         -15.9        -72.9
                 4       -2.0        0.0       -79.4         -25.3        -68.1
                 5       -1.0        0.0       -85.2         -35.6        -58.2
                 6        0.0        0.0       -41.0         -31.1        -24.2
                 7        1.0        0.0        -3.0           5.8       -292.5
                 8        2.0        0.0        24.5          57.9        136.5
                 9        3.0        0.0        42.0          92.9        121.3
                10        4.0        0.0        39.5          89.0        125.2
                11        5.0        0.0         7.0          68.2        874.4


RMS ERROR =       289.0
Strike any key to continue. . .
1LIST   2RUN 3LOAD"  4SAVE"  5CONT6,"LPT1 7TRONBTROFFKEY    0SCREEN
```

```
                              SP MAIN MENU

                        Choose one of the following actions:
                                      F1 - Input data
                    select ———————    F2 - Model data
                                      F3 - Graph data
                                      F4 - Reduce data
```

```
          hit the space bar to exit the program.
```

```
1LIST   2RUN 3LOAD"  4SAVE"  5CONT6,"LPT1 7TRONBTROFFKEY    0SCREEN
```

Line source entry

```
Enter an output filename:  LINE.OUT
SELECT SOURCE MODEL TYPE:
    ENTER 1 FOR SPHERICAL SOURCE
    ENTER 2 FOR POINT SOURCE
    ENTER 3 FOR HORIZONTAL LINE SOURCE——— select
    ENTER 4 FOR DIPOLAR SHEET SOURCE
    ENTER 5 FOR HORIZONTAL CYLINDER SOURCE
? 3
LINE SOURCE(S) PARALLEL TO Y-AXIS

Enter resistivity, number of source lines ( <20 ), scale factor
? 100,2,1
Enter source line center point X, Y, depth, current, line half-length
? 0,0,2,-2,10
? 3,0,2,2,10
   SOURCE    X SOURCE   Y SOURCE   Z SOURCE   CURRENT   LENGTH
      1          0          0          2         -2         10
      2          3          0          2          2         10
Strike any key to continue
```

```
1LIST   2RUN 3LOAD"  4SAVE"  5CONT6,"LPT1 7TRONBTROFFKEY    0SCREEN
```

MODEL NUMBER = 2

STATION	X	Y	V-MEASURED	V-CALCULATED	% ERROR
1	-5.0	0.0	-7.0	-22.5	221.7
2	-4.0	0.0	-37.8	-26.9	-28.9
3	-3.0	0.0	-58.6	-32.2	-45.1
4	-2.0	0.0	-79.4	-38.0	-52.1
5	-1.0	0.0	-85.2	-41.9	-50.8
6	0.0	0.0	-41.0	-36.2	-11.8
7	1.0	0.0	-3.0	-14.5	383.5
8	2.0	0.0	24.5	14.5	-40.8
9	3.0	0.0	42.0	36.2	-13.9
10	4.0	0.0	39.5	41.9	6.2
11	5.0	0.0	7.0	38.0	443.6

RMS ERROR = 191.4
Strike any key to continue. . .
1LIST 2RUN 3LOAD" 4SAVE" 5CONT6,"LPT1 7TRON8TROFFKEY 0SCREEN

SP MAIN MENU

Choose one of the following actions:
F1 - Input data
select ——— F2 - Model data
F3 - Graph data
F4 - Reduce data

hit the space bar to exit the program.

1LIST 2RUN 3LOAD" 4SAVE" 5CONT6,"LPT1 7TRON8TROFFKEY 0SCREEN

Sphere source entry

```
Enter an output filename:  SPHERE.OUT
SELECT SOURCE MODEL TYPE:
    ENTER 1 FOR SPHERICAL SOURCE ——— select
    ENTER 2 FOR POINT SOURCE
    ENTER 3 FOR HORIZONTAL LINE SOURCE
    ENTER 4 FOR DIPOLAR SHEET SOURCE
    ENTER 5 FOR HORIZONTAL CYLINDER SOURCE
? 1
  Enter number of spheres (<200)
? 1
ENTER SPHERE CENTER POINT (X,Y,Z), RADIUS, INCLINATION, AND VOLTAGE
? 0,0,4,2,120,500
     SOURCE  X     Y     Z        RADIUS  INCLINATION    VOLTAGE
       1     0     0     4          2          120          500
Strike any key to continue
                                          degrees
```

```
1LIST   2RUN 3LOAD"  4SAVE"  5CONT6,"LPT1 7TRON8TROFFKEY    0SCREEN
```

MODEL NUMBER = 3

STATION	X	Y	V-MEASURED	V-CALCULATED	% ERROR
1	-5.0	0.0	-7.0	-48.2	588.9
2	-4.0	0.0	-37.8	-60.4	59.7
3	-3.0	0.0	-58.6	-73.6	25.5
4	-2.0	0.0	-79.4	-83.5	5.1
5	-1.0	0.0	-85.2	-81.8	-4.0
6	0.0	0.0	-41.0	-62.5	52.4
7	1.0	0.0	-3.0	-32.4	978.5
8	2.0	0.0	24.5	-6.0	-124.5
9	3.0	0.0	42.0	9.6	-77.2
10	4.0	0.0	39.5	16.2	-59.0
11	5.0	0.0	7.0	17.8	153.6

```
RMS ERROR =      351.6
Strike any key to continue. . .
1LIST   2RUN 3LOAD"  4SAVE"  5CONT6,"LPT1 7TRON8TROFFKEY    0SCREEN
```

```
                    SP MAIN MENU

                Choose one of the following actions:
                          F1 - Input data
          select ———— F2 - Model data
                          F3 - Graph data
                          F4 - Reduce data
```

hit the space bar to exit the program.

```
1LIST   2RUN 3LOAD"  4SAVE"  5CONT6,"LPT1 7TRONBTROFFKEY    OSCREEN

                              Cylinder source entry
Enter an output filename:  CYL.OUT
SELECT SOURCE MODEL TYPE:
    ENTER 1 FOR SPHERICAL SOURCE
    ENTER 2 FOR POINT SOURCE
    ENTER 3 FOR HORIZONTAL LINE SOURCE
    ENTER 4 FOR DIPOLAR SHEET SOURCE
    ENTER 5 FOR HORIZONTAL CYLINDER SOURCE —— select
? 5
Cylinders of infinite strike extent parallel to y-axis

Enter resistivity,number of cylinders (<20), scale factor
? 100,1,1
Enter cylinder axis x-distance, radius, inclination, depth, current
? -1,2,-20,2,1
     SOURCE   X SOURCE RADIUS   INCLINATION   DEPTH   CURRENT
       1          -1      2          -20          2        1
Strike any key to continue          degrees


1LIST   2RUN 3LOAD"  4SAVE"  5CONT6,"LPT1 7TRONBTROFFKEY    OSCREEN
```

MODEL NUMBER = 4

STATION	X	Y	V-MEASURED	V-CALCULATED	% ERROR
1	-5.0	0.0	-7.0	-28.3	304.1
2	-4.0	0.0	-37.8	-34.3	-9.2
3	-3.0	0.0	-58.6	-40.8	-30.4
4	-2.0	0.0	-79.4	-41.3	-47.9
5	-1.0	0.0	-85.2	-21.8	-74.4
6	0.0	0.0	-41.0	6.5	-115.9
7	1.0	0.0	-3.0	19.0	-734.2
8	2.0	0.0	24.5	20.9	-14.6
9	3.0	0.0	42.0	19.6	-53.4
10	4.0	0.0	39.5	17.6	-55.4
11	5.0	0.0	7.0	15.8	125.3

RMS ERROR = 247.8
Strike any key to continue. . .
1LIST 2RUN 3LOAD" 4SAVE" 5CONT6,"LPT1 7TRONBTROFFKEY 0SCREEN

SP MAIN MENU

Choose one of the following actions:
F1 - Input data
select ——— F2 - Model data
F3 - Graph data
F4 - Reduce data

hit the space bar to exit the program.

1LIST 2RUN 3LOAD" 4SAVE" 5CONT6,"LPT1 7TRONBTROFFKEY 0SCREEN

Sheet source entry

```
Enter an output filename:  SHEET.OUT
SELECT SOURCE MODEL TYPE:
    ENTER 1 FOR SPHERICAL SOURCE
    ENTER 2 FOR POINT SOURCE
    ENTER 3 FOR HORIZONTAL LINE SOURCE
    ENTER 4 FOR DIPOLAR SHEET SOURCE ——— select
    ENTER 5 FOR HORIZONTAL CYLINDER SOURCE
? 4

ENTER SHEET INPUT PARAMETERS:

ENTER SHEET TOP DEPTH, BOTTOM DEPTH, STRIKE LENGTH 1,7,10
ENTER RHO1 (Y OR X NEG.), RHO2 (Y OR X POS.), SCALE FACTOR 10,5,250
ENTER SHEET CENTER COORDINATES (X,Y) 1,0
IS SHEET PARALLEL TO X OR Y AXIS? (ENTER X OR Y)Y

   AXIS  DTOP     DBOT      LENGTH      RHO1     RHO2       SCALE      XS      YS
    Y       1        7         10         10       5         250        1       0
DO YOU WISH TO ENTER A NEW MODEL WITH THE SAME STATIONS? (1=Y,2=NO)2



1LIST   2RUN 3LOAD"  4SAVE"  5CONT6,"LPT1 7TRON8TROFFKEY    0SCREEN


    MODEL NUMBER =           5

             STATION      X          Y      V-MEASURED   V-CALCULATED  % ERROR



                  1      -5.0        0.0         -7.0         -42.7       509.5
                  2      -4.0        0.0        -37.8         -50.3        33.0
                  3      -3.0        0.0        -58.6         -58.8         0.4
                  4      -2.0        0.0        -79.4         -67.2       -15.4
                  5      -1.0        0.0        -85.2         -71.6       -15.9
                  6       0.0        0.0        -41.0         -59.6        45.5
                  7       1.0        0.0         -3.0           0.0      -100.0
                  8       2.0        0.0         24.5          29.8        21.7
                  9       3.0        0.0         42.0          35.8       -14.7
                 10       4.0        0.0         39.5          33.6       -15.0
                 11       5.0        0.0          7.0          29.4       320.2


RMS ERROR =       185.1
Strike any key to continue. . .
1LIST   2RUN 3LOAD"  4SAVE"  5CONT6,"LPT1 7TRON8TROFFKEY    0SCREEN
```

End input of models

Begin graphic display option

SP MAIN MENU

Choose one of the following actions:
F1 - Input data
F2 - Model data
select ——— F3 - Graph data
F4 - Reduce data

hit the space bar to exit the program.

```
1LIST   2RUN 3LOAD"  4SAVE"  5CONT6,"LPT1 7TRON8TROFFKEY    0SCREEN
PLOT NEW MODELS ON PREVIOUS AXES (Y/N)? N
ENTER INITIAL AND FINAL STATIONS TO BE PLOTTED 1,11
PLOT ALONG X OR Y AXIS (ENTER X OR Y) X
ENTER XMIN,XMAX FOR GRAPH X-AXIS:  -5,5
ENTER YMIN,YMAX FOR GRAPH Y-AXIS:  -100,100
ENTER X-AXIS GRID LINE INTERVAL:  1
ENTER Y-AXIS GRID LINE INTERVAL:  20
ENTER X-AXIS TICK MARK INTERVAL:  .5
ENTER Y-AXIS TICK MARK INTERVAL:  10
ENTER A GRAPH TITLE:  POINT AND LINE SOURCES
ENTER AN X-AXIS TITLE:  STATION
ENTER A  Y-AXIS TITLE:  SP
Choose up to four (4) data sets, TOTAL, to graph.
GRAPH THE MEASURED (FIELD) DATA? (Y OR N):  ? Y
HOW MANY CALCULATED MODEL CURVES WOULD YOU LIKE TO GRAPH?  (0-4):  2
FOR CALCULATED DATA SET  1
ENTER MODEL #:  1
FOR CALCULATED DATA SET  2
ENTER MODEL #:  2
```

plot point sources (model 1), line sources (model 2) and field data

```
FOR CALCULATED DATA SET:    1
WHICH SYMBOL WOULD YOU LIKE :
    1       2       3       4
  Square  Dot  Triangle  Circle  (1,2,3, or 4):  1
DO YOU WISH TO CONNECT THE POINTS (Y OR N)?:  Y
WHAT COLOR LINE? (1-3) 1
FOR CALCULATED DATA SET:    2
WHICH SYMBOL WOULD YOU LIKE :
    1       2       3       4
  Square  Dot  Triangle  Circle  (1,2,3, or 4):  3
DO YOU WISH TO CONNECT THE POINTS (Y OR N)?:  Y
WHAT COLOR LINE? (1-3) 2
WHICH SYMBOL WOULD YOU LIKE FOR THE MEASURED DATA:
    1       2       3       4
  Square  Dot  Triangle  Circle  (1,2,3, or 4):  4
DO YOU WISH TO CONNECT THE POINTS (Y OR N)?:  Y
WHAT COLOR LINE? (1-3) 3
```

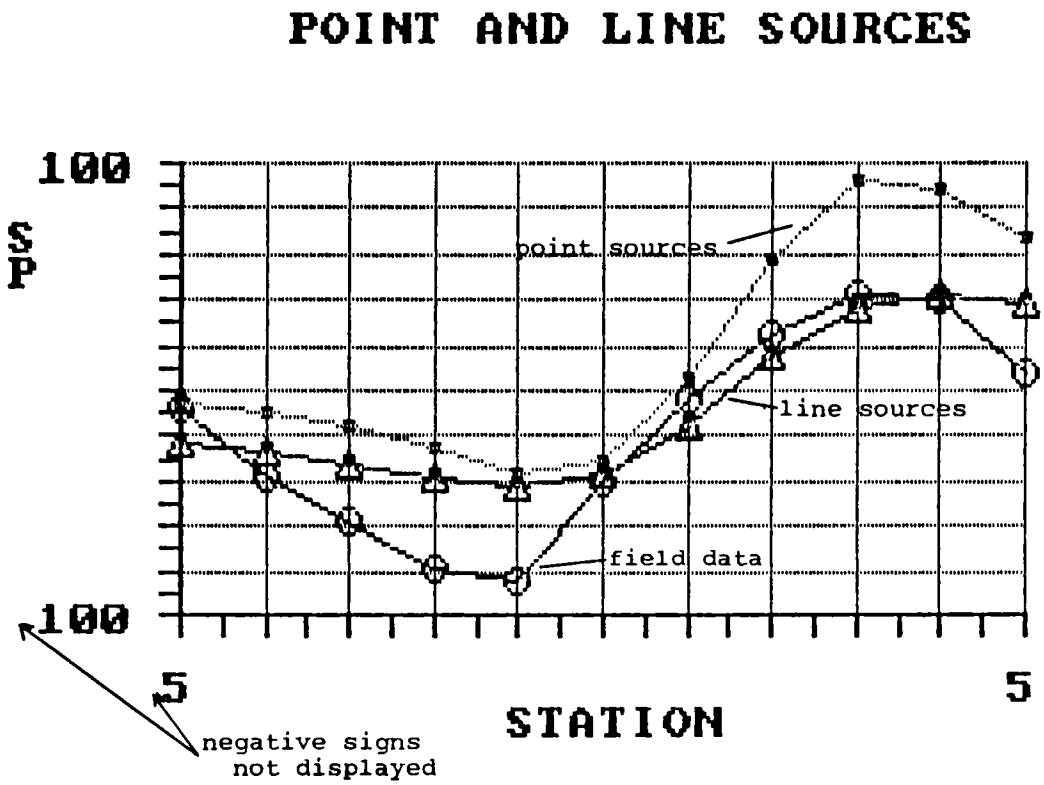

Strike space bar to clear display
and return to main menu

```
                    SP MAIN MENU

              Choose one of the following actions:
                        F1 - Input data
                        F2 - Model data
select ------           F3 - Graph data
                        F4 - Reduce data
```

hit the space bar to exit the program.

```
1LIST   2RUN 3LOAD"  4SAVE"  5CONT6,"LPT1 7TRON8TROFFKEY    0SCREEN
```

illustrates use of previous axes
note that previous title
also is used

```
PLOT NEW MODELS ON PREVIOUS AXES (Y/N)? Y
Choose up to four (4) data sets, TOTAL, to graph.
GRAPH THE MEASURED (FIELD) DATA? (Y OR N):  ? Y
HOW MANY CALCULATED MODEL CURVES WOULD YOU LIKE TO GRAPH?  (0-4):  3
FOR CALCULATED DATA SET  1
ENTER MODEL #:  3
```

plot sphere (model 3), cylinder (model 4), sheet (model 5), and field data

```
FOR CALCULATED DATA SET  2
ENTER MODEL #:  4

FOR CALCULATED DATA SET  3
ENTER MODEL #:  5

FOR CALCULATED DATA SET:   1
WHICH SYMBOL WOULD YOU LIKE :
    1       2       3         4
  Square  Dot  Triangle  Circle  (1,2,3, or 4):  1
DO YOU WISH TO CONNECT THE POINTS (Y OR N)?:  Y
WHAT COLOR LINE? (1-3) 1
```

```
FOR CALCULATED DATA SET:    2
WHICH SYMBOL WOULD YOU LIKE :
    1       2       3       4
  Square  Dot  Triangle  Circle  (1,2,3, or 4):  2
DO YOU WISH TO CONNECT THE POINTS (Y OR N)?:  Y
WHAT COLOR LINE? (1-3) 2
FOR CALCULATED DATA SET:    3
WHICH SYMBOL WOULD YOU LIKE :
    1       2       3       4
  Square  Dot  Triangle  Circle  (1,2,3, or 4):  3
DO YOU WISH TO CONNECT THE POINTS (Y OR N)?:  Y
WHAT COLOR LINE? (1-3) 3
WHICH SYMBOL WOULD YOU LIKE FOR THE MEASURED DATA:
    1       2       3       4
  Square  Dot  Triangle  Circle  (1,2,3, or 4):  4
DO YOU WISH TO CONNECT THE POINTS (Y OR N)?:  N
```

note incorrect title from previous plot

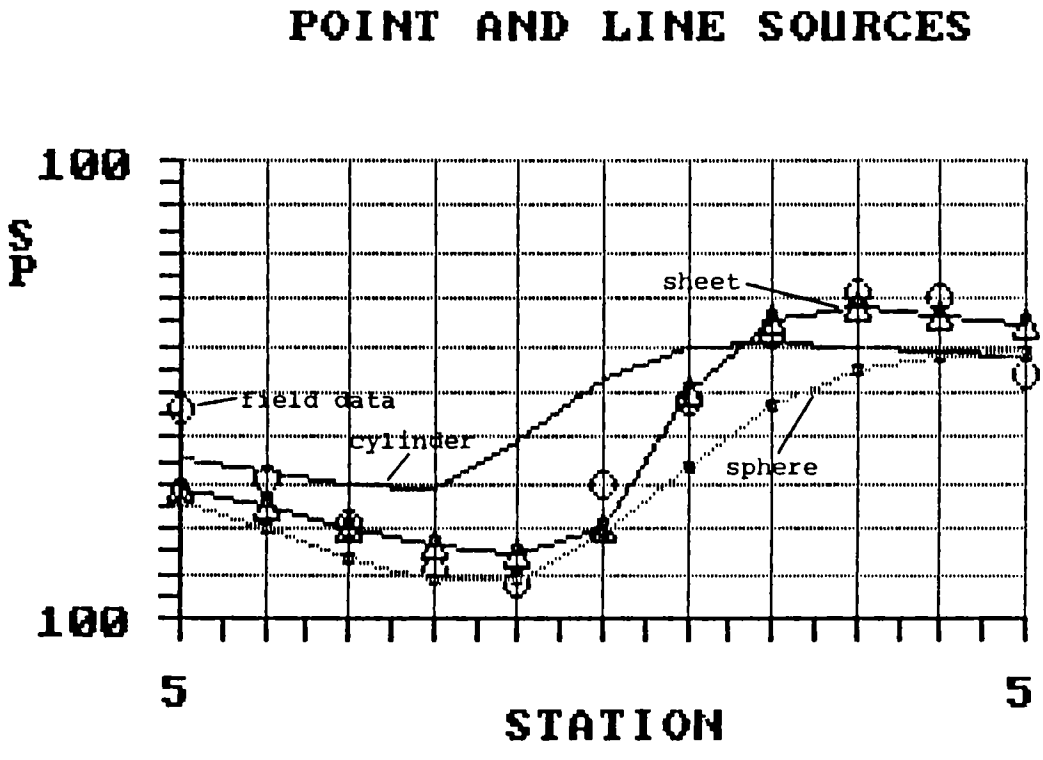

Re-plot entering new axes

SP MAIN MENU

Choose one of the following actions:
F1 - Input data
F2 - Model data
select ——— F3 - Graph data
F4 - Reduce data

hit the space bar to exit the program.

1LIST 2RUN 3LOAD" 4SAVE" 5CONT6,"LPT1 7TRONBTROFFKEY 0SCREEN

```
PLOT NEW MODELS ON PREVIOUS AXES (Y/N)? N
ENTER INITIAL AND FINAL STATIONS TO BE PLOTTED 1,11
PLOT ALONG X OR Y AXIS (ENTER X OR Y) X
ENTER XMIN,XMAX FOR GRAPH X-AXIS:  -5,5
ENTER YMIN,YMAX FOR GRAPH Y-AXIS:  -100,100
ENTER X-AXIS GRID LINE INTERVAL:  1
ENTER Y-AXIS GRID LINE INTERVAL:  20
ENTER X-AXIS TICK MARK INTERVAL:  .5
ENTER Y-AXIS TICK MARK INTERVAL:  10
ENTER A GRAPH TITLE:  MODELS 3, 4, AND 5   commas not allowed in titles
?Redo from start
ENTER A GRAPH TITLE:  MODELS 3 - 5
ENTER AN X-AXIS TITLE:  STATION (FT)
ENTER A  Y-AXIS TITLE:  mV
Choose up to four (4) data sets, TOTAL, to graph.
GRAPH THE MEASURED (FIELD) DATA? (Y OR N):  ? Y
HOW MANY CALCULATED MODEL CURVES WOULD YOU LIKE TO GRAPH?  (0-4):  3
FOR CALCULATED DATA SET  1
ENTER MODEL #:  3
```

plot sphere (model 3), cylinder (model 4), sheet (model 5) and field data

```
FOR CALCULATED DATA SET  2
ENTER MODEL #:  4

FOR CALCULATED DATA SET  3
ENTER MODEL #:  5

FOR CALCULATED DATA SET:   1
WHICH SYMBOL WOULD YOU LIKE :
    1       2       3         4
  Square  Dot  Triangle  Circle  (1,2,3, or 4):  1
DO YOU WISH TO CONNECT THE POINTS (Y OR N)?:  Y
WHAT COLOR LINE? (1-3) 1
FOR CALCULATED DATA SET:   2
WHICH SYMBOL WOULD YOU LIKE :
    1       2       3         4
  Square  Dot  Triangle  Circle  (1,2,3, or 4):  2
DO YOU WISH TO CONNECT THE POINTS (Y OR N)?:  Y
WHAT COLOR LINE? (1-3) 2
FOR CALCULATED DATA SET:   3
WHICH SYMBOL WOULD YOU LIKE :
    1       2       3         4
  Square  Dot  Triangle  Circle  (1,2,3, or 4):  3
```

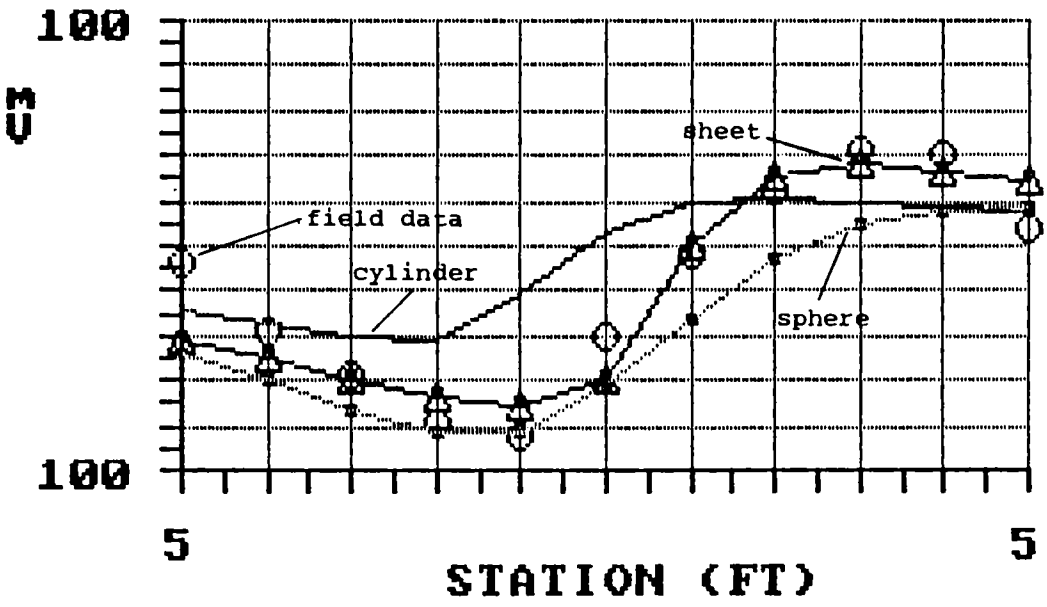

Program Listing

14. This section contains the complete listing for SP1.BAS. The program is written in BASIC and requires about 17500 bytes of storage. Data input and output files require a few hundred to a few thousand bytes, and machine memory requirements are minimal.

```
10 ' PROGRAM SP1.BAS
20 ' RFC/CM  JANUARY 1988
30 '
35 PI = 3.14159
40 ' MAIN MENU FOR SP PROGRAM
50 '
52 SCREEN 2:SCREEN 0:CLOSE#1
60 ON KEY (1) GOSUB 1000
70 KEY (1) ON
80 ON KEY (2) GOSUB 2000
90 KEY (2) ON
100 ON KEY (3) GOSUB 3000
110 KEY (3) ON
111 ON KEY (4) GOSUB 7000
112 KEY (4) ON
113 CLS
120 LOCATE 3,35:PRINT "SP MAIN MENU"
130 LOCATE 5,25:PRINT "Choose one of the following actions:  "
140 LOCATE 6,34:PRINT "F1 - Input data"
150 LOCATE 7,34:PRINT "F2 - Model data"
160 LOCATE 8,34:PRINT "F3 - Graph data"
162 LOCATE 9,34:PRINT "F4 - Reduce data"
170 LOCATE 22,10:PRINT "hit the space bar to exit the program."
180 IF INKEY$<>CHR$(32) THEN 180
200 END
1000
1010 '*******************************************************
1020 '
1030 ' DATA ENTRY SECTON
1040 '
1050 ' initialization
1060 '
1070 DEFDBL V,X
1080 DIM STAT(100),ELEV(100),X(100),Y(100),V(15,100),ISYM(5),Z(100)
1081 DIM LR(20),H(20),CURR(20)
1082 DIM RAD (200),ALF(200),E(200), ALFR(200), BETA (20)
1085 DIM XG(100),YG(100)
1087 DIM XS(200),YS(200),ZS(200),CUR(200)
1090 DIM LCOLR(5),C(15),RHO(15);X0(15),Y0(15),Z0(15),ERR0(100),PERERR(100)
1091 INCHECK=1
1100 CLS
1110 K=1:KK=1
1120 PRINT "IF YOUR DATA ARE ALREADY IN A DATA FILE THEY MUST BE IN "
1130 PRINT "THE FOLLOWING ORDER IN THE FILE:  ":PRINT
1140 PRINT "STATION NUMBER   ELEVATION   X   Y  V-MEASURED":PRINT " (X or Y and
 V-MEASURED must always be entered; ELEVATION and/or STATION may be omitted)
1150 PRINT: PRINT "IF THIS IS NOT THE FORMAT OF YOUR DATA THEN ENTER FROM ":PRIN
T "THE KEYBOARD OR EXIT AND EDIT THE FILE"
1160 PRINT "  "
1170 INPUT "DO YOU WISH TO INPUT DATA FROM THE KEYBOARD OR FROM A DATAFILE?  (K
OR D):  ",IN$:PRINT
1180 '
1190 ' variables used and units checks
1200 '
1210 INPUT "WILL YOU BE ENTERING ELEVATIONS?  (Y or N):  ",EL$
1220 INPUT "                                X's?          :  ",X$
1230 INPUT "                                Y's?          :  ",Y$
1240 INPUT "                          V-MEASURED?         :  ",V$
1250 INPUT "ENTER UNITS (F for Ft - M for meters - K for kms):  ",UNIT$
```

```
1260 IF UNIT$="F" THEN LABL$="FT" ELSE IF UNIT$="M" THEN LABL$="M" ELSE LABL$="K
M"
1270 CLS
1280 IF IN$="D" THEN 1680
1290 '
1300 LOCATE 2,30:PRINT "KEYBOARD ENTRY SCREEN"
1310 LOCATE 3,25:PRINT "Enter a 9999 in X column to quit"
1320 '
1330 LOCATE 4,1
1331 PRINT TAB(12) "STATION";
1332 PRINT TAB(24) "ELEVATION";
1333 PRINT TAB(36) "X";
1334 PRINT TAB(48) "Y";
1335 PRINT TAB(58) "V-MEASURED"
1337 PRINT TAB(24) LABL$;
1338 PRINT TAB(36) LABL$;
1339 PRINT TAB(48) LABL$;
1340 PRINT TAB(58) "mV"
1350 '
1360 LOCATE (K+6),1
1370 PRINT TAB(12) KK;
1380 '
1390 IF EL$<>"Y" THEN 1420
1400 LOCATE (K+6),24:INPUT "",ELEV(KK)
1410 '
1420 IF X$<>"Y" THEN 1460
1430 LOCATE (K+6),36:INPUT "",X(KK)
1440 IF X(KK)=9999 THEN 1560
1450 '
1460 IF Y$<>"Y" THEN 1500
1470 LOCATE (K+6),48:INPUT "",Y(KK)
1480 IF X$="N" AND Y(KK)=9999 THEN 1550
1490 '
1500 IF V$<>"Y" THEN 1530
1510 LOCATE (K+6),58:INPUT "",V(0,KK)
1520 '
1530 IF K=15 THEN K=0:FOR I=6 TO 22:LOCATE I,1:PRINT "
                                                    ";:NEXT I
1531 K=K+1:KK=KK+1
1540 GOTO 1360
1550 '
1560 NUMPTS=KK-1
1561 '
1562 ' datafile save
1570 '
1580 INPUT "If you wish to save this data set enter a filename:  ",DATFIL$
1590 IF DATFIL$="" THEN 1980
1600 OPEN DATFIL$ FOR OUTPUT AS #1
1610 FOR L=1 TO NUMPTS
1620   IF X$="Y" AND Y$="Y" AND EL$="Y" AND V$="Y" THEN DTA$=STR$(ELEV(L))+"  "+
STR$(X(L))+"  "+STR$(Y(L))+"  "+STR$(V(0,L))
1630   IF Y$="N" AND EL$="Y" THEN DTA$=STR$(ELEV(L))+"  "+STR$(X(L))+"  "+STR$(V
(0,L))
1640   IF EL$="N" AND Y$="N" THEN DTA$=STR$(X(L))+"  "+STR$(V(0,L))
1645 IF EL$="N" AND X$="N" THEN DTA$=STR$(Y(L))+"   "+STR$(V(0,L))
1650   PRINT#1 ,L;DTA$
1660 NEXT L
1670 GOTO 1980
1680 '
1690 ' datafile read
1700 '
1710 INPUT "ENTER DATAFILE NAME:  ",DATFIL$
```

```
1720 OPEN DATFIL$ FOR INPUT AS #1
1730 INPUT "ARE THERE STATION NUMBERS IN YOUR DATAFILE? (Y or N):",S$
1740 CLS:LOCATE 2,20:PRINT "DATA FILE:  ",DATFIL$
1750 LOCATE 4,5
1751 PRINT TAB(12) "STATION";
1752 PRINT TAB(24) "ELEVATION";
1753 PRINT TAB(36) "X";
1754 PRINT TAB(48) "Y";
1755 PRINT TAB(58) "V-MEASURED"
1757 PRINT TAB(24) LABL$;
1758 PRINT TAB(36) LABL$;
1759 PRINT TAB(48) LABL$;
1760 PRINT TAB(58) "mV"
1780 '
1790 FOR I=1 TO 1000
1800  IF EOF(1) THEN 1920
1810   IF S$="Y" THEN INPUT#1,STAT(I):LOCATE (II+6),11:PRINT STAT(I);
1820 '
1830   IF EL$="Y" THEN INPUT#1,ELEV(I):LOCATE (II+6),23:PRINT ELEV(I)
1840 '
1850   IF X$="Y" THEN INPUT#1,X(I):LOCATE (II+6),35:PRINT X(I);
1860 '
1870   IF Y$="Y" THEN INPUT#1,Y(I):LOCATE (II+6),47:PRINT Y(I)
1880 '
1890   IF V$="Y" THEN INPUT#1,V(0,I):LOCATE (II+6),57:PRINT V(0,I)
1900 '
1901   IF II MOD 15=0 AND II>14 THEN 1902 ELSE 1905
1902   PRINT "Strike any key to continue. . . "
1903   IF INKEY$="" THEN 1903
1904   LOCATE 6,1:II=0
1905   II=II+1
1910 NEXT I
1920 NUMPTS=I-1
1921  BLANK=NUMPTS MOD 15:FILL=15-BLANK+1
1922  FOR I=1 TO FILL
1923    PRINT"                                                                    ";
1924  NEXT I
1930 '
1940 LOCATE 22,1
1950 PRINT "Strike any key to continue. . . . ";
1960 IF INKEY$="" THEN 1960
1970 '
1980 CLOSE#1
1981 GOTO 52
1990 RETURN
2000 '*****************************************************
2001 ' MODEL INPUT SECTION
2020 '
2030 '
2040 CLS
2041 IF INCHECK=0 THEN 2042 ELSE 2047
2042 FOR I=1 TO 200:LOCATE 22,1:PRINT "NO DATA EXISTS YET!!":NEXT I:GOTO 52
2044 '
2046 '
2047 MODEL=MODEL+1
2048 INPUT "Enter an output filename:  ",OUTFIL$
2049 OPEN OUTFIL$ FOR OUTPUT AS #1
2051 PRINT "SELECT SOURCE MODEL TYPE:"
2052 PRINT "    ENTER 1 FOR SPHERICAL SOURCE"
2053 PRINT "    ENTER 2 FOR POINT SOURCE"
```

```
2054 PRINT "     ENTER 3 FOR HORIZONTAL LINE SOURCE"
2055 PRINT "     ENTER 4 FOR DIPOLAR SHEET SOURCE"
2057 PRINT "     ENTER 5 FOR HORIZONTAL CYLINDER SOURCE"
2061 INPUT STYP
2062 IF STYP = 1 THEN GOSUB 2346
2063 IF STYP = 2 THEN GOSUB 2400
2064 IF STYP = 3 THEN GOSUB 2600
2065 IF STYP = 4 THEN GOSUB 2800
2066 IF STYP = 5 THEN GOSUB 2500
2100 PRINT#1,       "                                        MODEL NUMBER:   ",MODEL
2110 PRINT#1,"  "
2120 PRINT#1,       "STATION     X       V-MEASURED    V-CALCULATED   % ERROR "
2135 FOR J = 1 TO NUMPTS
2136 IF V(0,J) = 0 THEN DERR = .1  ELSE DERR = V(0,J)
2140  ERRO(J)=(V(MODEL,J)-V(0,J))/DERR  :PERERR(J)=ERRO(J)*100
2171  PRINT#1,USING "######  #######.#    #######.#       #######.#     #######.#";J,X(J
),V(0,J),V(MODEL,J),PERERR(J)
2180 NEXT J
2185 SUMS = 0
2190 FOR K=1 TO NUMPTS
2200 SUMS = SUMS + PERERR(K)^2
2220 NEXT K
2230 RMS=(SUMS/NUMPTS)^.5
2240 PRINT#1, "RMS ERROR= ";RMS
2250 '
2260  CLS:LOCATE 3,1
2261  PRINT       "     MODEL NUMBER = ",MODEL
2263 PRINT
2270  PRINT "                STATION       X           Y      V-MEASURED    V-CALCULATE
D  % ERROR "
2280  LOCATE 10,1
2290  FOR L=1 TO NUMPTS
2300   PRINT,USING "######  #######.#  #######.#     #######.#       #######.#     #####
#.#";L,X(L),Y(L),V(0,L),V(MODEL,L),PERERR(L)
2301    IF L MOD 13 =0 THEN 2302 ELSE 2310
2302   PRINT "Strike any key to continue. . . "
2303   IF INKEY$="" THEN 2303
2304   LOCATE 10,1
2310  NEXT L
2311  BLANK=NUMPTS MOD 13 :FILL=13-BLANK+1
2312  FOR I=1 TO FILL
2313    PRINT"
          ";
2314  NEXT I
2315  PRINT "RMS ERROR = ";:PRINT USING"########.#";RMS
2316  PRINT "Strike any key to continue. . . ";
2317  IF INKEY$="" THEN 2317
2330 '
2340 CLOSE#1
2341 GOTO 52
2342 RETURN
2346 '  Model input for single point source
2350 ' Begin sphere model input
2352 PRINT "  Enter number of spheres (<200)"
2354 INPUT NSOUR
2356 PRINT "ENTER SPHERE CENTER POINT (X,Y,Z), RADIUS, INCLINATION, AND VOLTAGE"
2358 FOR I = 1 TO NSOUR
2360 INPUT XS(I), YS(I),ZS(I),RAD(I),ALF(I),E(I)
2361 ALFR(I) = ALF(I)/57.2958
2362 NEXT I
```

```
2364 PRINT "     SOURCE  X     Y     Z        RADIUS  INCLINATION    VOLTAGE"
2366 FOR I = 1 TO NSOUR
2368 PRINT  "       ";I;"    ";XS(I);"   ";YS(I);"   ";ZS(I);"        ";RAD(I);"
  ";ALF(I);"        ";E(I)
2370 NEXT I
2372 PRINT "Strike any key to continue";
2374 IF INKEY$="" THEN 2374
2378 PRINT
2380 FOR J = 1 TO NUMPTS
2382 SV = 0
2384 FOR I = 1 TO NSOUR
2386 NUMER = (X(J)-XS(I))*SIN(ALFR(I)) + ZS(I)*COS(ALFR(I))
2388 DEN = ((X(J)-XS(I))^2 + (Y(J)-YS(I))^2 + (ZS(I))^2 )^1.5
2390 VPART = E(I)*(RAD(I)^2)*NUMER/DEN
2392 SV = SV + VPART
2394 NEXT I
2395 V(MODEL%,J) = SV
2396 NEXT J
2397 RETURN
2400 '  Multiple point sources model
2404 F=1
2406 C4 = 0
2408 ' Begin model parameter input
2410 PRINT "  Enter resistivity, no. of source points (<200), scale factor"
2412 INPUT RHO(MODEL), NSOUR, F
2414 INPUT "SOURCE COORDINATE ENTRY: MANUAL (1) OR AUTO (2)";C3
2416 IF C3 = 1 THEN 2420
2418 IF C3 = 2 THEN 2438
2419 ' Manual source coordinate entry
2420 PRINT "ENTER SOURCE X, Y, Z, AND CURRENT"
2422 FOR I = 1 TO NSOUR
2424 INPUT XS(I), YS(I), ZS(I), CUR(I)
2426 NEXT I
2428 PRINT "     SOURCE   X SOURCE  Y SOURCE  Z SOURCE  CURRENT"
2430 FOR I = 1 TO NSOUR
2432 PRINT "       "; I;"        ";XS(I);"       ";YS(I);"       ";ZS(I);"
;CUR(I)
2434 NEXT I
2435 PRINT "Strike any key to continue";
2436 IF INKEY$="" THEN 2436
2437 GOTO 2470
2438 ' Auto source coordinate entry
2440 PRINT "ENTER INITIAL X SOURCE, Y SOURCE, Z SOURCE, CURRENT"
2442 INPUT XS1, YS1, ZS1, CUR1
2444 PRINT "ENTER INCREMENTS FOR X SOURCE, Y SOURCE, Z SOURCE, AND CURRENT"
2446 INPUT DXS, DYS, DZS, DCUR
2448 FOR I = 1 TO NSOUR
2450 XS(I) = XS1 + (I-1)*DXS
2452 YS(I) = YS1 + (I-1)*DYS
2454 ZS(I) = ZS1 + (I-1)*DZS
2456 CUR(I) = CUR1 + (I-1)*DCUR
2458 NEXT I
2460 PRINT "     SOURCE   X SOURCE  Y SOURCE  Z SOURCE  CURRENT"
2462 FOR I = 1 TO NSOUR
2464 PRINT "       ";I;"        ";XS(I);"       ";YS(I);"       ";ZS(I);"
;CUR(I)
2466 NEXT I
2467 PRINT "Strike any key to continue";
2468 IF INKEY$="" THEN 2468
2470 FOR J = 1 TO NUMPTS
```

```
2472 SV = 0
2474 FOR I = 1 TO NSOUR
2476 R= SQR((X(J)-XS(I))^2 +(Y(J)-YS(I))^2 +(Z(J)-ZS(I))^2)
2478 VPART= (F*CUR(I)*RHO(MODEL))/(2*PI*R)
2480 SV = SV + VPART
2482 NEXT I
2484 V(MODEL,J) = SV
2485 NEXT J
2494 RETURN
2500 'Cylinder model input
2502 F = 1
2504 PRINT "Cylinders of infinite strike extent parallel to y-axis":PRINT
2506 PRINT "Enter resistivity,number of cylinders (<20), scale factor
2508 INPUT RHO(MODEL),NCYLS,F
2510 PRINT "Enter cylinder axis x-distance, radius, inclination, depth, current"
2512 FOR I = 1 TO NCYLS
2514 INPUT XS(I),RAD(I),BETA(I),H(I),CURR(I)
2516 NEXT I
2518 PRINT "     SOURCE  X SOURCE RADIUS  INCLINATION  DEPTH  CURRENT"
2519 FOR I = 1 TO NCYLS
2520 PRINT "      ";I;"       ";XS(I);"   ";RAD(I);"        ";BETA(I);"      ";H
(I);"     ";CURR(I)
2522 NEXT I
2524 PRINT "Strike any key to continue";
2526 IF INKEY$="" THEN 2526
2528 FOR J = 1 TO NUMPTS
2530 SV = 0
2532 FOR I = 1 TO NCYLS
2534 BETAR = BETA(I)/57.2958
2536 F1 = 2*CURR(I)*RHO(MODEL)*RAD(I)/PI
2538 NUMER = (X(J)-XS(I))*COS(BETAR) + H(I)*SIN(BETAR)
2540 DENOM = (X(J)-XS(I))^2 + H(I)^2
2542 VPART = F*F1*NUMER/DENOM
2544 SV = SV + VPART
2546 NEXT I
2548 V(MODEL,J) = SV
2550 NEXT J
2552 RETURN
2600 ' Line source model
2602 F=1
2603 PRINT "LINE SOURCE(S) PARALLEL TO Y-AXIS": PRINT
2605 PRINT "Enter resistivity, number of source lines ( <20 ), scale factor "
2610 INPUT RHO(MODEL),NLINES, F
2615 PRINT "Enter source line center point X, Y, depth, current, line half-lengt
h"
2620 FOR I = 1 TO NLINES
2625 INPUT XS(I),YS(I),H(I),CURR(I),LR(I)
2630 NEXT I
2635 PRINT "   SOURCE   X SOURCE  Y SOURCE  Z SOURCE  CURRENT  LENGTH"
2640 FOR I = 1 TO NLINES
2645 PRINT "     "; I;"       ";XS(I);"       ";YS(I);"      ";H(I);"      ";CUR
R(I);"      ";LR(I)
2650 NEXT I
2655 PRINT "Strike any key to continue";
2660 IF INKEY$="" THEN 2660
2665 FOR J = 1 TO NUMPTS
2670 SV = 0
2675 FOR I = 1 TO NLINES
2680 F1 = CURR(I)*RHO(MODEL)/(2*PI)
2685 YPL = Y(J)-YS(I)+LR(I)
```

```
2690 YML = Y(J)-YS(I)-LR(I)
2695 NUMER = YPL+SQR(YPL^2 + (X(J)-XS(I))^2 + H(I)^2)
2700 DENOM = YML+SQR(YML^2 + (X(J)-XS(I))^2 + H(I)^2)
2705 VPART = F1 * LOG (NUMER/DENOM) * F
2710 SV = SV + VPART
2715 NEXT I
2720 V(MODEL,J)=SV
2725 NEXT J
2750 RETURN
2800 PRINT
2802 ' Fitterman Sheet Model
2805 PRINT "ENTER SHEET INPUT PARAMETERS:"
2808 PRINT
2810 INPUT "ENTER SHEET TOP DEPTH, BOTTOM DEPTH, STRIKE LENGTH ",A,B,L
2815 INPUT "ENTER RHO1 (Y OR X NEG.), RHO2 (Y OR X POS.), SCALE FACTOR " ,R1,R2,
NF
2820  INPUT "ENTER SHEET CENTER COORDINATES (X,Y) ",XS,YS
2822 INPUT "IS SHEET PARALLEL TO X OR Y AXIS? (ENTER X OR Y)",FAX$
2823 PRINT
2824 PRINT "   AXIS  DTOP    DBOT     LENGTH     RHO1    RHO2       SCALE      XS
   YS"
2825 PRINT "    ";FAX$;"     ";A;"     ";B;"      ";L;"      ";R1;"    ";R2;"
  ";NF;"     ";XS;"    ";YS
2832 NTOT = NUMPTS
2833 IF FAX$="X" THEN 2835 ELSE 2920
2835 FOR I = 1 TO NTOT
2840 YD = Y(I)-YS
2845 XD = X(I)-XS
2850 IF YD = 0 THEN 2855 ELSE 2865
2855 V(MODEL,I)=0
2860 GOTO 2915
2865 IF YD<0 THEN FE = NF/(PI*(1+R2/R1))
2870 IF YD>0 THEN FE = NF/(PI*(1+R1/R2))
2875 XP = X(I)-XS+L/2
2880 XM = X(I)-XS-L/2
2885 FA = ATN ( (B*XP)/(YD*SQR(XP^2 + YD^2 +B^2) )  )
2890 FB = ATN ( (A*XP)/(YD*SQR(XP^2 + YD^2 +A^2) )  )
2895 FC = ATN ( (B*XM)/(YD*SQR(XM^2 + YD^2 +B^2) )  )
2900 FD = ATN ( (A*XM)/(YD*SQR(XM^2 + YD^2 +A^2) )  )
2905 V(MODEL,I) = FE * (FA -FB -FC +FD)  \
2915 NEXT I
2920 FOR I = 1 TO NTOT
2922 YD = Y(I)-YS
2924 XD = X(I)-XS
2926 IF XD = 0 THEN 2928 ELSE 2932
2928 V(MODEL,I) = 0
2930 GOTO 2952
2932 IF XD<0 THEN FE = NF/(PI*(1+R2/R1))
2934 IF XD>0 THEN FE = NF/(PI*(1+R1/R2))
2936 YP = Y(I)-YS+L/2
2938 YM = Y(I)-YS-L/2
2940 FA = ATN((B*YP)/(XD*SQR(YP^2+XD^2+B^2)))
2942 FB = ATN((A*YP)/(XD*SQR(YP^2+XD^2+A^2)))
2944 FC = ATN((B*YM)/(XD*SQR(YM^2+XD^2+B^2)))
2946 FD = ATN((A*YM)/(XD*SQR(YM^2+XD^2+A^2)))
2948 V(MODEL,I) = FE * (FA-FB-FC+FD)
2952 NEXT I
2985 INPUT "DO YOU WISH TO ENTER A NEW MODEL WITH THE SAME STATIONS? (1=Y,2=NO)"
,CF2
2990 IF CF2 = 1 THEN 2800 ELSE 2995
```

```
2995 RETURN
3000 '*********************************************
3001 ' PLOTTING ROUTINES
3015 CLS: KEY OFF
3016 INPUT "PLOT NEW MODELS ON PREVIOUS AXES (Y/N)? ",REPLT$
3017 IF REPLT$ = "Y" GOTO 3070 ELSE GOTO 3020
3020 ' CM 9/28/86
3022 INPUT "ENTER INITIAL AND FINAL STATIONS TO BE PLOTTED ",STP1,STP2
3024 NPLT = STP2 - STP1 + 1
3026 INPUT "PLOT ALONG X OR Y AXIS (ENTER X OR Y) ",PAX$
3028 IF PAX$ = "X" THEN 3030 ELSE 3036
3030 FOR I = 1 TO NPLT
3032 XG(I) = X(STP1 + I - 1)
3034 NEXT I
3036 FOR I = 1 TO NPLT
3038 YG(I) = Y(STP1 + I - 1)
3040 NEXT I
3042 INPUT "ENTER XMIN,XMAX FOR GRAPH X-AXIS:  ",XMIN,XMAX
3044 INPUT "ENTER YMIN,YMAX FOR GRAPH Y-AXIS:  ",YMIN,YMAX
3046 INPUT "ENTER X-AXIS GRID LINE INTERVAL:  ",XGINT
3048 INPUT "ENTER Y-AXIS GRID LINE INTERVAL:  ",YGINT
3050 INPUT "ENTER X-AXIS TICK MARK INTERVAL:  ",XTINT
3052 INPUT "ENTER Y-AXIS TICK MARK INTERVAL:  ",YTINT
3054 INPUT "ENTER A GRAPH TITLE:  ",TITLE$
3056 INPUT "ENTER AN X-AXIS TITLE:  ",XTITL$
3058 INPUT "ENTER A  Y-AXIS TITLE:  ",YTITL$
3070 PRINT "Choose up to four (4) data sets, TOTAL, to graph.  "
3080 INPUT "GRAPH THE MEASURED (FIELD) DATA? (Y OR N):  ";F$
3090 INPUT "HOW MANY CALCULATED MODEL CURVES WOULD YOU LIKE TO GRAPH?  (0-4):
,MODLN
3100 IF MODLN = 0 THEN 3210
3110 FOR I=1 TO MODLN:PRINT "FOR CALCULATED DATA SET ";I:INPUT "ENTER MODEL #:
",MODL(I):PRINT "  ":NEXT I
3120 FOR I=1 TO MODLN
3130   PRINT "FOR CALCULATED DATA SET:  ";I
3140   PRINT "WHICH SYMBOL WOULD YOU LIKE :  "
3150   PRINT "    1      2      3       4"
3160   INPUT "  Square  Dot  Triangle  Circle  (1,2,3, or 4):  ",ISYM(I)
3170   INPUT "DO YOU WISH TO CONNECT THE POINTS (Y OR N)?:  ",CONN$(I)
3180   IF CONN$(I)="n" OR CONN$(I)="N" THEN 3210
3190   INPUT "WHAT COLOR LINE? (1-3) ",LCOLR(I)
3200 NEXT I
3210 IF F$<>"Y" THEN 3380
3220 PRINT "WHICH SYMBOL WOULD YOU LIKE FOR THE MEASURED DATA:  "
3230 PRINT "    1      2      3       4"
3240 INPUT "  Square  Dot  Triangle  Circle  (1,2,3, or 4):  ",ISYM(0)
3250 INPUT "DO YOU WISH TO CONNECT THE POINTS (Y OR N)?:  ",CONN$(0)
3260 IF CONN$(0)="n" OR CONN$(0)="N" THEN 3380
3270 INPUT "WHAT COLOR LINE? (1-3) ",LCOLR(0)
3271 '
3272 '
3380 '
3390 '   calculate scaling factors
3400 '
3410 XSCL=216/(XMAX-XMIN):'            216= total length of x axis
3420 YSCL=104/(YMAX-YMIN):'            104= total length of y axis
3430 SCREEN 1:COLOR 0,1:CLS
3440 '
3450 '   draw ticks
3460 '
```

```
3470 YINC=50
3480 IF YINC>155 THEN 3530:'                          154=bottom of graph
3500   LINE (60,YINC)-(55,YINC):'                    horizontal
3510   YINC=YINC+YSCL*YTINT
3520   GOTO 3480
3530
3540 XINC=60
3550 IF XINC>277 THEN 3600:                         276=right side of graph
3570   LINE (XINC,154)-(XINC,159):'                   vertical
3580   XINC=XINC+XSCL*XTINT
3590   GOTO 3550
3600 '
3610 '    draw grid lines
3620 '
3630 IF YGINT=0 AND XGINT=0 THEN 3790
3640 IF YGINT=0 THEN 3720
3650 YGINC=50  .
3660 IF YGINC>155 THEN 3710
3680   LINE (60,YGINC)-(276,YGINC),1:'              horizontal
3690   YGINC=YGINC+YSCL*YGINT
3700   GOTO 3660
3710 '
3720 XGINC=60
3730 IF XGINT=0 THEN 3790
3740 IF XGINC>277 THEN 3790
3760   LINE (XGINC,154)-(XGINC,50),1:'              vertical
3770   XGINC=XGINC+XSCL*XGINT
3780   GOTO 3740
3790 '
3800 '    draw axes
3810 '
3820 LINE (60,154)-(276,154),3:'                    x axis
3830 LINE (60,154)-(60,50),3:'                      y axis
3840 '
3850 '  label endpoints
3860 '
3870 TEMP$(1)=STR$(YMAX):TEMP$(2)=STR$(YMIN):'    set up temp. arrays
3880 TEMP$(3)=STR$(XMIN):TEMP$(4)=STR$(XMAX)
3890 XPOS(1)=7:YPOS(1)=6:XPOS(2)=20:YPOS(2)=6
3900 XPOS(3)=22:YPOS(3)=8:XPOS(4)=22:YPOS(4)=35
3910 '
3920 FOR I= 1 TO 4:'                              right justify 4 labels
3930  JPOS=0
3940  FOR J= 1 TO LEN(TEMP$(I))-1
3950   A$=MID$(TEMP$(I),LEN(TEMP$(I))-JPOS,1)
3960   LOCATE XPOS(I),YPOS(I)-JPOS:PRINT A$
3970   JPOS=JPOS+1
3980  NEXT J
3990 NEXT I
4000 '
4010 '    graph title
4020 '
4030 XPOS=INT(23-(LEN(TITLE$)/2)):'               center title
4040 LOCATE 3,XPOS:PRINT TITLE$
4050 '
4060 '    axes titles
4070 '
4080 XPOS=INT(23-(LEN(XTITL$)/2)):'               center x axis label
4090 LOCATE 23,XPOS:PRINT XTITL$
4100 FOR I = 1 TO 15:'                           write y axis vertically
```

```
4110  A$=MID$(YTITL$,I,1)
4120  LOCATE I+8,3
4130  PRINT A$
4140 NEXT I
4150 LOCATE 23,1
4160 '
4170 '   post data points
4180 '
4181 IF F$="Y" THEN J=0 ELSE J=1
4182 FOR JJ=J TO MODLN
4190   FOR I=1 TO NPLT
4191    YG(I)=V(MODL(JJ),I+STP1-1)
4200    XPT=(XG(I)-XMIN)*XSCL+60
4210    YPT=200-((YG(I)-YMIN)*YSCL+46)
4220 '
4240    IF ISYM(JJ)<>1 THEN 4280
4250    LINE (XPT-1,YPT-1)-(XPT+1,YPT+1),2,B:'      rectangle
4260    GOTO 4381
4270 '
4280    IF ISYM(JJ)<>2 THEN 4320
4290    PSET (XPT,YPT),2:'                          dot
4300    GOTO 4381
4310 '
4320    IF ISYM(JJ)<>3 THEN 4380
4330    LINE (XPT-3,YPT+3)-(XPT,YPT-3):'            triangle
4340    LINE -(XPT+3,YPT+3)
4350    LINE -(XPT-3,YPT+3)
4360    GOTO 4381
4370 '
4380    CIRCLE (XPT,YPT),3,,,,1:'                    circle
4381  NEXT I
4390 NEXT JJ
4400 '
4410 '   connect the data points
4420 '
4421 IF F$="Y" THEN J=0 ELSE J=1
4422 FOR JJ=J TO MODLN
4423   IF CONN$(JJ)="N" OR CONN$(JJ)="n" THEN 4520
4424   FOR I=1 TO NPLT -1
4425    YG(I)=V(MODL(JJ),I+STP1-1):YG(I+1)=V(MODL(JJ),I+STP1)
4460    XPT=(XG(I)-XMIN)*XSCL+60
4470    YPT=200-((YG(I)-YMIN)*YSCL+46)
4480    XPT2=(XG(I+1)-XMIN)*XSCL+60
4490    YPT2=200-((YG(I+1)-YMIN)*YSCL+46)
4500    LINE (XPT,YPT)-(XPT2,YPT2),LCOLR(JJ)
4510   NEXT I
4520 NEXT JJ
4521 '
4530 '  legend
4540 '
4550 '
4560 '  pause
4570 '
4580 IF INKEY$="" THEN 4580
4585 KEY ON
4590 '
4600 GOTO 52
4610 RETURN
5000 '
5005 KEY ON
```

```
5010 GOTO 52
5020 RETURN
7000 '*************************************************************
7001 CLS
7005 'Data reduction option: Gradient and constant correction
7010 INPUT "Enter first station number, correction  ";SF,C1
7020 INPUT "Enter last station number, correction  ";SL,C2
7030 INPUT "Enter constant correction  ";C3
7040 NS = SL-SF+1
7050 NCOR = SL-SF
7060 DCOR = (C2-C1)/NCOR
7065 COUNT = 0
7070 FOR I = SF TO SL
7075 COUNT = COUNT + 1
7080 V(0,I) = V(0,I) +C1 +DCOR*(COUNT-1) +C3
7081 'Round off calculated values using integer division
7082 V(0,I) = V(0,I)\1
7090 NEXT I
7100 INPUT "Correct another set of stations (Y/N)?  ";MSTAT$
7110 IF MSTAT$ = "Y" THEN 7000 ELSE 1562
7120 RETURN
```

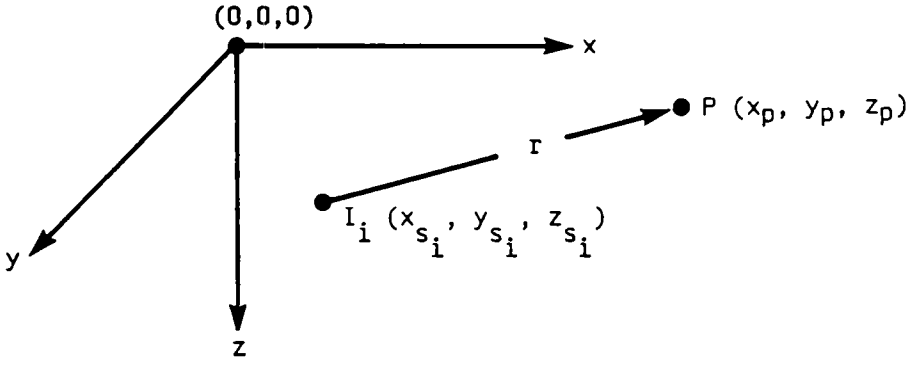

$$V_p\,(x_p,\ y_p,\ z_p) = \sum_{i=1}^{n} \frac{I_i\ \rho}{2\ \pi\ r_i}$$

where V_p = generated voltage

I_i = source or sink current intensity

ρ = resistivity of medium

$$r_i = \sqrt{(x_p - x_{s_i})^2 + (y_p - y_{s_i})^2 + (z_p - z_{s_i})^2}$$

References

Telford et al., 1976
Corwin et al., 1981

Point Current Sources

Line source is parallel to y-axis, centered at (x_s, y_s)

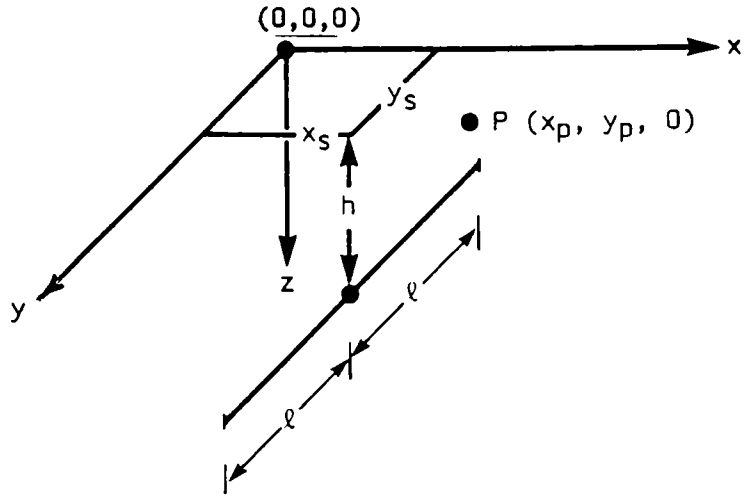

$$P(x_p, y_p, 0) = \frac{I\rho}{2\pi} \ln \frac{(y_p - y_s + \ell) + (y_p - y_s + \ell)^2 + (x_p - x_s)^2 + h^2}{(y_p - y_s - \ell) + (y_p - y_s - \ell)^2 + (x_p - x_s)^2 + h^2}$$

where V_p = generated voltage

I = current per unit length

ρ = resistivity of medium

References:

Rao et al., 1970

Broughton Edge and Laby, 1931

Semenov, 1974

Horizontal Line Source

PLATE A2

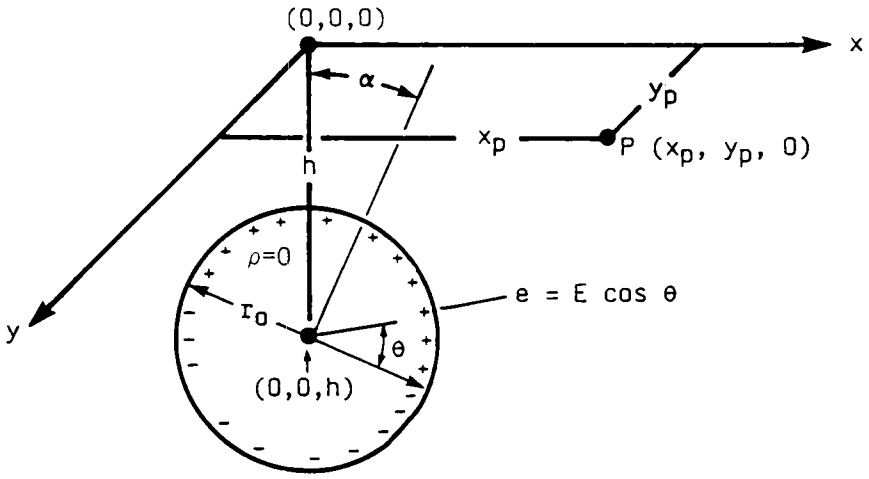

$$V_p\,(x_p,\ y_p,\ 0) = E\ r_o^2\ \frac{x_p \sin\alpha + h\cos\alpha}{(x_p^{\,2} + y_p^{\,2} + h^2)^{3/2}}$$

where V_p = generated voltage

E = maximum potential at surface of sphere (at $\theta = 0$)

r_o = radius of sphere

$h \gg r_o$

resistivity of sphere = 0

References

Petrowsky, 1925
Semenov, 1974

Spherical Source

PLATE A3

Cylinder is of infinite length and parallel to y-axis.
Polarization is uniform.

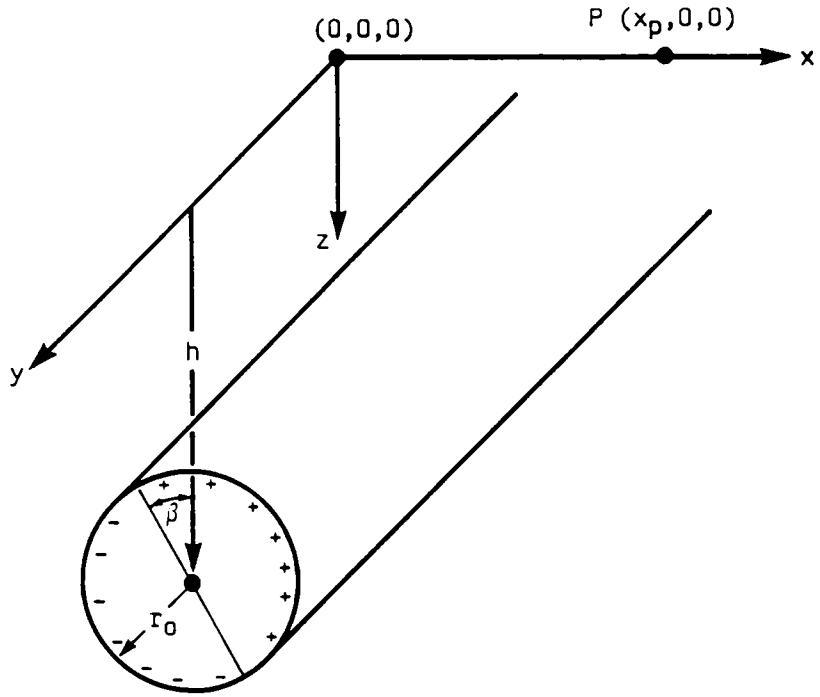

$$V_p\ (x_p,\ 0,\ 0) = \frac{2I\rho}{\pi}\ r_o\ \frac{(x \cos \beta + h \sin \beta)}{(x^2 + h^2)}$$

where V_p = generated voltage

I = current per unit of circumference

ρ = resistivity of medium

r_o = radius of cylinder

$h \gg r_o$

resistivity of cylinder = 0

References

Murty and Haricharan, 1985
Bhattacharya and Roy, 1981
Semenov, 1974

Horizontal Cylindrical Source

PLATE A4

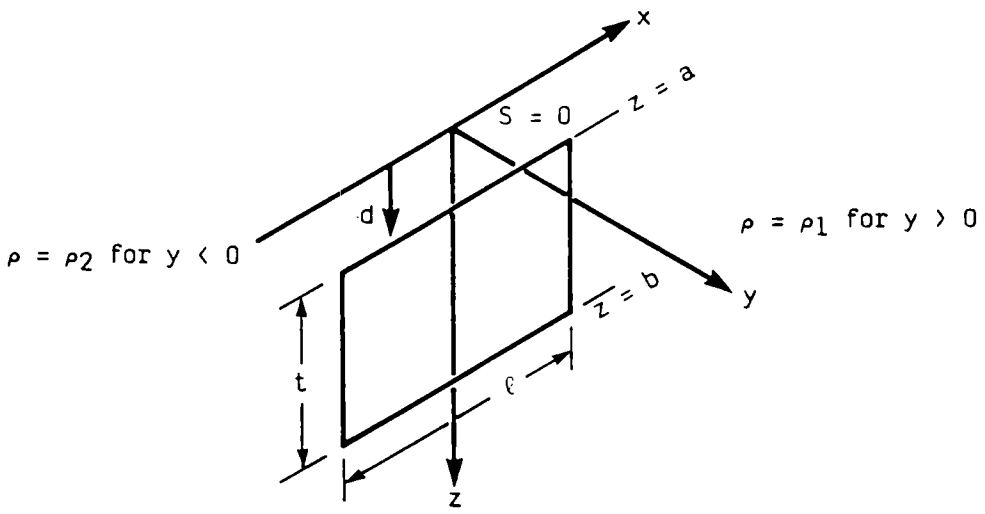

$$V_{\substack{1\\2}}(x, y, 0) = \frac{S}{\pi(1 + \rho_2/\rho_1)_{1\ 2}} (\tan^{-1} F_1 - \tan^{-1} F_2 - \tan^{-1} F_3 + \tan^{-1} F_4)$$

where $V_{\substack{1\\2}}$ = generated voltage in region 1 ($y > 0$) or 2 ($y < 0$)

S = source strength $b > a > 0$

$$F_1 = \frac{(x + \ell/2)\, b}{y\,[(x + \ell/2)^2 + y^2 + b^2]^{1/2}}$$

$$F_2 = \frac{(x + \ell/2)\, a}{y\,[(x + \ell/2)^2 + y^2 + a^2]^{1/2}}$$

$$F_3 = \frac{(x - \ell/2)\, b}{y\,[(x - \ell/2)^2 + y^2 + b^2]^{1/2}}$$

$$F_4 = \frac{(x - \ell/2)\, a}{y\,[(x - \ell/2)^2 + y^2 + a^2]^{1/2}}$$

Notes: 1. F_1, F_2, F_3, F_4 are expressed in radians

2. V is positive for x and y positive and s positive

3. Interchange x and y for plane parallel to y-axis

References: Fitterman, 1979
Fitterman and Corwin, 1982

Vertical Dipolar Sheet Source

PLATE A5

APPENDIX B: SELF-POTENTIAL FIELD PROCEDURE AND DATA REDUCTION

1. The self-potential (SP) survey procedures described below have been found to give data of acceptable reproducibility for seepage studies, mineral and geothermal exploration, and other applications of the SP method. More elaborate procedures involving multiple base or measurement stations, repeated reoccupation of stations, monitoring of electrode temperatures, etc. may result in better data quality, but the increased time and expense involved must be compared with anticipated improvements in data quality to determine whether such procedures will be cost-effective for a particular application.

2. The procedures given are necessarily general in nature, and may have to be modified somewhat for special conditions such as frozen or very rocky soil, high telluric or stray current noise levels, etc. It is recommended that a telluric monitor, consisting of a battery-operated strip chart recorder continuously measuring the potential between a pair of stationary electrodes, be installed in the survey area to detect SP time variations that could erroneously be recorded as spatial anomalies.

3. The recommended "fixed-base" survey configuration has been found to give much more reproducible results than the "leapfrog" or "gradient" configuration, in which a length of wire equal to the station separation is moved along the survey line and the total SP reading at a given station is calculated by successive addition of individual dipole readings. The cumulative error inherent in this process has been found to generate significant spurious "anomalies", and it is recommended that this type of configuration be used only in situations where it is impossible to deploy the longer wire lengths needed for the fixed-base technique.

Fixed-Base Survey Configuration

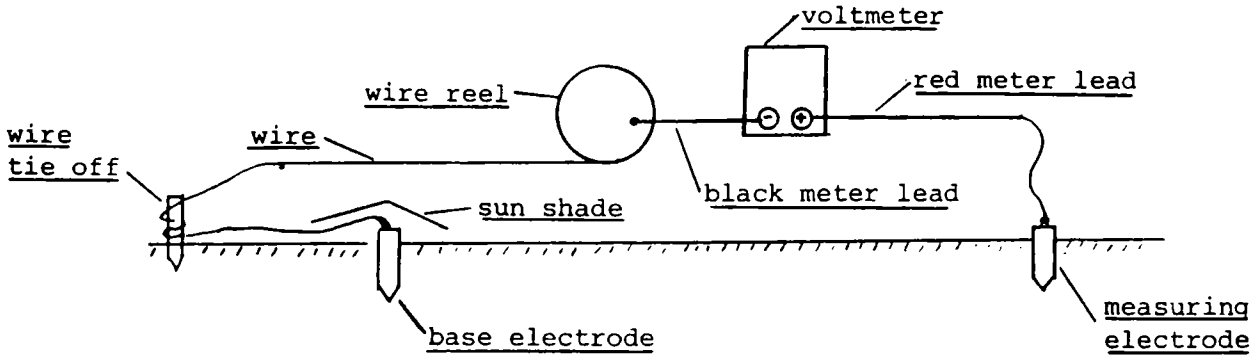

Survey Procedure
(using copper-copper sulfate electrodes and digital multimeter)

1. Record initial information on data sheet (see sample following text).

2. Reel and meter check

   a. Check wire insulation for breaks.

   b. Measure and record reel wire resistance (infinite reading indicates open wire).

   c. Measure resistance between either end of wire and frame of reel for short circuits between wire and frame. Reel must not contact ground during readings if short is present.

3. Initial electrode polarization check

   Measure and record voltage between all three electrode pairs in copper sulfate bath as shown on sample data sheet. These values will be used later for drift corrections. Measurements should be made on meter range having 0.1 or 1.0 mV resolution.

4. Base electrode installation

   a. Select base station site where conditions are unlikely to change during the survey period. If tying into previous station, re-occupy previous hole.

   b. Tie off end of reel wire and attach to base electrode terminal.

c. Dig hole into moist soil below surface layer. Do not add water to hole. Clean loose soil and rocks from bottom of hole.

d. Install base electrode by pushing down and rotating to ensure good soil contact. Pile soil around electrode and tamp down firmly. Be sure that no soil contacts electrode terminal.

e. Place sun shade over electrode and weight down with soil or rocks.

f. Be sure to note base station location on data sheet.

5. Measurement procedure

a. Minimum equipment needed by survey operator includes multimeter, data sheet, digging tool, flagging tape, and "portable reference electrode" carried in a bath of copper sulfate solution.

b. Transport reel and equipment above to first measuring station.

c. Select station location in area of uniform, undisturbed soil, if possible. Dig hole to moist soil below surface layer and clean loose soil and rocks from bottom of hole.

d. Insert measuring electrode in hole with firm downward pressure and rotate to ensure good soil contact. Hold electrode firmly in place or pack soil around it to hold it upright.

e. Connect positive lead of meter to electrode and negative lead to connector on reel. Shade electrode from sun.

f. Make SP reading:

1) Read potential on meter range having 0.1 or 1.0 mV resolution.

2) Read value for at least 10 to 20 seconds to check for drift or telluric fluctuations. If reading fluctuates, read long enough to obtain a reasonable average value. Record final value in mV, with + or - sign to indicate polarity.

3) Measure contact resistance between electrodes using appropriate kOhm range of multimeter. Resistance should be measured for only a few seconds or less to avoid undue

polarization of electrodes. If resistance differs considerably from previous values, try re-seating electrode or relocating station. Note that large SP values may produce erroneous resistance readings on the meter. In such cases, measure resistance with meter leads reversed and record average value. Return meter to voltage range after reading resistance.

4) Note soil conditions, vegetation, cultural features, etc. in "Comments" column of data sheet.

5) Remove electrode and clean loose soil from ceramic tip. Carry electrode in shaded location.

6) If there is any chance that the station will be a future tie-in point or will be re-occupied for any other reason, put flagging tape in hole to mark it and re-fill it to keep the soil from drying.

g. Move to next station and repeat procedure above. About once every half hour to hour, or at the end of a survey line, measure the potential between the measuring electrode and the portable reference electrode in the copper sulfate bath and record as shown on the sample data sheet. These readings will be used for later drift corrections, as discussed below.

h. After completing survey line, reel wire in and return to base station. Remove and clean base electrode and re-measure polarization between all three electrode pairs in copper sulfate bath as shown on sample data sheet.

Data Reduction Procedures

4. It is assumed that the polarization between the base and the portable reference electrodes remains constant, and that the measuring electrode drifts relative to these two. Therefore two electrode corrections are superimposed on the measured values: an initial polarization between the base and measuring electrodes (which is assumed to remain constant throughout the survey) and a drift of the measuring electrode, which is

determined by periodically measuring its potential relative to the portable reference. If in a given case it is apparent that the portable reference has drifted with respect to the base, then drift corrections should be made using only the initial and final readings between the base and measuring electrodes instead of the procedure below.

5. On the sample data sheet, the initial polarization between the base (#1) and measuring (#3) electrodes is +5 mV. This is corrected by subtracting 5 mV from all the measured values.

6. At the first reading between the portable reference and measuring electrodes at 0935 the #2(-) #3(+) reading (#2 electrode to the negative voltmeter lead; #3 electrode to the positive lead) has gone from an initial reading of +3 mV to a new value of +10 mV, i.e., the measuring electrode is 7 mV more positive than it was at the beginning of the survey. Therefore, an additional 7mV is subtracted from the initial -5 mV correction for a total electrode correction of -12 mV. Electrode corrections between drift measurements are interpolated linearly.

7. At 1005, the #2(-) #3(+) reading is +8 mV, so the measuring electrode now is 5 mV positive with respect to the initial reading of +3 mV. Therefore, 5 mV is subtracted from the original -5 mV polarization correction, giving a total electrode correction of -10 mV. Again, electrode correction values are interpolated back to the previous drift reading.

8. If the base station was at a point where SP had been measured previously, the SP value at that point must be added to all the measured and drift-corrected values as a tie-in correction (e.g., the +12 mV value on the sample data sheet). The final corrected SP value is the sum of the measured, electrode drift correction, and tie-in values.

SAMPLE

SELF-POTENTIAL SURVEY DATA

DATE 2 April 1980
LOCATION Honeybunny Mine, Nevada
LINE A-A'
BASE ELECTRODE LOCATION 0E, 200N, Line 13-B'
PERSONNEL G. Fox, M. Faraday

VOLTMETER Fluke 8020A
BASE ELECTRODE #1
PORTABLE REFERENCE ELECTRODE #2
MEASURING ELECTRODE #3
REEL CHECKS: RESISTANCE 170 Ω
SHORT CIRCUITS OK

Time	Station (m)	ΔV measured (mV)	Resistance (kΩ)	Electrode correction (mV)	Tie-in correction (mV)	ΔV corrected (mV)	ΔV smoothed (mV)	Comments
(	Previous SP	at base	station =		+12mV	wrt	survey zero)	
0817	In bath #1⁻	#2⁺	= +2mV,	#1⁻#3⁺ =	+5mV,	#2⁻#3⁺ = +3mV		
0823	10E	+3	15	−5	+12	+10		Dry, rocky soil
0830	20E	−3	12	−6	+12	+3		Soil wetter
0840	30E	+2	19	−8	+12	+6		at dirt road
0850	40E	−10	14	−9	+12	−7		metal well casing 10m to north
0910	50E	−40	3	−11	+12	−39		dry soil
0930	60E	−80	5	−12	+12	−80		mine shaft 5m to South pyrite outcrop 2m to North
0935	In	bath	#2⁻	#3⁺ =	+10	mV		
0940	70E	−30	2	−12	+12	−30		heavy brush, wet soil
0945	80E	−10	8	−11	+12	−9		serpentine outcrop 2m N
0950	90E	−2	15	−11	+12	−1		wet soil, grassy area
1002	100E	−5	20	−10	+12	−7		dryer soil
1005	In	bath	#2⁻	#3⁺ =	+8 mV			
	End	line.	Reel	in	wire			
1020	At base station							
	In	bath	#1⁻#2⁺	= +2mV,	#1⁻#3⁺ =	+6	mV,	#2⁻#3⁺ = +3mV

APPENDIX C: COMPREHENSIVE SEEPAGE ASSESSMENT, BEAVER DAM, ARKANSAS*

* Llopis, J. L., Deaver, C. M., Butler, D, K., and Hartung, S. C., 1988, article reprinted from Proceedings: Second International Conference on Case Histories in Geotechnical Engineering, Paper No. 3.33, pp 519-526, St. Louis, Missouri.

Proceedings: Second International Conference on Case Histories in Geotechnical Engineering, June 1-5, 1988, St Louis, Mo., Paper No. 3.33

Comprehensive Seepage Assessment: Beaver Dam, Arkansas

J.L. Llopis
U.S. Army Engineers Waterways Experiment Station, Vicksburg, Mississippi

D.K. Butler
U.S. Army Engineers Waterways Experiment Station, Vicksburg, Mississippi

C.M. Deaver
U.S. Army Engineers District, Little Rock, Arkansas

S.C. Hartung
U.S. Army Engineers District, Little Rock, Arkansas

SYNOPSIS: A general philosophy of the role of engineering geology and engineering geophysics in seepage assessment is presented. Practical application of this philosophy is illustrated by a case history. A large dike continues to have anomalous seepage in spite of pre-construction and post-construction grouting. The dike is founded over a graben of cavernous limestone with about a 200-ft. vertical offset along the bounding fault zones, which are horizontally separated by about 1000 ft. Objectives of the seepage assessment program were to define the geological and hydrological conditions beneath the dike in sufficient detail to allow rational remedial planning.

Integration of results of a geophysical investigation with the overall assessment program is emphasized: preliminary interpretation of the geophysical results is used to site new piezometers; detailed analysis of the geophysical results is used to site exploratory borings; feedback from exploratory borings and new piezometers is used to refine geophysical interpretation.

INTRODUCTION

Background

Earth dams and dikes are expected to seep, and their designs include drainage systems to collect and discharge seepage water into the downstream channel. Sometimes, however, seepage occurs in an unplanned manner, exceeding the capacity of the drainage system or along a path not considered in the seepage design. Excessive unplanned seepage may be just unsightly (though possibly disconcerting to the public), or it may threaten the integrity of the embankment. In these cases it may be necessary to conduct a seepage assessment program to detect and map seepage paths in order to more rationally plan remedial measures.

Dike 1, at Beaver Dam has been experiencing a general increase in seepage rates since initial reservoir filling in 1966. Recently however, the proliferation of seepage exits along the toe of Dike 1 has prompted the Little Rock District, U.S. Army Corps of Engineers (SWL) to undertake a comprehensive seepage assessment program. This program consisted of examining the project history, mapping and topographic surveying, surface geophysical testing, extending the piezometer network (including drilling, sampling and testing), exploratory drilling, seepage flow measurements, planning for and installing an automated piezometer and flow measurement data acquisition system, and remedial measure analysis. In support of this effort the U.S. Army Engineer Waterways Experiment Station (WES) was requested to perform a detailed geophysical investigation of the dike and its foundation.

Purpose

The purpose of this paper is to present the general philosophy of a seepage assessment program conducted at Beaver Dam, Arkansas. Described are the various phases of the program and how they are integrated to allow for a more rational approach to remedial planning.

Site Location and Description

Beaver Dam is located on the White River at river mile 609.0 in Carroll County, Arkansas, approximately 6 miles northwest of Eureka Springs, Arkansas. Beaver Dam is a straight, gravity-type, concrete structure flanked to the north by an earth embankment and three saddle dikes. The location of Dike 1 relative to the concrete dam and main embankment is shown in Figure 1. The reservoir (Beaver Lake) is used for flood control, power generation, and water supply. Construction of the dam was started in November 1960 and ended in June 1966. Dike 1 is approximately 1,000 ft in length and 30 ft high. The top of the conservation pool is elevation 1,120 ft while the top of the dike is elevation 1,142 ft. Dike 1 is founded on severely weathered limestone and is experiencing seepage from various exits.

GEOLOGY

General Geology

Beaver Dam and reservoir area are located in an area known as the Ozark uplift, a region consisting of flat-lying sedimentary rocks composed chiefly of limestone and dolomitic limestone. The strata are nearly horizontal over the greater part of the area but are locally deformed by simple dislocations along southwest-northeast trending normal faults and shallow basins that in places of are of considerable magnitude.

Physiography

The upland area around the dam is a part of the Springfield Plateau, the surface of which is developed at approximate elevation 1500 ft the cherty limestone of the Boone Formation. In the dam and reservoir area, the White River has cut a channel approximately 600 ft in depth. This

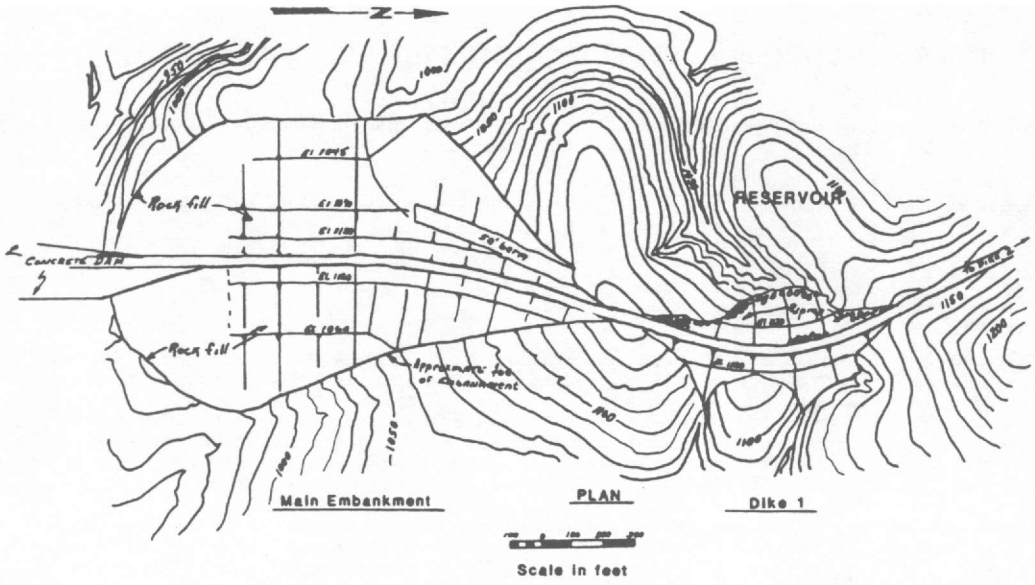

Figure 1. Location of Dike 1 relative to concrete dam and main embankment

incision into the Plateau surface has resulted in a deeply and intricately dissected type of topography. The entrenched river follows a meandering course across the area.

Stratigraphy

Five formations are exposed at the dam site. They are (moving upsection) the Powell Formation, the Cotter and the Jefferson City Formations of the Jefferson City Group which is of Ordovician age, the Chattanooga Formation of Devonian age, and the Boone Formation of Mississippian age. The Chattanooga and the Boone Formations are generally above reservoir level except in the vicinity of the left abutment of the dam and Dike 1 where the units are downfaulted. In the vicinity of the dam site, the Boone Formation caps the higher ridges and forms the sides of the valley down to approximate elevation 1200 ft. Beneath this lies the Chattanooga Shale member (Chattanooga Formation), which in turn is underlain by its Sylamore Sandstone member. Beneath these and forming the valley walls below elevation 1180 ft and underlying the greater part of the valley bottom are limestones and dolomitic limestones of the Jefferson City Group (Design Memorandum No. 5, 1959).

Structural geology

The general structural geology of the region is that of flat lying rocks which are locally deformed by simple dislocations along southwest-northeast trending normal faults that extend for considerable distances, and by monoclines, low domes, and shallow basins. The Beaver Dam site lies near the northeast end of a very gentle, shallow, elongate, northeast-southwest trending structural basin known as the Price Mountain syncline. This basin is often faulted in areas where the downfolding is most pronounced. In the greater part of the lower end of the reservoir, Ordovician strata underlie the valley floor and extend up the sides of the valley to about elevation 1,180 ft. Overlying these and almost everywhere above pool level are formations of Devonian and Mississippian age. In localized areas, these units have been downfaulted to form a part of the foundation under the most topographically desirable dam sites in the valley. This is the case at Dike 1.

Dike 1 Foundation Materials

Figure 2 shows the foundation materials underlying Dike 1. Dike 1 is founded on a downfaulted block of the Boone formation. This downfaulted block (graben) extends approximately between station 63+00 at the northern end to approximate station 75+00 at the southern end, a total distance of approximately 1,200 ft. The graben is bounded by steeply dipping normal faults on either side trending roughly in a northeast-southwest direction. The vertical displacement of these faults is approximately 200 ft. Cores of the rock adjacent to the northern fault zone show evidence of fracturing; however, the fractures appear to be filled or cemented and sound. Boring information from the southern fault zone area indicates the presence of many clay-filled cavities. The southern fault gouge does not appear to have the same degree of soundness as the northern fault zone. The Boone Chert which makes up the foundation of Dike 1 can be divided into two distinct sub-units. The upper sub-unit of the Boone Chert (estimated thickness, 100 ft) is composed of calcium carbonate and chert which upon weathering has resulted in the removal of calcium carbonate and left a spongy, vuggy, residual material that is predominately chert. The lower sub-unit of the Boone Chert (estimated thickness, 60 ft) is also composed of calcium carbonate and silica; however, this sub-unit is characterized as being slightly weathered to unweathered and contains more crystalline calcium

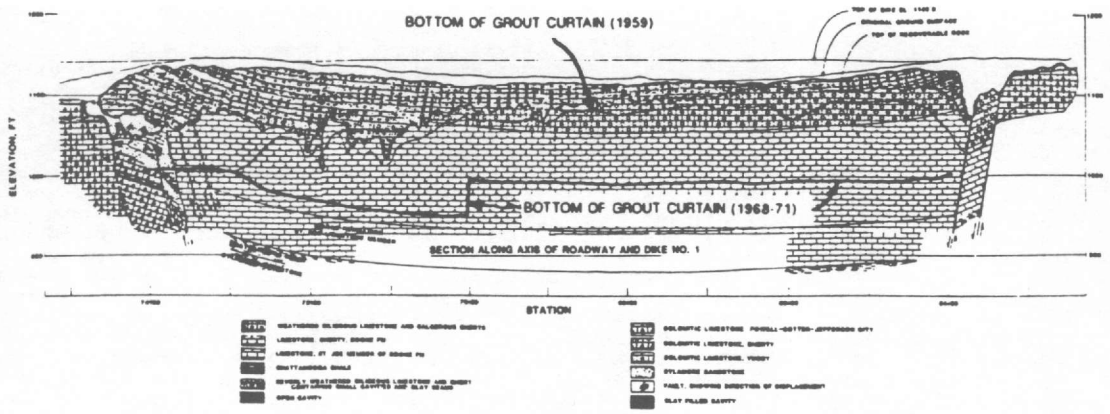

Figure 2. Foundation materials underlying Dike 1

carbonate. The lower sub-unit is moderately to closely jointed and this jointing has allowed the passage of water which has led to the dissolution of calcium carbonate and in turn has resulted in open channels and cavities.

Underlying the Boone Chert Unit is the St. Joe Limestone, described as non-cherty, gray to green-gray, crystalline, very fossiliferous, and containing numerous thin shale seams and partings. Underlying the St. Joe Limestone is the Chattanooga Shale described as black, firm, and fissile. The shale is considered to be an effective barrier to any downward movement of ground water.

SEEPAGE HISTORY OF DIKE 1

Pre-Construction Grout Curtain

The foundation materials of Dike 1 were recognized as being susceptible to seepage during the early phases of the site selection. In June 1959 it was decided that an economical solution to prevent a potential seepage problem was to install a grout curtain. The grout curtain consisted of two lines of holes spaced 5 ft apart with 10-ft hole spacings which extended to a depth of 5 ft below the top of sound or unweathered rock at all locations except between stations 72+70 and 74+70, where the grout curtain was extended deeper (16 to 65 ft) into sound rock (Figure 2). A total of 284 holes (24,200 linear ft) were drilled in this grouting program. The grout (31,000 cu. ft) was placed by gravity flow (Reconnaissance Report, Beaver Dam, 1984).

During initial filling of the reservoir (April 1966) seepage was detected in a small valley downstream of Dike 1. The reservoir pool elevation at this point was 1,102+ ft and the seep was flowing at a rate of 150-200 gpm By June 1966 the reservoir elevation was 1114 ft and eight additional seeps were detected with a combined flow rate of approximately 400 gpm By the time remedial grouting operations were initiated in 1968, the combined flow rate of these seeps had risen to approximately 800 gpm Conclusions from studies conducted at Dike 1, including flow measurements and dye tracing, indicated seepage was coming from the lake through two possible passages, either beneath the grout curtain through open cavities in the foundation rock, or along the top of rock or both. Seepage was occurring along the entire length of Dike 1 with the most concentrated flow occurring in the vicinity of station 71+00 near the southern portion of the dike (Reconnaissance Report, 1984).

Several possible explanations why the pre-construction grout curtain did not perform satisfactorily are as follows:

a. Grout holes were not drilled deep enough to sound rock to intercept open joints.

b. Since grout was placed by gravity flow, it is possible many small cavities and joints were not filled.

c. Grout was too thick to enter some of the cavities and joints.

d. Since drilling was performed with tricone roller bits using compressed air to remove cuttings, the cuttings could have plugged some of the cavities preventing them from being grouted.

e. Many cavities and joints could have been missed altogether because of the grout hole spacing.

Early Seepage Flow Studies

Flow measurements, exploratory drilling, pressure tests, and dye and temperature tests were conducted from the time of leakage (1966) until 1968 to determine the extent and routes of seepage through and beneath the dike and to formulate possible remedial measures. These measurements were accomplished by installing two weirs, a Parshall flume, and twenty-seven piezometers. The data suggested that the leakage was issuing both through cavities below the original grout curtain and along the top of

crystalline/weathered rock interface. It was concluded that seepage occurred along the entire length of Dike 1 and to the fault zone beneath the main embankment at station 73+00, with the greatest seepage occurring along the shortest flow path in the vicinity of station 71+00.

Remedial Grout Curtain

During the period July 1968 to December 1971 an extensive grouting program was conducted in an effort to abate the seepage occurring at the dike. The program consisted of 30,040 linear ft being drilled in 228 holes. Also, 38,900 cubic ft of grout solids were pressure injected into these holes with the heaviest grout takes occurring in an area between stations 70+50 and 72+00 (Figure 2). Problems encountered during the grouting operations were collapsing boring walls (cave-in), insufficient seating of casing, and incapability of grout pump to grout some large cavities to refusal.

As a result of the remedial grouting program, seepage was reduced to approximately 450 to 500 gpm for mid-pool elevations (1120-1130 ft), a decrease in flow of 30 to 35 percent. During the period 1971 through 1984 piezometers were manually read approximately twice a year by SWL personnel while the Parshall flume was read on a monthly basis by project personnel. During a periodic inspection in 1980, a new seepage area was located on the downstream right abutment of the dike. This prompted SWL personnel to undertake an effort to locate, inspect, and describe all known seepage exits.

Dam Safety Assurance Program

When the U.S. Army Engineer Southwest Division's (SWD) Division-wide Master Plan for the Dam Safety Assurance Program was submitted in 1983, Beaver Dam was listed as requiring studies for a Reconnaissance Report under designated priorities of spillway adequacy and major seepage. The Reconnaissance Report (May 1984) concluded that seepage at Dike 1 would increase to near pre-grouting flows (800+ gpm.) during a Spillway Design Flood (Probable Maximum Flood, pool elevation 1,139.9 ft) and continue flowing at this rate even after the flood receded due to expansion of existing cavities. This conclusion was proven to be valid on 23 December 1984 when a Pool of Record (el 1,130.4 ft) occurred. During the emergency flood procedure inspection on that date the project superintendent observed a new seepage exit 500 feet downstream from Dike 1 with a flow rate of approximately 25 gpm. The alarming factor at the newly discovered exit however, was the large amounts of detrital material (sediment), ranging from clay- to gravel-size being discharged in the flow, i.e. muddy water. Another new seep was discovered on 2 January 1985 near the left dike/abutment contact at approximate elevation 1,106 ft (Figure 3). Water from this new seep was described as jetting vertically with a flow rate of approximately 7 gpm. at pool elevation 1,125.1 ft (Feature Design Memorandum, 1987). The 1984 Reconnaissance Report recommended that a seepage investigation be undertaken to determine the location and extent of seepage and develop remedial measures to control seepage at Dike 1.

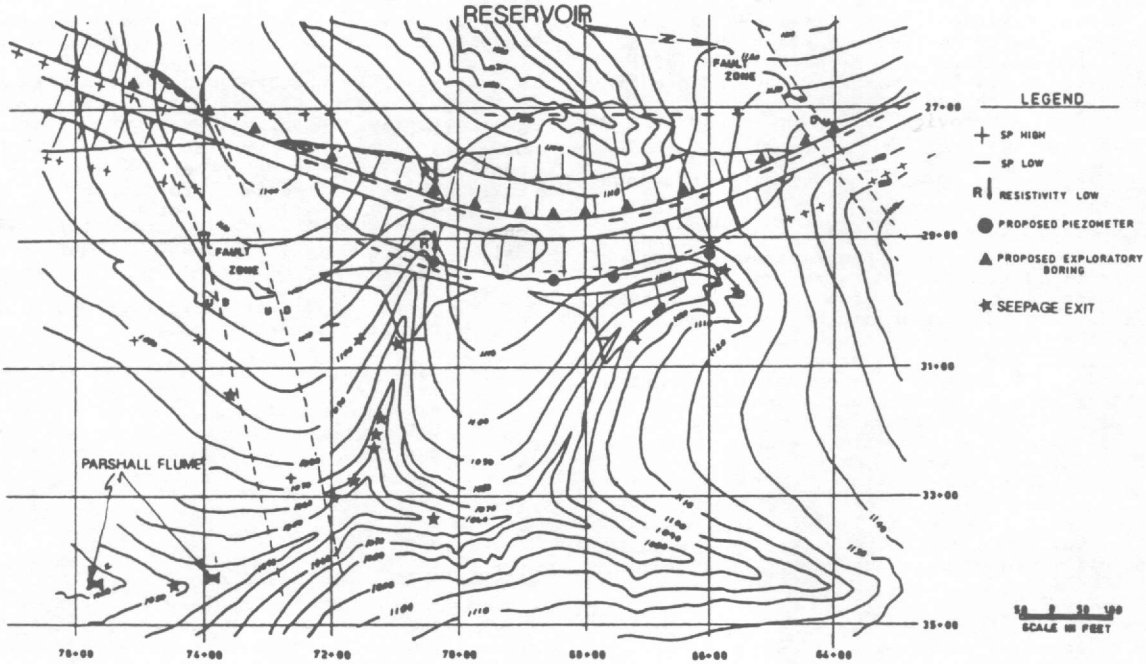

Figure 3. Location of seepage exits and proposed piezometer and exploratory borings.

A combined SWD/SWL/WES meeting was held at Beaver Dam on 14-16 January 1985 to discuss the proposed seepage investigations, which were initiated in February 1985.

SEEPAGE INVESTIGATIONS

General

The new muddy seepage exit below Dike 1 discovered during a pool-of-record (1,130.4 ft) in December 1984 not only substantiated the need for seepage investigations, but also added an element of urgency and a necessity to expedite the investigations, and recommendations of measures to control seepage. In 1985 the monitoring /inspection of instrumentation and seepage was revised to more frequent scheduling, especially for pool levels above elevation 1,128 ft. The action having the greatest impact on project operations, due to severe seepage, is the request and approval for a deviation (loss) of the authorized flood storage pool in Beaver Lake from elevation 1,130 to 1,128 ft until the seepage the seepage problem is resolved. The major elements of the seepage investigation are described below.

Geophysical Investigations

In March 1985 WES personnel conducted a geophysical investigation at Dike 1. Several geophysical methods were used for this study including self-potential (SP), electrical resistivity, electromagnetic induction (EM), seismic refraction, magnetic profiling, and borehole water conductivity/temperature measurements. The objectives of the geophysical investigation were to (a) detect, map, and monitor seepage through the foundation of Dike 1, (b) delineate geologic structure beneath and immediately adjacent to Dike 1, and (c) provide input to the planning of remedial measures.

The geophysical methods necessary for a seepage analysis are not difficult to use. However, a geophysical survey program must be planned based, to the maximum extent possible on knowledge of the (1) surface geometry of the dam and associated features, (2) design and construction details of the structure, and (3) the geology of the foundation and abutments (Butler, 1985).

The primary, long-term geophysical method was the self-potential (SP) method, which was monitored throughout the duration of the investigation. SP data were obtained during various pool levels to determine relationships of seepage flows and pool levels. The SP arrays were installed by SWL personnel in February 1985. Initial SP readings were made by WES in March 1985. Subsequent readings, during various pool levels, were taken by SWL personnel and forwarded to WES for interpretation. Detailed results of the geophysical studies pertaining to the seepage investigation are presented in Supplement No. 1 of the Reconnaissance Report, 1986.

Additional geophysical studies were conducted at Beaver Dam in conjunction with the Corps of Engineers' Repair, Evaluation, Maintenance, and Rehabilitation Program (REMR). These REMR sponsored geophysical tests included high-resolution seismic reflection, ground-penetrating radar, microgravimetry, and additional SP investigations. The ground-penetrating radar survey was conducted in September 1985 with an additional survey being conducted in February 1986. In August 1986 a high-resolution seismic reflection and a "low pool level" SP survey was conducted. Detailed results of these geophysical surveys are presented in the Feature Design Memorandum, 1987.

The geophysical investigation was successful in delineating the fault zones bounding Dike 1, which are believed to act as channels for lake water to exit downstream, as well as identifying other faults which were not previously known to exist. The tests also identified fractured and saturated zones as well as determining the vertical extent of the weathered Boone Chert. The tests also indicated that seepage is occurring along the entire length of the dike. The geophysical tests suggest that both axial and transverse seepage flows are occurring along the south fault zone, but that the north fault zone is relatively tight (impermeable) to those flows. Based on results of the geophysical tests an integrated seepage map was produced showing that seepage flows are moving primarily in an east-southeasterly direction with the greatest flows occurring between stations 69+00 and 73+00, and along the south fault zone (Figure 4).

Exploratory Borings

Twenty-five exploratory borings were drilled along the upstream crest of Dike 1 and its abutments during the period April 1986 to August 1987. The primary purpose of these borings was to delineate the limits and geologic characteristics of the downthrown faulted block of the Boone Formation beneath Dike 1 and the North and South fracture zones that bound the Dike. Originally, the boring locations were selected based on areas that had experienced high grout takes during the previous grouting program. However, locations for the borings were later changed to take advantage of information obtained from geophysical testing. Based on results of the SP, resistivity, and other geophysical testing and also considering previous grout takes, fault locations, and piezometer data, WES submitted a list of proposed locations for exploratory borings to SWL for approval. Figure 3 shows the WES suggested exploratory boring locations.

Extensive investigations were conducted on each of the borings, typically included soil sampling, diamond core drilling, detailed descriptive logging of rock core, dye testing at zones of drill fluid loss, pressure testing of rock, downhole geophysical logging, inspection with downhole video equipment, and laboratory testing of rock core samples.

The investigations conducted in the exploratory borings determined that the northern fault zone has a vertical offset of 230 ft while the southern fault zone's vertical displacement measures approximately 146 ft. The unsound nature of the fault zones was evidenced during drilling by noting the complete loss of drill fluid and large core losses. This condition was substantiated by SWD laboratory personnel while

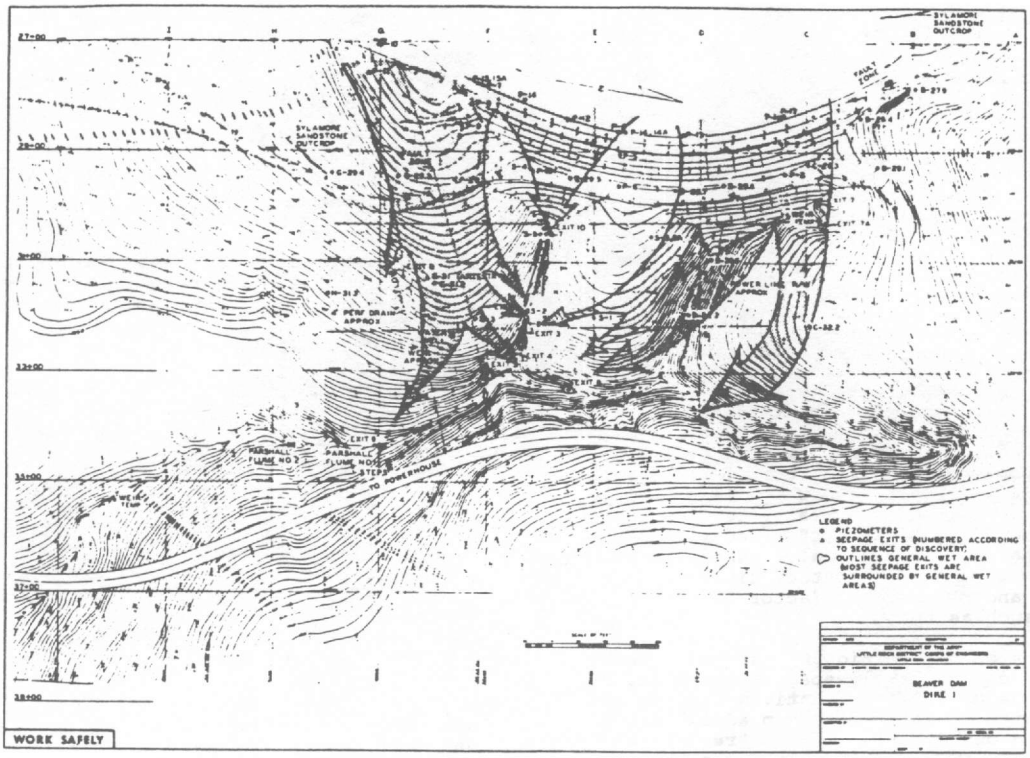

Figure 4. Integrated seepage map

performing "down-looking" and "side-wall looking" observations with a down-hole video camera. Numerous open cavities, channels, joints, and intensely fractured zones were encountered in the the fault zones as well as in the upper cherty Boone Formation. Subsurface flows through channels in rock were apparent in several borings where normally suspended fines could be seen moving rapidly.

Piezometers

There were 26 open (well point) piezometers at Dike 1 prior to the seepage investigation. A review and analysis of locations and depths of the existing piezometers was made to determine key areas (and depths) where piezometric data was inadequate for analyzing the overall groundwater (seepage) flow network beneath Dike 1. The new piezometers were located in a directional alignment pattern (grid) with existing piezometers to facilitate preparation of cross sections through the piezometers, both parallel and perpendicular to the dike. Piezometers were also located to give broader coverage (north/south) of the fault zones and downstream seepage areas (east/west). The new piezometers were dual-tipped and were designed such that the lower tip was placed at or near elevation 1040 ft, which is within the zone between known seepage exits and Parshall flumes located further downstream, and the upper tip placed within the upper weathered Boone Formation, at an average depth of 11 feet below top-of-rock.

Four of the new piezometer sites were relocated in May 1985 based on results of SP and resistivity geophysical tests conducted by WES. Figure 3 shows the WES proposed piezometer locations. Thirty piezometers were installed at Dike 1 between the period May and September 1985, giving a total of 56 piezometers at the structure.

The piezometer borings drilled in 1985 at Dike 1 were sampled and tested to determine subsurface conditions prior to installing the piezometers. A common difficulty was heavy loss of drilling (circulation) fluid, with most borings having a total circulation loss at some point during drilling. A downhole camera lowered into several of the piezometers in August 1985 indicated rock characteristics and features which contribute to subsurface seepage such as open cavities, channels, intensive fracturing, and weathering.

Seepage Flow Measurements

Prior to the seepage investigation there was only one Parshall flume used for measuring seepage flow rates downstream of Dike 1. The frequency of the flow measurements were taken based on pool level. Measurements were made by reading the water level on a scaled gauge on the interior wall of the flume and converting the readings to gpm. In October 1985, a flow recorder was installed on the Parshall flume allowing the seepage to be monitored continuously. In November 1985, a second Parshall flume and

recorder were installed approximately 170 ft downstream of the first flume. The necessity for a flume at this second location came from the appearance of the new muddy seepage flow which bypassed the first flume.

Topographic Surveys and Mapping

Field control for the seepage investigations, boring locations, and geophysical surveys was established by installing a 200-foot survey point grid. Also, the topographic map of Dike 1 was updated by a new planetable survey, with a final plan on 2-foot contour lines.

Seepage Study Findings and Recommendations

In April 1986 SWL reported the findings of the seepage study in Supplement No. 1 of the Reconnaissance Report. The report concluded that the foundation beneath Dike 1 was in an advanced stage of deterioration, and that seepage could be generally described as pervasive. Also, the risk factor and potential existed during a high (flood) pool condition for one of the numerous seepage flows to seek a new and larger exit path, by removal of detrital material (cavity clays, etc.), and "blowout" through the overburden in the downstream area. Finally the report concluded that the element of time was both a critical and a debatable factor on a seepage problem such as this.

The report also investigated various alternatives for controlling seepage beneath the dike. The seepage control alternatives considered at Dike 1 were construction of an additional grout curtain, a cutoff wall, a downstream berm, placement of an upstream blanket, or do nothing and continue monitoring the seepage. The recommended remedial technique was a concrete diaphragm cutoff wall installed upstream of the centerline of the dike. The report concluded that this was the most feasible method to adequately provide a positive cutoff of the seepage. The other methods were considered to be only temporary measures to control seepage and inadequate for providing a positive cutoff, which was deemed necessary from seepage investigations.

Automated Piezometer System

During the period November 1986 through April 1987 an automated monitoring network was installed at Beaver Dam to read all (88) open well point piezometers at Dike 1 and the main embankment and Dike 3. The system transmits the piezometer information via telephone modem to the District Office (250 miles). Readings are routinely taken every 4 hours and can be read with a higher frequency if needed. Since the installation of the automated system a high degree of interconnection between piezometers has been detected. This was evidenced during periods of drilling or performing down-hole tests when piezometers were being monitored at intervals as short as 1 hour. The automated system should aid in constructing more accurate piezometric profiles of the site since short term piezometric head versus pool level can be determined.

PLAN FOR REHABILITATION

In September 1987 a Feature Design Memorandum was prepared by SWL. The report described the recommended design for a concrete diaphragm cutoff wall.The plan for the wall consists of constructing the wall through the embankment and permeable zone of the foundation rock. The wall will be a minimum of 1,400 feet long, 2 feet wide, and vary in depth from 130 to 205 feet. The estimated cost of constructing the cutoff wall is $16,000,000.

A rock-mill type excavation system will be used to excavate the cutoff wall trench, using bentonite slurry to stabilize the trench during both excavation and concrete placement. The rock-mill was determined to be the most efficient and cost effective method to construct the proposed wall due to the amount and characteristics of rock that will be encountered. More detailed information on this excavation method is given by Hess, 1985.

Also included in the Feature Design Memorandum was a recommendation by WES to install and maintain an automated geophysical monitoring network to monitor seepage before, during, and after implementation of a remedial measure (such as a concrete cutoff wall). The result of the monitoring network analysis will be an assessment of the effectiveness of the remedial measure. The computer controlled network is envisioned as consisting of a permanently installed SP array and borehole resistivity probes with the capability of scanning the network at any desired time interval.

SUMMARY AND CONCLUSIONS

The results of the seepage investigation indicated that the foundation beneath Dike 1 was in an advanced stage of deterioration, and that seepage can be generally described as pervasive. Also, the risk factor and potential exists during a high (flood) pool condition for one of the numerous seepage flows to "blowout" through the overburden in the downstream area. Finally the report concluded that the element of time is both a critical and debatable factor on a seepage problem such as the one above.

The investigation also recommended that a concrete diaphragm wall be installed upstream of Dike 1 as a mean of controlling seepage.

By conducting a comprehensive seepage program such as the one performed at Beaver Dam it has been demonstrated that integration of results from various phases of the investigation has led to a more rational approach to remedial seepage planning. In a program of this magnitude it is very important to consider the geophysical surveys as an integral part of the seepage analysis. It is also important for the project engineer and the geophysicist to communicate with each other and share their knowledge of the project in order to make more meaningful interpretations of test data and to more efficiently plan any future testing.

ACKNOWLEDGMENTS

The tests described and the resulting data presented herein, unless otherwise noted, were obtained from research conducted under the Dam Safety Assurance and Repair, Evaluation, Maintenance, and Rehabilitation programs of the U.S. Army Corps of Engineers by the U.S. Army Engineer District, Little Rock and the U.S. Army Engineer Waterways Experiment Station. Permission was granted by the Chief of Engineers to publish this information.

REFERENCES

Butler, D. K. (1985), "Geophysical Methods Applied to Detect and Map Seepage Paths at Clearwater Dam", The REMR Bulletin, Vol 2, No. 2, U.S. Army Engineer Waterways Experiment Station, Vicksburg, Miss.

Hess, C. M. (1985), "French Drilling Machine Shows Advantages in Excavating for Concrete Cutoff Wall", The REMR Bulletin, Vol 2, No. 2, U.S. Army Engineer Waterways Experiment Station, Vicksburg, Miss.

U.S. Army Engineer District, Little Rock, 1959. Design Memorandum No. 5, Geology and Soils, Little Rock, Ark.

U.S. Army Engineer District, Little Rock, 1984. Reconnaissance Report, Little Rock, Ark.

U.S. Army Engineer District, Little Rock, 1986. Reconnaissance Report Supplement No. 1, Beaver Dam, Little Rock, Ark.

U.S. Army Engineer District, Little Rock, 1987. Feature Design Memorandum, Beaver Dam, Little Rock, Ark.

The following two letters used as part of the number designating technical reports of research published under the Repair, Evaluation, Maintenance, and Rehabilitation (REMR) Research Program identify the problem area under which the report was prepared:

	Problem Area		Problem Area
CS	Concrete and Steel Structures	EM	Electrical and Mechanical
GT	Geotechnical	EI	Environmental Impacts
HY	Hydraulics	OM	Operations Management
CO	Coastal		

Destroy this report when no longer needed. Do not return it to the originator.

The findings in this report are not to be construed as an official Department of the Army position unless so designated by other authorized documents.

The contents of this report are not to be used for advertising, publication, or promotional purposes. Citation of trade names does not constitute an official endorsement or approval of the use of such commercial products.

COVER PHOTOS:

TOP — Methodology and strategy for mapping anomalous subsurface seepage paths.

MIDDLE — View of Beaver Dam and Lake, Arkansas.

BOTTOM — Concept of self-potential generation by fluid flow.

DEPARTMENT OF THE ARMY
WATERWAYS EXPERIMENT STATION, CORPS OF ENGINEERS
P.O. BOX 631
VICKSBURG, MISSISSIPPI 39180-0631

Official Business
Penalty for Private Use, $300
WESIM-TS-T

SPECIAL FOURTH CLASS RATE
POSTAGE & FEES PAID
Department of the Army
Permit No. G-5

54004/21/01

UNIVERSITY OF ILLINOIS
ATTN: METZ REFERENCE ROOM
B106 NEWMARK CIVIL ENGR LAB
208 NORTH ROMINE STREET
URBANA IL 61801-2374